MORPHOLOGICAL ANALYSES OF SENESCENT MICROGLIA IN HUMAN AND RODENT BRAINS UNDER CONDITIONS OF DISEASE AND INJURY

By

KRYSLAINE OLIVEIRA LOPES

A DISSERTATION PRESENTED TO THE GRADUATE SCHOOL
OF THE UNIVERSITY OF FLORIDA IN PARTIAL FULFILLMENT
OF THE REQUIREMENTS FOR THE DEGREE OF
DOCTOR OF PHILOSOPHY

UNIVERSITY OF FLORIDA

2008

To my family.

ACKNOWLEDGMENTS

Completion of this dissertation was made possible by the contribution of a number of people. I thank my mentor Dr. Wolfgang J. Streit for nurturing my intellectual curiosity about glial cells and for encouraging me not to give up after disappointing experiments. I thank the other members of my committee, Dr. David Borchelt, Dr. Christiaan Leeuwenburgh, and Dr. John Petitto, for their assistance and suggestions. I am grateful to the Neuroscience office staff members, John Neeley and B.J. Streetman, for making sure I had all the necessary paperwork to complete my coursework and to present my research at conferences.

I would also like to thank the past and present members of the Streit lab for their research assistance. In particular, I would like to thank Dr. Chris Mariani, Dr. Sarah Fendrick, Robby Sweeney and Celeste Karch for their technical help and friendship. I am indebted to Dr. Qing-Shan Xue and Nichole Fife for their multitude of assistance and suggestions. I appreciate the help eMalick Njie gave me in various aspects of my research, from providing antibodies and helpful comments to creating a fun workplace in the late night/weekend shifts. I am very grateful to my colleague Kelly Miller for her continuous encouragement, friendship and for making graduate school an enjoyable experience.

Special thanks go to my parents, Roberto and Elizabeth; and my siblings, Rodrigo and Vanessa, for always believing in me. Despite all the emotional and financial struggles, my family never stopped supporting my choice to stay miles away from home while I pursued my career interests. I am particularly thankful to my dad for his long-time commitment to my academic success. Finally, I am principally indebted to Dr. Baler Bilgin for his unwavering support throughout my academic career. This milestone would not have been possible without him.

TABLE OF CONTENTS

page

LIST OF TABLES

LIST OF FIGURES

Abstract of Dissertation Presented to the Graduate School
of the University of Florida in Partial Fulfillment of the
Requirements for the Degree of Doctor of Philosophy

MORPHOLOGICAL ANALYSES OF SENESCENT MICROGLIA IN HUMAN AND RODENT BRAINS UNDER CONDITIONS OF DISEASE AND INJURY

By

Kryslaine Oliveira Lopes

August 2008

Chair: Wolfgang J. Streit
Major: Medical Sciences--Neuroscience

Little is currently known about microglial cells in the aging brain. Recently, microglia have been shown to undergo senescence-related changes with advancing age, including dystrophy (i.e., degeneration) of their typically branched morphology and alterations in metabolic functions. The cause(s) and consequences of such alterations to microglial cells themselves as well as to the central nervous system as a whole are not known. In this study we characterized the defining morphological features of dystrophic microglia in both human and rodent brains. The central focus of this application was in the assessment of whether aging-related degeneration of microglial cytoplasmic structure is secondary to prolonged iron storage via expression of the iron storage protein ferritin. Since aging in the brain is accompanied by an accumulation of iron in ferritin proteins, particularly L-rich ferritins expressed by microglia, it is hypothesized that aged microglia are highly susceptible to iron-induced oxidative damage. The findings presented herein shed light not only on the effects of the aging process on microglial structural and functional integrity, but they also introduce ferritin immunohistochemistry as a useful method for detecting microglial cells that are in danger of being lost. Furthermore, our findings support a possible connection between microglial cytoplasmic deterioration and impaired glial neuroprotection. Understanding the underlying mechanisms responsible for the

degeneration of microglial cells in aged brains may be important for elucidating the pathogenesis of aging-related neurodegeneration and neurodegenerative diseases.

CHAPTER 1
INTRODUCTION AND LITERATURE REVIEW

Microglia: An Overview

Microglial cells constitute a functionally dynamic and morphologically heterogeneous cell population within the central nervous system (CNS; Hanisch and Kettenmann 2007). Ramified microglia, which are the most prevalent in the healthy CNS, are characterized by highly branched processes arising from the cell body in every direction. These processes engage in pinocytosis and are highly motile, continually going through renewal cycles as they inspect the CNS homeostatic status (Booth and Thomas, 1991; Nimmerjahn et al., 2005; Davalos et al., 2005). Typically, ramified microglia are uniformly spaced in the healthy brain parenchyma (Streit, 2005) although on occasion they have also been shown to contact neuronal cell bodies, astrocytes, and blood vessels (Nimmerjahn et al., 2005). The implication is that in the normal, healthy brain, ramified microglia are constantly monitoring the well-being of neighboring cells as well as the status of their extracellular milieu. In response to a disturbing stimulus, the first immediate reaction of microglial cells is to project all of their ramified processes in the direction of the stimulus epicenter, forming a shield as a first line of defense (Davalos et al., 2005). Taken together, these findings strongly suggest that the highly branched morphology of microglia serves an essential purpose in CNS protection and normal functioning.

Microglia can react to a number of endogenous (e.g., abnormal protein aggregation, neuronal dysfunction/death) and exogenous (e.g., blood brain barrier [BBB] disruption by injury/ infection) signals. When the disturbing stimulus persists, local ramified microglia become ‘activated’. That is, they lose their fine branches, enlarge their processes (hypertrophy), increase expression of immunophenotypic markers, proliferate, and increase secretion of cytokines and other inflammatory mediators, including hydrogen peroxide (H_2O_2) and superoxide (Colton and

Gilbert, 1987; Perry et al., 1995). Activation of microglial cells is an elaborate, graded process, whereby precise immune effector functions are matched to the specific stimulus at hand (Streit, 2002; Schwartz et al., 2006). Moreover, activation is under strict control and occurs only in response to strong stimuli (Kreutzberg 1996). In extreme levels of activation, when cellular debris must be cleared (i.e., phagocytosed and degraded), activated microglia metamorphose into rounded brain macrophages. The acquired functions of activated microglia are matched by changes in morphological configuration, going from ramified over rodlike to rounded morphology depending on the nature of the activating agent and accompanied by changes in gene expression profiles. Cumulatively, these observations emphasize the significance of microglial cytoplasmic structure for the proper execution of their cellular functions.

Recently, several histological studies in human brain have identified microglial cells exhibiting an aberrant cytoplasmic structure, termed dystrophic microglia (Conde and Streit 2006; Ferraro 1931; Lopes et al. 2008; Simmons et al. 2007; Streit 2002; Streit 2004; Streit et al. 2004; von Eitzen et al. 1998; Wierzba-Bobrowicz T et al. 2004). Their morphology is marked by degenerative changes, such as thinning and loss of distal branches, fragmentation of cytoplasm (cytorrhexis), and the formation of rounded swellings (spheroids) along major processes. This type of microglia is more prevalent in the aged brain, and thus microglial dystrophy is thought to be a reflection of cellular senescence and ongoing degeneration (Flanary et al. 2007; Streit 2006; Streit et al. 2004). It is not yet known what functional changes result from the degeneration of microglial cytoplasmic structure. It is possible that microglial dystrophy leads to an impairment of their normal cellular functioning, possibly resulting in a significant reduction of their normal neurotropic support functions.

Microglial Senescence

Neurons, oligodendrocytes and astrocytes originate from the neuroectoderm. In contrast, microglia arise from myeloid progenitors derived from the hemangioblastic mesoderm (Streit 2001). Reminiscent of their monocytic lineage is the ability of microglia to proliferate and undergo self-renewal. The proliferative capacity of microglia is relevant to the study of microglia in the aging brain because it underlies their senescence potential: microglia, as mitotic cells, have a finite replicative lifespan. Upon reaching a critical shortening of telomeres, the tandem-repeat sequences at the end of chromosomes, the cell enters the senescent state. Analyses of telomere length revealed that microglia become senescent with mitotic stimuli *in vitro* (Flanary and Streit 2004) and with normal aging *in vivo* (Flanary and Streit 2003). The primary consequence of this replicative senescence is the cessation of cell division through the cell's arrest in the G1-S boundary of the cell cycle (Yanishevsky et al. 1974).

Cells that have entered the senescent state remain metabolic active, although there are gradual changes in cellular structure and function. For instance, senescent cells accumulate lipofuscin granules in their cytosol (Brunk and Terman 2002; Sitte et al. 2001; Vogt et al. 1998). Lipofuscin is a mixture of autofluorescent lysosomal lipo-pigments and proteins that cannot be excreted or degraded (Gary and Woulfe 2005; Seehafer and Pearce 2006). The amount of lipofuscin in mitotic cells is dependent on both its rate of formation and its rate of dilution by cell division (Sitte et al. 2001). Recently, microglia have been shown to progressively accumulate lipofuscin-containing dense bodies in their cytoplasm (Sierra et al. 2007; Xu et al. 2008; Yamasaki et al. 2007), thus providing further evidence for their replicative senescence potential with advancing age. Other age-related changes in microglial metabolic functioning include a

decrease in proteolytic activity, an increased production of pro-inflammatory mediators, and an apparent 'primed' state of activation. These results are summarized in Table 1-1.

Structural Deterioration

The morphology of senescent microglia is quite different from the ramified appearance of resting microglia or the bushy morphology of hypertrophic (activated) microglia (Figure 1-1) (Streit 2006; Streit et al. 2004). As a result, to emphasize their degenerative cytoplasmic structure, these cells were named 'dystrophic' microglia (Streit et al. 2004). The most pervasive feature of microglial cytoplasmic degeneration is the presence of atypical, tortuous processes, often found in deramified microglia (v Eitzen et al., 1998; Streit et al., 2004a; Wierzba-Bobrowicz et al., 2004). Microglial dystrophy is also manifested by the formation of spheroids (various-sized bulbous formations) on branches, either singly or in succession (beading); by fusion with other microglial cells (clusters), indicative of loss of normal contact inhibition; by fragmentation (cytorrhexis) of processes (i.e., severing of main branches); and by atrophy (i.e., nearly complete loss of cytoplasmic structure). The observation that dystrophic microglia are found scattered randomly in the brain parenchyma, often alongside ramified microglial cells, suggests that they may form a subset of older (senescent) microglia (Streit et al. 2004).

In regards to their incidence, microglial cells exhibiting dystrophic characteristics have been identified in the normal aging brain (Conde and Streit 2006; Flanary et al. 2007; Streit et al. 2004), as well as in several neurological disorders, including Alzheimer's disease (AD) (Ferraro 1931; Streit 2002; Streit et al. 2004), Creutzfeldt-Jakob disease (von Eitzen et al. 1998), Huntington's disease (HD) (Simmons et al. 2007), and schizophrenia (Wierzba-Bobrowicz T et al. 2004). Degenerative changes have also been reported in rat primary microglial cultures exposed to AD-associated amyloid-β deposits (Korotzer et al. 1993), and in murine disease

models of HD (Ma et al. 2003; Simmons et al. 2007) and amyotrophic lateral sclerosis (Fendrick et al. 2007). Recent findings on the characterization of microglial dystrophy in various animal species are summarized in Table 1-2. Given that microglial functioning is highly dependent on their morphological state (Kreutzberg 1996), it is likely that these morphological alterations serve as an impediment to the normal surveillance function of these cells (Davalos et al. 2005; Nimmerjahn et al. 2005), which could lead to deleterious consequences for the CNS as a whole.

Self-Renewable Capacity of Microglia in the Aging Brain

Iron is indispensable for DNA synthesis and therefore it plays a crucial role in cell proliferation rate. As a cofactor of the enzyme ribonucleotide reductase, iron mediates the production of deoxy-ribonucleotides from the corresponding ribonucleotides (the rate-limiting step in the synthesis of DNA precursors and, therefore, a key control point in DNA synthesis) (Hoffbrand et al. 1976). Numerous studies have shown that iron limitation arrests cell proliferation (Le and Richardson 2002). In the aged brain, microglia proliferate more vigorously than in younger brain tissues (Conde and Streit 2005). A plausible explanation for this increased proliferation rate is the age-related increase in microglial intracellular iron levels. The observed increase in microglial proliferation rate likely reflects an imbalance in microglial self-regulatory mechanisms. Inevitably, higher levels of microglial proliferation in the aged brain would result in further propagation of microglial senescence in the affected tissue.

An interesting question is how microglia can reach replicative senescence in the normal aging brain that is devoid of obvious inflammatory/proliferative stimuli such as infection, neurological trauma or extracellular proteinaceous aggregates. Although the underlying mechanisms of microglial proliferation are well-understood in specific injury models (e.g., facial nerve axotomy) and in cell culture systems, little is known about how normal aging may promote

microglial replicative senescence. It is possible, that in addition to stimuli inherent to the CNS, alterations in systemic functioning also play a role in microglial senescence. One such mechanism may be linked to the body's response to stressful events. Microglia express receptors for stress-related hormones (Wang et al. 2002) and respond to physical/emotional stress and related hormones with proliferation (Nair and Bonneau 2006; Wang et al. 2003) and morphological and functional activation (Sugama et al. 2007). Similarly, microglial activation also occurs in response to closed head trauma (Schmidt et al. 2005), systemic infection (Lemstra et al. 2007; Semmler et al. 2005), and even diet (e.g., cholesterol-rich diet) (Crisby et al. 2004; Streit and Sparks 1997). The accumulation of these processes during a lifetime, in addition to age-related changes in neural homeostasis, is likely to lead to senescence of at least a subpopulation of microglial cells.

Microglial senescence was once considered an immaterial process because microglia are self-renewable cells (Lawson et al. 1992). Besides mitosis, microglial replenishment can occur via recruitment of a specific subpopulation of bone marrow-derived cells, which migrate into the neural parenchyma and differentiate into microglia (Mildner et al. 2007). However, the recruitment of microglial myeloid progenitors across the BBB has been shown to decline with age (Simard et al. 2006), albeit the change is not highly substantial. Nonetheless, the mechanisms of microglia replenishment described herein might put a heavy load on a system already compromised by old age. As a result, senescent microglia accumulate in the aged CNS. Higher incidences of senescent microglia may contribute to aging-related neurodegeneration and neurodegenerative diseases by at least two mechanisms: (i) Hyperactivation or hypersensitivity to stimuli and/or misregulation of the activation process, leading to an increased production of toxins, such as reactive oxygen species (ROS); and (ii) Hypoactivation and undernourishment of

neighboring neurons in both the quiescent and disturbed CNS. Either one of these two possibilities would produce a devastating effect on the welfare of neural cells, potentially exacerbating cytotoxic signals already present in the tissue or directly ensuing cellular death.

Brain Iron Metabolism

Iron is an essential nutrient required for the proper functioning of virtually all cells. It is crucial for oxygen transport (function and biosynthesis of hemoglobin), energy production as a cofactor of several enzymes in the mitochondrial electron transport chain, immune function, cellular growth (i.e., RNA and protein synthesis), and proliferation (i.e., DNA synthesis) (Lieu et al. 2001). In the CNS, iron participates in additional roles, including: 1) The synthesis of monoamine (Ramsey et al., 1996; Beard et al., 2003) and GABA (Taneja et al. 1986) neurotransmitters; 2) Normal brain development, specifically in myelin synthesis (Connor et al., 1995), 3) Cognition (Black, 2003); 4) Memory formation, through the development of dendritic spines in the hippocampus (Jorgenson et al., 2003) and many others. These examples highlight the importance of the availability of iron for brain cell viability. However, high levels of free iron in and around cells is very toxic due to its propensity to catalyze the generation of the highly reactive hydroxyl radical ($^{\bullet}OH$), which can lead to lethal consequences by permanently altering the molecular structure of lipids, DNA and proteins (Crichton et al., 2002). Physiologically, iron exists in one of two oxidation states: ferrous (Fe^{2+}) iron or ferric (Fe^{3+}) iron. The generation of $^{\bullet}OH$ occurs via the oxidative conversion of Fe^{2+} to Fe^{3+} in the presence of H_2O_2 by means of the Fenton reaction: $Fe^{2+} + H_2O_2 \rightarrow Fe^{3+} + {}^{\bullet}OH + OH^-$ (Crichton et al., 2002).

The coordinated expression of two types of protein with high affinity (transferrin) and high capacity (ferritin) for iron is largely responsible for the maintenance of adequate levels of intracellular iron (Levenson and Tassabehji, 2004). Apo (iron free)-transferrin is an iron carrier

glycoprotein primarily involved in iron uptake. Each molecule of transferrin (Tf) binds two ferric iron molecules. Iron is taken up by cells primarily after Tf, the principal iron-carrying protein of the plasma, binds to a specific cell surface receptor and the transferrin-receptor complex is internalized (Dautry-Versat et al., 1983). The acidic environment of early endosomes induces a conformational change in Tf resulting in the release of Tf-bound Fe^{3+} (Bali et al. 1991). Subsequently, Fe^{3+} is reduced to Fe^{2+} by a yet unidentified reductase, allowing divalent metal transporter 1 (DMT-1; also known as DCT1 or Nramp2) to transfer Fe^{2+} to the cytosol (Fleming et al. 1998). Apo-Tf and TfR are then recycled to the plasma membrane, where each can undergo further cycles of iron binding and uptake. Once iron enters the cell, any portion in excess (i.e., not needed for immediate use in enzymatic reactions) is stored by ferritin (Ft), a ubiquitous and highly conserved hollow protein shell that constitutes the main intracellular iron storage protein (Torti and Torti 2002). As a consequence of their inherent functional dichotomy, Ft and TfR expression levels are reciprocally related in their responses to changes in iron levels.

Iron-Dependent and –Independent Regulation of Ferritin mRNAs

Ferritin and transferrin receptor levels are primarily regulated by intracellular iron concentrations at the level of translation (Ponka and Lok 1999; Torti and Torti 2002). The nucleotide sequence of both Ft and TfR mRNAs contain a stem-loop structure, termed an iron-response element (IRE), which in the case of Ft mRNA is located in its 5' untranslated region (UTR), while in the TfR mRNA it is located in the 3' UTR. When iron is scarce, the IRE binds a 90-kDa IRE-binding protein (IRE-BP) which has an approximate 30% identical amino acid sequence with the citric acid cycle enzyme aconitase from mitochondria (Kim et al. 1996). In the case of Ft, IRE-BP bound to IRE blocks the initiation of translation of the Ft mRNA, while inducing TfR mRNA stability and translation (Ponka and Lok 1999). When iron levels increase,

the IRE-BP binds iron as a 4Fe-4S cluster. Because the binding sites of iron and RNA overlap considerably, the resulting IRE-BP-iron complex cannot bind RNA. Thus, in condition of iron surplus, ferritin mRNA is released from the IRE-BP cap and translated to produce ferritin, which sequesters the excess iron. On the other hand, TfR mRNA freed from IRE-BP is rapidly degraded (Ponka and Lok 1999).

In addition to iron levels, other factors have been demonstrated to affect cellular ferritin. Of interest to the present investigation are factors produced by microglial cells under activation conditions, including cytokines (Torti et al., 1988; Rogers, 1996) and oxidants (Cairo et al., 1995; Mehlhase et al., 2006). Superoxide in particular has been shown not only to modulate Ft expression but also iron leakage from ferritin (Bolann and Ulvik, 1990; Yoshida et al., 1995). The propensity of labile iron to catalyze the generation of oxygen radicals means that the intracellular concentration and chemical form of the element must be kept under tight control.

Structure and Function of Ferritin

Apo-ferritin is a large (450 kDa) protein located in the cytosol of virtually every cell. It consists of a hollow protein shell composed of 24 functionally distinct heavy (H)-chain and light (L)-chain subunits, which store up to 4500 atoms of iron per molecule of protein (reviewed in Harrison and Arosio, 1996). The H-chain has a metal-binding site associated with its ability to catalyse the oxidation of the highly toxic Fe^{2+} to the less reactive iron form Fe^{3+} (Bakker and Boyer, 1986, (Lawson et al. 1989). This ferroxidase activity occurs only at the H-chain subunit and it is of great importance because although ferritin can only take up iron in the Fe^{2+} form, this is a highly reactive cation and must be quickly converted to Fe^{3+} to prevent any iron-induced toxicity. H-rich ferritins take up iron faster than L-rich in vitro (Lawson et al. 1989; Levi et al., 1988), and are found predominantly in such tissues as heart, kidney and brain (Harrison and

Arosio 1996). The L subunit lacks the ferroxidase site but contains additional glutamate residues on the interior surface of the protein shell which produce a microenvironment that facilitates mineralization of Fe^{3+} for long-term storage (Santambrogio et al., 1996). L-ferritin subunits are mostly found in tissues principally involved in iron storage, such as the liver and spleen (Harrison and Arosio 1996). While ferritin is mainly a cytosolic protein, small amounts are present in the nucleus (Surguladze et al., 2004) and in mitochondria (Corsi et al., 2002) as well as in lysosomes where it is degraded (Sibille et al., 1989).

Since all cells contain ferritins composed of both subunits (even though the H:L ratio is cell- and tissue-specific), iron enters the protein as Fe^{2+} by the action of the H-subunit, but is always stored as Fe^{3+} in the central core via the L-subunit. In order for iron release to occur a reductive conversion back to Fe^{2+} is required (Jones et al., 1978). Iron mobilization happens more quickly in H-rich ferritins, since most Fe^{3+} cations are not mineralized and can be easily recruited and released. This is a defining feature behind the cellular composition of ferritin proteins. In the CNS, H-rich ferritins are mostly present in neurons and oligodendrocytes, which are two cell types with high demand for iron participation in a number of enzymatic reactions. On the other hand, L-rich ferritins are primarily expressed by microglia and oligodendrocytes (Cheepsunthorn et al. 1998; Connor et al. 1994). Because iron is constantly needed for normal myelin production, oligodendrocytes retain a large concentration of iron atoms in both L-rich and H-rich ferritin for their own use. As a consequence, microglia are the principal cells responsible for maintaining adequate iron levels within the CNS (Connor and Menzies 1995).

Microglia and Iron Dyshomeostasis

A common feature of both aging and several of the neurological diseases in which dystrophic microglia are present is iron dyshomeostasis. Iron levels must be tightly regulated to

prevent iron-mediated toxicity. Too little iron impedes the normal functioning of cells, whereas too much iron promotes iron-induced oxidative stress. Iron metabolism is thought to be disregulated with advancing age because iron progressively accumulates in the aged brain (Bartzokis et al. 1997; Benkovic and Connor 1993; Connor et al. 1990; Roskams and Connor 1994), especially in brain regions affected by age-dependent neurodegenerative diseases such as AD, Parkinson's disease (PD), and HD (Bartzokis et al. 1999; Connor et al. 1995; Dexter et al. 1991). This increase in brain iron levels places a large toll on microglia, since prolonged storage of excess iron is performed primarily by microglial cells (Connor et al. 1994; Connor et al. 1990). The combined effects of microglial senescence, in which cellular functions are at suboptimal conditions, and increased intracellular iron levels may predispose microglial cells to degeneration in the aging brain.

Alzheimer's Disease

First described by Alois Alzheimer in 1907, AD is an incurable, late-onset neurodegenerative disorder that primarily affects areas of the brain that are essential for cognitive function. As the disease progresses, other brain regions are affected as well. The loss of memory, judgment and emotional stability that AD inflicts on its victims occurs gradually and inevitably, usually leading to death in a severely debilitated, immobile state between four and twelve years after onset. No treatment that retards the progression of the disease is known. AD affects approximately 20 million people worldwide, making it the leading cause of dementia in the elderly (Cummings and Cole 2002). As more people survive to the seventh, eighth, and ninth decades, AD is rapidly becoming an urgent public health problem. The clinical diagnosis of probable AD is based on family history, physical examination, neuropsychological testing, laboratory studies and neuroimaging techniques. However, there is no specific laboratory marker

to support the definite diagnosis of AD or for monitoring the progression of the disease. A postmortem histological examination is often required for confirmation of its clinical diagnosis. This is because AD is defined pathologically by specific abnormally folded proteins that aggregate extracellularly in senile plaques and as neurofibrillary tangles within affected neurons.

In AD, acetylcholine-releasing neurons, whose cell bodies lie in the basal forebrain, primarily (and selectively) degenerate. These cholinergic neurons provide widespread innervation of the cerebral cortex and related structures and play an important role in cognitive functions, especially memory. Stereological and biochemical analyses have recently shown, however, that the loss of synaptic density correlates better with cognitive decline than either the decrease in neuronal cell numbers or the accumulation of plaques and tangles (DeKosky and Scheff 1990; Masliah et al. 1989). Despite rigorous efforts to understand the pathogenesis of AD, its etiology remains unknown. Most cases of AD occur sporadically, that is, without any known familial predisposition.

Pathology

Histopathologically, AD is characterized by a generalized atrophy of the cerebral cortex and the widespread appearance of senile plaques (SP) and neurofibrillary tangles (NFT). Extracellular SPs contain a core of beta-amyloid peptide (Aβ), which is derived from the proteolytic processing of the amyloid-β precursor protein (APP). When this proteolytic cleavage occurs by the actions of both β- and γ-secretases, a soluble Aβ peptide with a length between 39-42 amino acids is generated, with $A\beta_{40}$ being the most common isoform. The newly generated Aβ peptide forms an α-helix structure and remains mostly soluble. For yet poorly understood reasons, in AD the multimeric γ-secretase complex cleaves APP preferentially at residue 42 instead of 40. The resulting $A\beta_{42}$ is highly susceptible to conformational changes leading to

aggregation into fibrils with an insoluble β-pleated sheet. Once Aβ forms a β-pleated structure it becomes resistant to degradation resulting in permanent extracellular deposition in the brain parenchyma as the main constituent of senile plaques. Similar to Aβ fibrils, NFTs are composed of misfolded proteins. NFts, however, aggregrate within the cell bodies of selectively vulnerable neurons as insoluble paired helical filaments containing hyperphosphorylated microtubule-associated tau protein.

Although these pathological lesions constitute the histological hallmarks of the AD brain they can also be found in nondemented elderly people (Arriagada et al. 1992). Thus, for the most part, the distinction between normal brain aging and AD is quantitative rather than qualitative. Usually patients with progressive dementia of the Alzheimer type have moderately or markedly more mature SPs and NFTs than age-matched nondemented people do. However, the principal difference between demented AD patients and nondemented elderly people lies in the prevalence and distribution pattern of NFTs and SPs (Thal et al. 2006).

In cognitively normal individuals, SPs are usually restricted to the cerebral cortex, the basal ganglia, the thalamus and hypothalamus, while in AD patients SPs are found not only in those areas but also in the midbrain, brain stem and cerebellum (Thal et al. 2006). Likewise, NFT pathology is only seen in the primary and secondary neocortical areas in AD patients (Braak and Braak 1991). The progressive incursion of anatomical regions by AD-related pathologies facilitated the establishment of histological staging systems for the NFT (Braak Stages I-VI) and SP (Stages 1-5) pathological expansion throughout the neuropil (Table 1-3) (Braak and Braak 1991; Thal et al. 2006). Progression through these stages also symbolizes the increase in the severity of cortical destruction. Of note, at early (clinically silent) stages, plaques first accumulate in the neocortex, while tangles concentrate in the hippocampus. Only at late stages of

the disease the two pathologies become interactive. Taken together, these findings indicate that although these plaques and tangles are also present in normal aging brain, they are far less severe and less prevalent than in AD.

Classification of Senile Plaques

The senile plaque is a complex, slowly evolving structure and the time required to generate fully formed, "mature" plaques may be years or even decades. For unknown reasons, this maturation seems to occur much more commonly in the symptom-producing cerebral cortex than in, for example, the symptom-free cerebellum. SPs can be classified into two representative subtypes (diffuse and neuritic) based primarily on morphological and histological characteristics as illustrated in Figure 1-5 (Oide et al. 2006). Amorphous, nonfilamentous deposits of Aβ protein that are sharply delineated are called 'diffuse' plaques. Significantly, most diffuse Aβ protein deposits contain few or no degenerating neurites or reactive glial cells. The presence of degenerating neuronal processes and reactive astrocytes and microglia within and around the plaque is often associated with the presence of a homogeneous appearing, darkly stained central core of Aβ protein and plaques containing such are called dense core plaques. Dense core plaques are also called 'neuritic' plaques. In the late 1990s several investigators noticed that diffuse plaques are actually much more abundant than the classic neuritic plaques (Yamaguchi et al. 1988), occurring in a variety of degenerative and non-degenerative conditions, while neuritic plaques are particularly likely to exist in persons with AD (Thal et al. 2006). Electron microscopic examinations have revealed that much of the tissue in the vicinity of the diffuse plaque is indistinguishable from surrounding normal brain tissue, suggesting a potential innocuous effect at this stage of the disease (Yamaguchi et al. 1988).

Dystrophic Microglia and AD Pathogenesis

Although the pathogenesis of AD is not yet understood, several risk factors have been associated with the development of the disease. Age is the strongest known risk factor. Most AD patients are 65 or older and according to the National Institute on Aging the number of patients approximately doubles every 5 years after age 65. Despite the apparent contribution to AD development, the exact mechanisms by which aging contributes to neuronal degeneration remain unresolved. To date several changes in brain homeostasis have been linked to the aging process, a large number of which is linked to microglial cell functioning, including an increase in oxidative stress markers, the accumulation of iron deposits within the brain parenchyma, and an apparent age-related increase in microglial activation.

It is possible that among the various factors that are involved in AD pathogenesis, a loss of normal function by senescent dystrophic microglia, leading for example to an iron metabolic malfunction and/or a loss of neuronal trophic support, over an extended period of time may play a contributory or acceleratory role. This notion, which is based in the microglial dysfunction hypothesis originally proposed by Streit (2002), highlights the significance of microglial functioning for the maintenance of neuronal cell viability. Since increasing evidence implicates a role of iron in many neurodegenerative disorders (Dexter et al. 1991; Hallgren and Sourander 1958; Qian and Wang 1998), the study of ferritin-containing microglia in the aged and AD brain can provide important clues about the changes that may lead to iron imbalance in the brain and possibly a model for therapeutic intervention in case of iron storage dysfunction.

Facial Nerve Axotomy Paradigm

The cell bodies of facial motoneurons (FMN) are located in the brainstem but axons are projected out of the CNS through the ipsilateral facial nerve (FN) to innervate the musculature of

the face (Fig. 1-2). Corollary to this anatomical structure, the axotomy of the rat FN offers a reliable and useful model in which to study the underlying principles of microglial activation *in vivo* as well as microglial responses to neurodegeneration and regeneration. In this model, the FN can be transected, resected or crushed near its exit from the skull at the stylomastoid foramen resulting in retrograde, non-lethal injury of cell bodies in the facial motor nucleus (FNu), which can then be microdissected and processed for histological examination. The advantages of the FN axotomy paradigm over other *in vivo* and *in vitro* models is sevenfold: 1) Remote lesion (responses not due to surgery itself); 2) BBB remains intact (no influx of peripheral macrophages that could confound the results); 3) High reproducibility; 4) Endogenous transient glial responses (as opposed to persistent glial activation in *in vitro* models); 5) Neuronal regeneration (mild severity); 6) Neuron-glia interactions (intrinsic microenvironment of the brain is maintained); and 7) Analytical strength (contralateral, unlesioned side serves as an internal control) (reviewed in Moran and Graeber, 2004). This type of lesion is reversible and does not lead to neurodegeneration, resulting primarily in a transient and graded activation of microglial cells in the vicinity of injured cell bodies (Moran and Graeber 2004; Streit 2000).

Microglial Response to Facial Nerve Axotomy

The microglial response to FN axotomy proceeds though a series of graduated steps, commencing within 24 hours post-injury with hypertrophy of processes resulting in a 'bushy' appearance and an increase in the expression of the immune markers, such as type 3 complement receptors (CR3) and major histocompatibility complex (MHC) antigens (Graeber et al., 1988: Streit et al., 1989; Raivich et al. 1999). At this stage microglia are activated and approximately 2-3 days post-axotomy they start to proliferate forming a sheath around the injured neuronal cell bodies (Fig. 1-3), and their numbers reach maximal levels after 4-7 days (Graeber et al., 1988b).

Activated microglia also begin stripping the injured neuron of synaptic terminals (Blinzinger and Kreutzberg 1968). Once the stimulus has dissipated, microglial cell numbers return to pre-injury levels by programmed cell death mechanisms (Gehrmann and Banati, 1995; Jones et al., 1997). Complete regeneration of motoneurons is dependent on the severity of the lesion, requiring for instance approximately 2 weeks in the mildest (crush) lesions (Moran and Graeber, 2004). The purpose of using the axotomy model in this investigation was two-fold: 1) To determine whether microglial activation by an acute injury (ie, FN axotomy) induces microglial ferritin expression; and 2) To determine whether the appearance of dystrophic microglia is increased after acute microglial activation in aged animals.

Project

This thesis had two main objectives: 1) To elucidate the morphological similarities and differences between senescent microglia in human and rodent brains; and 2) To determine whether long-term iron storage function via expression of L-rich ferritin proteins can be associated with microglial dystrophy, possibly by increasing their vulnerability to iron-catalyzed oxidative stress reactions. In addition, we also wanted to assess the contribution of disease and injury conditions to indices of microglial cytoplasmic degeneration in aged brains. Our findings support a possible connection between microglial cytoplasmic deterioration and impaired glial neuroprotection. We propose that a loss of microglial neuroprotective function by dystrophic microglia may contribute to the neuronal dysfunction and/or death that characterize neurodegenerative diseases, such as Alzheimer's disease.

Table 1-1. Age-related changes in microglial metabolic activity

CHANGES IN PROTEOLYTIC ACTIVITY	REFERENCE
▪ Impaired protein turnover	(Stolzing and Grune 2003)
▪ Decline in proteasomal function	(Stolzing and Grune 2003; Stolzing et al. 2002)
▪ Decreased protein synthesis	(Stolzing and Grune 2003)
▪ Decreased degradation of proteins from apoptotic vesicles	(Stolzing et al. 2006)
▪ Accumulation of lipofuscin granules	(Sierra et al. 2007; Xu et al. 2008)
▪ Increase of inclusions, vacuoles, and granularity	(Peinado et al. 1998; Sierra et al. 2007)
CHANGES IN CELL SURFACE MOLECULE EXPRESSION	
▪ Increase in MHC class II antigen expression	(McGeer et al. 1987; Sheffield and Berman 1998)
▪ Increase in CD40, CD45, and CD86 expression	(Stolzing and Grune 2003)
CHANGES IN CYTOKINE PRODUCTION	
▪ Increased production of IL-6, TNF-α, and IFN-γ	(Stolzing et al. 2006; Ye and Johnson 1999)
▪ Increased production of TNF-α, IL-1β, IL-6, IL-10, and TGF-β1 mRNA expression	(Buckwalter and Wyss-Coray 2004; Sierra et al. 2007)
▪ Decreased production of IL-12	(Stolzing et al. 2006)
CHANGES IN ROS PRODUCTION	
▪ Higher basal nitric oxide release	(Stolzing and Grune 2003)
▪ Higher production of ROS	(Heppner et al. 1998; Stolzing et al. 2006)
▪ Diminished capacity to evoke oxidative burst	(Stolzing and Grune 2003; Stolzing et al. 2006)
CHANGES IN ACTIVATION DYNAMICS	
▪ Ostensibly continuous activation	(Dipatre and Gelmann 1997; Overmyer et al. 1999; Rozovsky et al. 1998; Sloane et al. 1999)
▪ Increased release of inflammatory mediators	(Bodles and Barger 2004; Godbout et al. 2005; Sierra et al. 2007)
▪ Insufficient de-activation by astrocytes	(Stolzing et al. 2005)

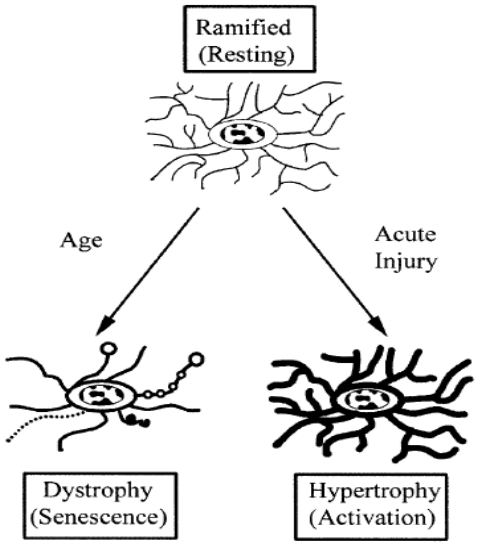

Figure 1-1. Schematic representation of transformation of ramified microglia into hypertrophic and dystrophic forms. Microglia become hypertrophic when activated by CNS injury, resulting in the formation of greatly enlarged cytoplasmic processes. With aging, microglia develop dystrophic cytoplasmic processes characterized by slight enlargement, distinct loss of fine branches (deramification), formation of cytoplasmic spheroids, gnarling, beading, and fragmentation. It is rare to see all of these dystrophic changes occurring in a single cell; instead, most dystrophic microglia display just one or two of these characteristics. (Streit et al., 2004)

Table 1-2. Microglial degeneration in the literature

Species	Method	Classification	Characteristics of degenerating cells	Ref.
Human	IHC	Aging	Deramification, cytorrhexis	(Streit et al. 2004)
		AD	Deramification, bulbous swellings, cell clusters, cytorrhexis	(Ferraro 1931; Streit 2002; Streit 2004)
		AD, HPC	Atrophy, bulbous swellings, cytorrhexis	(Flanary et al. 2007)
		Schizophrenia	Deramification, atrophy, cytorrhexis	(Wierzba-Bobrowicz T et al. 2004; Wierzba-Bobrowicz et al. 2005)
		HD	Tortuous processes, cytorrhexis	(Simmons et al. 2007)
Rat	IHC	$SOD1^{G93A}$	Deramification, cytorrhexis	(Fendrick et al. 2007)
	Cell Culture	Aβ- exposed	Atrophy, beaded processes, cytorrhexis	(Korotzer et al. 1993)
Mouse	IHC	R6/2 model of HD	Deramification, bulbous swellings, cytorrhexis	(Ma et al. 2003; Simmons et al. 2007)

IHC, immunohistochemistry; AD, Alzheimer's disease; HPC, High amyloid plaque pathology control; HD, Huntington's disease

Table 1-3. Alzheimer's disease-related pathological hallmarks develop in a hierarchical manner

Stage	Senile Plaque Pathology	Neurofibrillary Tangle Pathology
I	• Neocortex	• Transentorrhinal region
II	• Allocortical Areas – entorrhinal cortex – subiculum/CA1 region	• Entorrhinal Cortex • Ammon's Horn
III	• Basal Ganglia • Thalamus • Hypothalamus	• Hippocampal Formation
IV	• Midbrain • Medulla Oblongata	• Inferior Temporal Cortex
V	• Pons • Cerebellum	• Neocortex Association Areas – Frontal – Parietal – Occipital
VI		• Occipital Lobe

Senile Plaque Pathology: stages 1-3= preclinical stages; 4-5= clinical stages. Neurofibrillary Tangle Pathology: Braak stages I-II (clinically silent); III-IV= (incipient AD); V-VI= (fully developed AD). Braak Stages V-VI are conventionally used as criteria for neuropathologic confirmation of the clinical diagnosis of AD. (Based on Thal et al., 2006; Braak and Braak, 1991).

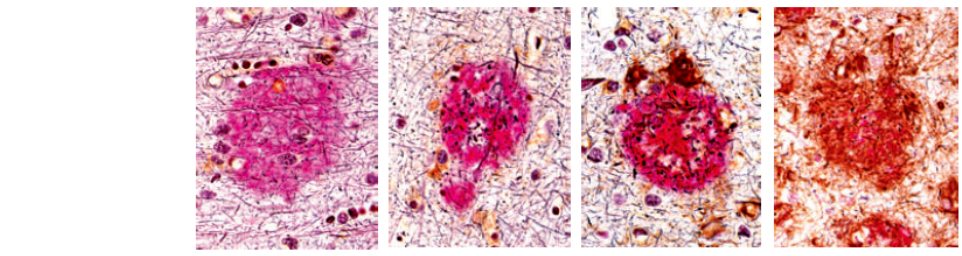

Senile plaque subtypes	*Diffuse plaque*	*Neuritic plaque*		
		Primitive plaque	*Classical plaque*	*Remnant plaque*
Senile plaque components				
Amyloid deposits	Diffuse	Fibrillar	Dense-cored	Ragged, debris-like
Dystrophic neurites	Absent – scarce	Few – many	Many	Few
Astrocytic participation	Absent – scarce	Absent – few in marginal zone	Few in marginal zone	Intense, entire plaque portion
Histological profiles				
H&E	Unrecognizable	Unrecognizable	Recognizable due to amyloid core	Recognizable due to glial fibrils
Bodian	Unrecognizable	Recognizable	Recognizable	Less recognizable
Congo red	Unrecognizable	Barely recognizable	Recognizable	Barely recognizable
Holzer	Unrecognizable	Unrecognizable	Barely recognizable	Recognizable
Aβ immunoreactivity	Weak, diffuse	Intense, fibrillar	Intense, cored	Weak, ragged
GFAP immunoreactivity	Absent	Absent – weak	Moderate	Intense

Aβ, amyloid β-protein; GFAP, glial fibrillary acidic protein; H&E, haematoxylin and eosin.

Figure 1-2. Classification of senile plaques based on Bodian, Aβ and GFAP triple staining. (Oide et al., 2006)

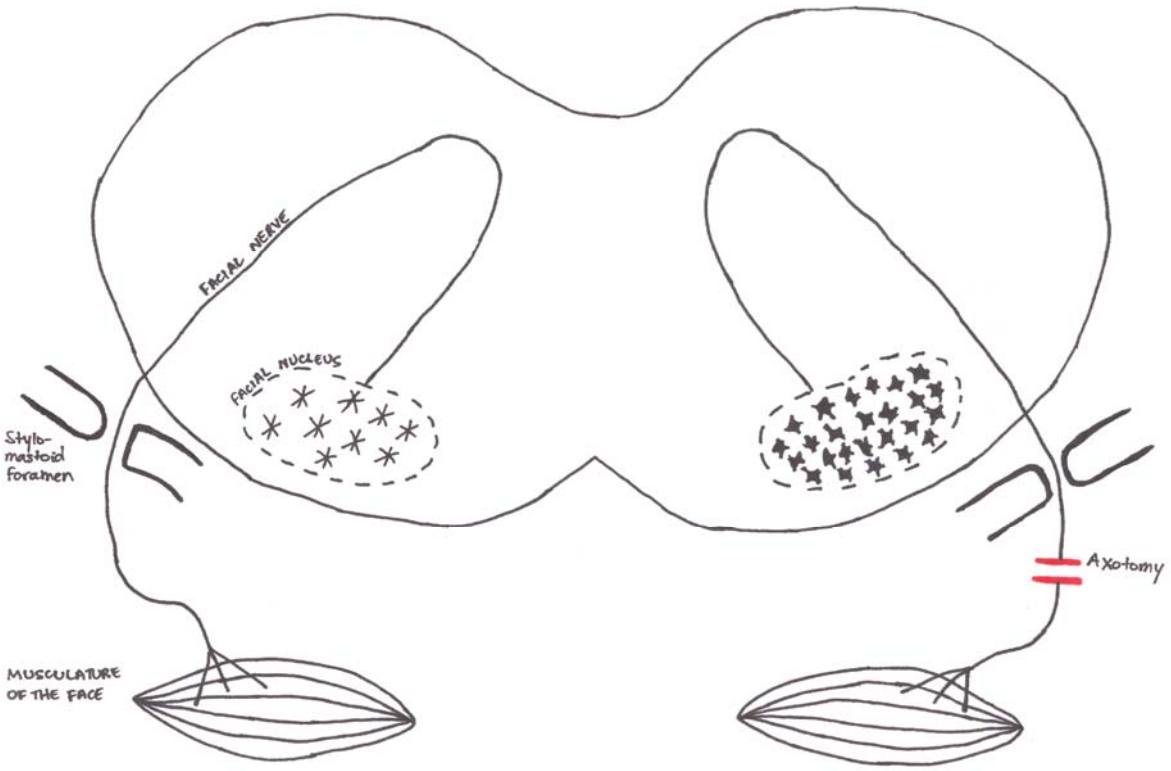

Figure 1-3. Schematic diagram of the facial nerve axotomy model. The facial nerve nuclei containing motoneuron cell bodies are located on either side of the ventral region of the brain stem (dotted-line area). The motoneuron axons loop around the genu of the abducens nucleus in the dorsal region of the brainstem and exit the skull at the stylomastoid foramen to innervate the musculature of the face. In the axotomy procedure, the facial nerve is either crushed or transected after its exit from the skull, inducing a reaction that is propagaded retrogradely to the motoneuron cell bodies. Signals released from the injured neurons activate microglial cells locally, resulting in proliferation as well as morphological (hypertrophy) and immunophenotypic alterations in parenchymal microglia within the ipsilateral facial nucleus.

CHAPTER 2
MATERIALS AND METHODS

Supplier Information

Adobe Photoshop (San Jose, CA), Assay Designs (Ann Arbor, MI), Calbiochem (Gibbstown, NJ), DAKO (Carpinteria, CA), Chemicon (Temecula, CA), Fisher Scientific (Pittsburg, PA), Media Cybernatics (Silver Spring, MD), Molecular Probes (Eugene, OR), MP Biomedicals (Santa Ana, CA), Promega (Madison, WI), SAS Institute Inc. (Cary, NC), Serotec (Raleigh, NC), Sigma Aldrich (St. Louis, MO), Spot Diagnostic Instruments (Sterling Heights, MI), Vector Labs (Burlingame, CA), Wako Chemicals (Richmond, VA).

Tissue Specimens

Human brain specimens were obtained from the Sun Health Research Center (SHRC) Brain Bank, Sun City, Arizona. Brain tissues were obtained at autopsy from 24 subjects aged 34-97 years. Subject groups were classified based on clinical history and neuropathological findings as follows: 1- Younger (mean age 36.66 ± 2.08 years), nondemented individuals (Y) free of amyloid-β immunoreactivity; 2- Aged (mean age 79.86 ± 8.05 years), nondemented and amyloid-free individuals (ND); 3- Aged (mean age 83.43 ± 5.19 years), non-demented individuals with high amyloid-β burden, designated as high pathology controls (HPC); and 4- Demented individuals (mean age 80.29 ± 11.64 years) that met the clinicopathological criteria of AD, including high amyloid load. There was no significant difference in age between the AD and the elderly nondemented control groups ($P > 0.5$). The postmortem intervals (PMI) between death and tissue retrieval ranged from 1.5 to 4.83 hours. Age at death, gender, and PMI are shown in Table 2-1.

In order to study the potential relevance of postmortem autolysis to microglial degeneration, nine additional brain tissue samples were obtained from the Kentucky Medical Examiner's Office. These specimens ranged in PMI from 3 to 20 hrs as summarized in Table 2-2. For the FN axotomy study, young adult (3 months; n= 15) and old (30 months; n=15) male Fisher 344-Brown Norway F1 hybrid rats obtained from the National Institute on Aging were used.

Antibody List

The list of primary antibodies used in this study can be found on Table 2-3, along with specificity of the antibody, dilution used, application and source. The following secondary antibodies were used: Biotinylated anti-rabbit and anti-mouse raised in goat (1:500; Vector Labs); Alexa Fluor-488 and -568 goat anti-mouse (1:500; Molecular Probes); and Alexa Fluor 488 and -568 goat anti-rabbit (1:500; Molecular Probes).

Methods

Facial Nerve Axotomy

Experiments were done in accordance with the regulations of the University of Florida Institutional Animal Care & Use Committee (IACUC). Under isofluorane anesthesia, the right facial nerve of both groups of rats was exposed near its exit from the stylomastoid foramen and crushed with a fine pair of hemostats for 10s. Animals were euthanized at 1, 3, 7, 10, and 14 days postaxotomy (n=3 for each time point) by an overdose of pentobarbital and perfused with 4% paraformaldehyde (PFA). The brains were removed, postfixed for 24hr in 4% PFA, and cryoprotected by infiltration with 30% sucrose overnight.

Tissue Sectioning and Storage

After fixation in 4% PFA for 48 hours at 4ºC, human brain samples were sectioned at the SHRC in the coronal plane in a vibratome at 50µm prior to shipment to the University of Florida and stored in 30% glycol solution until use. The brain areas represented in this study are the superior frontal gyrus, the superior, middle and inferior temporal gyri, the hippocampus and amygdala. From the 50µm free-floating tissue samples obtained, equivalent regions of gyri, hippocampi or amygdala were cut from adjacent sections using a razor blade and rinsed with PBS. For the PMI study, serial 50µm-thick sections were cut from formalin (10%)-fixed, tissue blocks of temporal and frontal cortices in a vibratome and rinsed with PBS.

For the rat axotomy study, brainstem sections containing both right (axotomized) and left (control) sides of the rat FNu were serially cut either on a vibratome at 50µm for free floating sections or on a cryostat into 20µm coronal sections., in which case the sections were immediately mounted onto SuperFrost Plus slides (Fisher Scientific).

Single Label Immunohistochemistry

After inhibition of endogenous peroxidase with 3% H_2O_2 for 5 min, rat and human free-floating sections were incubated for 2 hr in blocking buffer composed of 10% normal goat serum (NGS) diluted in PBS, pH 7.4. The sections were then incubated overnight at 4°C with an antiserum to rabbit anti-horse spleen (L) ferritin (Sigma) diluted 1:500 in PBS containing 5% NGS. In the case of human samples, adjacent tissue sections were also stained with a mouse monoclonal antibody (mAb) against human HLA-DR (LN-3; MP Biomedicals; 1:500). On the following day, the sections were incubated for 1 hr with biotinylated secondary antibodies raised in goat (anti-mouse or anti-rabbit) diluted 1:500 in 5% NGS/PBS solution. Next, the sections were incubated for 45 min with horseradish peroxidase (HRP)-avidin D (Vector Labs) diluted at

1:500 in PBS. Between each step, the sections were rinsed three times in PBS for 5 min. Following peroxidase development with 0.05% 3,3'-diaminobenzidine tetrahydrochloride (DAB; Sigma) and 0.01% H_2O_2 for 1-15 min, the sections were rinsed in PBS, mounted on subbed slides and air dried. The sections were then dehydrated through ascending series of ethanol and coverslipped out of xylene with Permount (Fisher Scientific). In the human study, a few sections were also processed for double staining immunohistochemistry. As a negative control, omission of either the primary or secondary antibodies yielded no immunoreactivity. Selected sections were counterstained with either hematoxylin or cresyl violet, dehydrated through ascending alcohols, cleared in xylenes, and coverslipped with Permount.

Double Label Immunohistochemistry

In double staining experiments on human brain specimens, after development with DAB/H_2O_2 stained sections were incubated overnight at 4°C with mouse anti-human β-amyloid clone 6F3D (6F3D; Dako; 1:100) in 5% NGS in PBS. 6F3D is a monoclonal antibody reactive to amino acid residue 8-17 of the human β-amyloid peptide. Some sections labeled first with LN-3 were also processed for double immunohistochemistry using Ferritin as a primary antibody in the second reaction. After the same sequences of washes as for the first label, the antigen was visualized by incubating biotinylated anti-mouse or anti-rabbit secondary antibodies (1:500; 1h at RT) followed by a 45 min incubation with HRP-avidin D diluted 1:500 in PBS. The color reaction product for Aβ was developed using a PBS solution containing 0.05% DAB, 0.01% H_2O_2 and 1% cobalt chloride as the chromogenic substrate for horseradish peroxidase. This substrate produced a dark black color which could be differentiated from the brown color obtained after staining with the first primary antibody. These double labeled sections were then

mounted, dehydrated and coverslipped as described for the single label procedure. In all cases, elimination of either primary or secondary antibodies yielded no immunoreactivity.

Immunofluorescence

Human samples

Free-floating, adjacent tissue sections from the superior frontal gyri of all groups examined were pre-treated with 0.5% Triton-X in PBS for 15 min followed by 30 min incubation with 0.3% Triton-X/10% NGS blocking solution. The sections were then incubated overnight at 4ºC with both LN-3 and Ferritin antibodies at the same concentrations listed above in 0.3% Triton-X/3% NGS/PBS. Next, the sections were rinsed in PBS and incubated for 1 hr at 37ºC with goat anti-rabbit IgG conjugated to Alexa Fluor 568 and goat anti-mouse IgG conjugated to Alexa Fluor 488 diluted 1:500 in 0.3% Triton-X/3% NGS/PBS. After another series of PBS rinses, the sections were immersed in 70% ethanol for 5 min, followed by a 3 min treatment with Autofluorescence Eliminator Reagent (Chemicon). This fluorescence immunohistochemistry counterstain reduces the intensity of the autofluorescent pigment lipofuscin which accumulates in the cytoplasm of post-mitotic cells with increasing age. Next, the sections were rinsed with 70% ethanol, mounted onto slides and coverslipped with Vectashield anti-fading mounting media (Vector Labs). Fluorescent images of tissue sections were obtained using a Zeiss Axioskop-2 Plus fluorescent microscope and photomicrographs were adjusted for contrast and brightness using Adobe Photoshop C2S.

Rat samples

Frozen sections at the level of the brainstem containing both axotomized and uninjured FNu of young and old rats were processed for double-label immunofluorescence. These sections

were pretreated with 10% NGS/0.3% Triton-X-100 in PBS for 1 hr at 37ºC, followed by overnight incubation at 4ºC in a primary antibody cocktail diluted in 5% NGS/0.1% Triton-X-100 in PBS. The following primary antibody combinations were used: 1) anti-ferritin (1:1000) plus the microglial marker OX-42 (Serotec; 1:500); and 2) the macrophage marker ED1 (Dako; 1:300), plus a microglial marker against ionized calcium binding adaptor molecule 1 (Iba-1; Wako Chemicals; 1:500). Following several PBS washes, the sections were incubated at room temperature for 2 hr with corresponding Alexa-Fluor 568 and Alexa-Fluor 488 IgGs each diluted 1:500 in the same buffer solution as for the primary antibodies. Next, the sections were washed again in PBS, coverslipped using anti-fading Vectashield mounting media with DAPI (Vector Labs) and photographed with a Zeiss Axioskop 2 Plus microscope equipped with an RT Color Spot camera model 2.2.1 (Spot Diagnostic Instruments). For all staining procedures, omission of primary antibodies resulted in the absence of immunoreactivity and served as negative controls.

Morphometric Analyses and Cell Quantification

Human Study

The quantitative evaluation of microglial cells immunolabelled with either anti-HLA-DR or anti-ferritin was performed in all 24 cases on adjacent sections by randomly sampling 10 microscopic fields of gray matter, each measuring 0.3×0.225 mm^2. Digital images of fields were acquired through a 20x objective lens with a Zeiss Axioskop 2 Plus microscope using a Spot RT Color CCD camera and Spot RT software (Spot Diagnostic Instruments). Image Pro Plus v.4.6 image analysis software (Media Cybernetics) was used to manually calculate the instances (i.e., number of cells per microscopic field) of microglial cells stained with either marker as well as the instances of immunoreactive dystrophic microglia. Only microglia with a clearly visible cell body were counted.

Incidences of microglial structural abnormalities were evaluated based of a set of predefined criteria (Streit 2006; Streit et al. 2004), including deramification and tortuosity of processes, cluster formation, processes containing small but conspicuous spheroid-like structures, and cytorrhexis. Figure 3-2 shows representative sections used for quantitative analysis of each of the four cohorts in this study. The photomicrographs presented were taken using a higher magnification lens (40x) for better visualization of the microglial cytoplasmic structure. All cell counts and morphometric analyses were performed without knowledge of the case number by coding the specimens.

Rat Axotomy Study

The quantitative evaluation of lipofuscin (LF)-containing microglial cells was performed 'blind' on coded slides using a 40x objective lens. Six adjacent FNu sections per animal at each time point postaxotomy were selected and ten microscopic fields per section, each measuring 200 x 400 μm^2, were randomly sampled within both control and axotomized sides of the FNu. Because LF residues also accumulate in other neural cells, ImagePro Plus v.4.6 analysis software (Media Cybernetics) was used to manually calculate the instances of LF-positive microglia in Iba-1/ED1 double labeled sections by merging digital photographs of fluorescent material using ultraviolet, blue, and green excitation lights (360-460, 440-490, and 490-570 nm, respectively). Only immunoreactive microglial cells with a clearly visible cell body and a DAPI-positive nucleus were counted in order to carry out a consistent semi-quantitative evaluation of the number of cells stained between and within groups.

Statistical Analyses

Data were expressed as the mean ± standard error of the mean. In the human study, differences among groups were determined by one-way ANOVA followed by Bonferroni's *t* test

for multiple comparisons. All data were analyzed using the software program SAS 9.1 (SAS Institute Inc.). For the rat axotomy study, statistical significance among the means was determined using the paired Student's t test also using the SAS 9.1 program. In all instances, *P* values less than 0.05 were considered statistically significant.

TABLE 2-1. Clinical and pathological features of human cases

Case ID	Age	Gender	PMI (h)	Group
Younger controls (n=3)				
1	34	F	3	Y
2	37	M	3.25	Y
3	38	M	2.25	Y
Average	36.33		2.83	
S.D.	2.08		0.52	
Non-demented aged controls (n=7)				
4	69	M	2.16	ND
5	73	M	2.25	ND
6	74	M	2	ND
7	81	M	2.75	ND
8	85	M	3.16	ND
9	86	F	2.5	ND
10	91	M	2.5	ND
Average	79.86		2.53	
S.D.	8.05		0.41	
Non-demented high plaque pathology controls (n=7)				
11	77	F	3.25	HPC
12	78	M	2.25	HPC
13	82	M	3	HPC
14	83	F	4.83	HPC
15	84	M	3	HPC
16	89	M	1.5	HPC
17	91	M	2.5	HPC
Average	83.43		2.90	
S.D.	5.19		0.98	
Demented high plaque pathology cases (n=7)				
18	60	M	3.33	AD
19	73	F	2	AD
20	79	M	2	AD
21	81	M	3	AD
22	85	F	1.66	AD
23	87	M	2.41	AD
24	97	F	1.5	AD
Average	80.29		2.27	
S.D.	11.64		0.82	

Y, younger controls; ND, non-demented aged controls; HPC, aged, non-demented high plaque pathology controls; AD, sporadic, Alzheimer's disease cases

TABLE 2-2. Profile of postmortem interval (PMI) cases

Case ID	PMI (h)	Expired Age (y)	Gender
1	3	40	M
2	4	57	M
3	8	60	M
4	9	47	M
5	11	57	M
6	12	15	F
7	14	54	M
8	17.5	19	M
9	20	43	M

Table 2-3. Source, species reactivity, cell specificity and dilution of primary antibodies

Antigen (Ab name)	Reactivity	Specificity	Antibody/ dilution	Source
L-Ferritin	Human/rodent	microglia/oligodendrocytes	Rabbit pAb/ 1:1000	Sigma
HLA-DR (LN-3)	Human	microglia	Mouse mAb/ 1:500	MP Biomedicals
Iba-1	Rodent	microglia	Rabbit pAb/ 1:500	Wako Chemicals
CR3 (OX-42)	Rodent	microglia	Mouse mAb/ 1:500	Serotec
CD-68 (ED-1)	Human/rodent	macrophages	Mouse pAb/ 1:300	Dako
Myelin CNPase	Human/rodent	oligodendrocytes	Mouse mAbl/ 1:500	Calbiochem
6F3D	Human/rodent	β-amyloid peptide	Mouse mAb/ 1:100	Dako

Ab, Antibody; CR3, complement receptor type 3; HLA-DR, human leukocyte antigen D-related; mAb, mouse monoclonal antibody; pAb, polyclonal antibody;

CHAPTER 3
RESULTS

Morphological Analyses of Senescent Microglia in the Human Brain under Conditions of Normal Aging and Neurodegenerative Disease

Ferritin-Positive Microglia Exhibit Abnormal Morphological Features

The ferritin antibody used in this thesis specifically labels the light (L)-chain subunit of ferritin proteins (Kaneko et al. 1989), therefore both microglia and oligodendrocytes could be resolved by light microscopy. Both cell types were promptly distinguished from one another based on morphological characteristics. Identification and distribution of microglia was confirmed by using LN-3, an antibody specific for human leukocyte antigen (HLA-DR) expressed by microglia in both normal and pathological human brain (Miles and Chou 1988). Ft-positive cells exhibiting a dense perinuclear staining, a large rounded nucleus and a lack of processes (Fig. 3-1A) fitted the morphological criteria of oligodendrocytes, which was verified by immunostaining for CNPase, a protein expressed exclusively by oligodendrocytes in the CNS (Fig. 3-1D). Other Ft-positive cells, however, presented a highly branched morphology with small, rounded and/or irregularly-shaped nuclei (Fig. 3-1C), all of which are hallmark features of microglial cells as evidenced by immunoreactivity for HLA-DR antigens (Fig. 3-1F). Based on these morphological characteristics Ft-positive oligodendrocytes could be readily distinguished from Ft-positive microglia (Fig. 1B, 1E). For the purposes of the present study, analysis of ferritin expression was limited to microglial cells.

Figure 3-2 shows typical staining patterns of microglial cells labeled with either LN-3 or Ferritin antibodies in adjacent tissue sections. In all groups examined, microglia immunoreactive for HLA-DR exhibited the typical branched morphology of ramified microglia with small cell bodies, multiple long proximal branches extending in all directions, and extensive ramification of

the distal processes (Fig. 3-2A, -2C, -2E, -2G). Ferritin-positive microglia in the younger control group appeared less ramified, but still maintained mostly a branched morphology (Fig. 3-2B). In contrast, the majority of ferritin-positive microglia in aged groups (ND, HPC, and AD) exhibited aberrant cytoplasmic structures indicative of dystrophy (Fig. 3-2D, -2F, -2H), which suggests an age-related component.

Morphological Characteristics of Dystrophic Microglia

In all groups examined, the majority of HLA-DR immunoreactive (IR) microglia exhibited a ramified morphology (Table 3-1). In sharp contrast, most Ft-positive microglial cells exhibited dystrophic changes, including deramification of processes, which produced unilateral ramification patterns and long, single processes devoid of distal branches. Any remaining fine processes on dystrophic microglia were often unusually tortuous and coiled (Table 3-1).

In many instances, Ft-positive microglial cells appeared in clusters of two or more cells, suggesting that dystrophic cells had lost contact inhibition that normally keeps microglia apart. Another defining characteristic of Ft-positive, dystrophic microglia was the formation of spheroid-like structures occurring either singly or in succession to produce beading. These changes often coincided with atrophy of processes. A cardinal feature of microglial dystrophy was cytorrhexis, in which cytoplasmic processes were broken up into two or more parts. These defining dystrophic morphological characteristics are depicted in Table 3-1, along with their frequency in the various cohorts examined in this study. What appears to be the most severe form of cytoplasmic deterioration, cytorrhexis, was most widespread in AD tissues than in aged-matched controls, while in younger brains, no examples of microglial cytorrhexis were encountered.

Ferritin-Positive Microglia Are Less Abundant than HLA-DR-Positive Microglia and Appear Mostly Dystrophic

Comparing the total number of stained cells with either marker showed that only a fraction of microglial cells was immunoreactive for L-ferritin (Fig. 3-3A). The difference in the number of ferritin-positive versus HLA-DR-positive microglial cells was highly significant for all the groups examined ($P < 0.01$). The number of HLA-DR-positive microglial cells increased significantly with age ($P < 0.05$) (Fig. 3-3A), particularly with AD pathology, in accordance with previous reports (Carpenter et al. 1993; Luber-Narod and Rogers 1988). Although comparison of the number of HLA-DR-positive microglia in the ND and HPC groups showed no significant difference ($P > 0.5$), the number of HLA-DR-positive microglia was significantly different between all other groups (i.e., Y and ND, Y and HPC, Y and AD, HPC and AD groups) ($P < 0.01$). In contrast to HLA-DR expression, microglial L-chain Ft expression appeared to decrease with advancing age ($P < 0.05$), although a smaller subject pool in the young control group (n=3 versus n=7 in aged groups) may preclude a conclusive comparison of the number of stained microglial cells among aged groups and young controls. In HPC and AD tissues, the number of Ft-IR microglia was slightly higher than in ND tissues but this difference did not reach statistical significance.

Figure 3-3B shows the number of stained cells quantified in Fig. 3-3A that presented dystrophic changes. Microglial dystrophy was more prevalent in Ft-positive microglia than in HLA-DR-positive microglia for all groups ($P < 0.01$), except for the Y subjects ($P > 0.5$). Table 3-2 shows the percentage of microglial cells stained with either LN3 or Ferritin (Fig. 3-3A) that shows dystrophic changes (Fig. 3-3B). In younger brains, about 8% of Ft-IR microglial cells and 4% of HLA-DR positive microglia exhibited dystrophic changes. In ND tissues, approximately 5% of the HLA-DR-IR microglia were found to exhibit dystrophic changes whereas 83% of Ft-

positive microglia appeared dystrophic. In the HPC group, HLA-DR-positive, dystrophic microglia amounted to 11% of the total number of LN-3 stained microglial cells. For this group, approximately 57% of the Ft-IR microglial cells exhibited signs of dystrophy. Microglial cells immunoreactive for HLA-DR antigens in the AD tissues were found to exhibit mostly ramified and hypertrophic profiles, with only about 9% of these cells showing signs of dystrophy. In contrast, 83% of Ft-IR microglial cells in AD tissues possessed a dystrophic morphology.

In younger brains, Ft-positive dystrophic microglia were less conspicuous in comparison with Ft-IR dystrophic microglia in aged tissues. Moreover, in regards to the instances of dystrophic microglia immunoreactive for HLA-DR antigens, independent t-tests showed statistically significant differences ($P < 0.01$) in multiple comparisons between all groups, except for HPC versus AD ($P > 0.5$) (Fig. 3-3B). Similar comparisons were made for the instances of Ft-positive dystrophic microglia. The only non-significant comparison found was between the ND and HPC groups ($P > 0.5$) (Fig. 3-3B).

Ferritin-Positive Microglia Constitute a Subset of the Larger Microglial Pool

Direct evidence for the finding that Ft-positive microglia constitute a subpopulation of the overall microglial pool was obtained by fluorescently double labeling microglial cells with both HLA-DR and Ft markers (Fig. 3-4). In immunofluorescence staining preparations, HLA-DR-positive microglial cells outnumbered Ft-positive microglia, as evidenced by comparing single labeling for each marker. By merging color channels, it was confirmed that only a subset of microglial cells express L-Ft by co-localization with HLA-DR antigens. Moreover, in a given microscopic focal plane, Ft immunoreactivity was found to occur throughout the extent of microglial cell processes in a similar manner as for HLA-DR immunoreactivity, suggesting a similar cellular localization for the antigens analyzed in this study.

Microglial Dystrophic Changes are Not Due to Postmortem Tissue Autolysis

Postmortem delay defines the time interval in hours from death to tissue preservation. In order to determine whether or not microglial dystrophic changes could be caused by tissue autolysis during prolonged post-mortem intervals (PMIs), ferritin immunohistochemistry was performed on the frontal and temporal cortices of 9 forensic cases with postmortem delays ranging from 3 to 20 hours (Table 2-2). The subjects studied included 8 men and one woman; their mean age at death was 43.56 years with a standard deviation of 16.52 years. Review of clinical records and general autopsy reports revealed no evidence of neurologic disease, drug intake, or metabolic disease. Moreover, temperature, mode of fixation and storage, and staining technique were thoroughly controlled.

At a PMI of 3 hrs, Ft-IR microglial cells exhibited a mostly branched morphology (Fig. 3-5A), although distal processes were largely devoid of fine ramifications. Similar morphological characteristics were observed at longer PMIs (Fig. 3-5B-D), and most Ft-positive microglia in these tissues displayed deramified and beaded processes as described before (Table 3-1). Instances of deramified microglial cells remained constant from shortest to longest PMI. However, non-specific background staining was found to increase after a PMI of 8 hrs. These results suggest that Ft antigenicity is resistant to postmortem delay autolysis. In contrast, HLA-DR immunoreactivity, as demonstrated by LN-3 staining, proved very sensitive to prolonged postmortem delay and was of poor quality following immunohistochemistry (data not shown). Taken together, our results suggest that the structural changes associated with microglial dystrophy are not associated with postmortem interval tissue autolysis, but instead to inherent metabolic changes.

Ferritin-Positive Dystrophic Microglia are Prominent in the Brains of Alzheimer's Disease Patients

In our evaluation of microglial dystrophy, it became apparent that dystrophic microglia in aged specimens differed in the extent of cytoplasmic degeneration from those in younger brain tissue samples. Consequently, we set out to analyze in detail the morphological characteristics of both ramified and overtly dystrophic (i.e., cytorrhectic) microglia immunoreactive for both HLA-DR and Ferritin markers in all groups examined. In both control and AD tissues, HLA-DR-positive microglia predominantly exhibited a highly branched morphology including distal ramifications (Fig. 3-6A-D). However, a few HLA-DR immunoreactive microglia presented signs of dystrophy (Fig. 3-6B). Cytorrhexis, which appears to be the most severe form of microglial degeneration, could be observed in HLA-DR-positive microglia but only in aged groups (Fig. 3-6F-H) and not in young controls (Fig. 3-6E). In most cases, only a small number of HLA-DR-positive microglia in younger control subjects presented deramification of processes (Fig. 3-6E), which often did not progress into further degeneration of cytoplasmic structure. Cytorrhexis is thought to progress from deramified, beaded processes (as shown in Fig. 3-6F) into a complete fragmentation of cytoplasmic processes (Fig. 3-6G-H).

Ferritin-positive microglial cells ramified to the same extent as HLA-DR-IR microglia were rarely observed. For the most part, Ft-positive microglia never fully exhibited the branched morphology of HLA-DR positive microglia. Instead, they appeared in a deramified, atrophied morphology regardless of the age group in question (Fig. 3-6I-L). The majority of L-Ft-positive microglia in aged groups displayed all of the previously established characteristics of dystrophy (Table 3-1), while in young control subjects most Ft-positive microglia presented only a deramified morphology (Fig. 3-6M). Cytorrhectic microglia in ferritin-stained sections were

more readily identified as well as more pronounced than in LN-3 stained sections and they were largely limited to aged groups (Fig. 3-6N-P and Table 3-1), particularly in AD brain specimens.

In contrast to the other two aged groups examined, only 57% of Ft-positive microglia in HPC tissues appeared dystrophic (Fig. 3-3B; Table 3-2). The remainder of Ft-IR microglial cells did not fit the criteria for microglial dystrophy as outlined in Table 3-1, but their processes were often stripped of fine ramifications similar to Ft-positive microglial cells in younger tissues (Figs. 3-6I, 3-6M). AD tissue specimens exhibited the most severe dystrophic changes compared to the other groups, both for HLA-DR-positive and Ft-positive microglia.

Morphological analyses of microglia in the proximity of senile plaques

Because microglial cells exhibiting characteristics of cytoplasmic deterioration were readily noticeable in the AD brain (Figure 3-7), we subsequently wanted to know whether there was any relationship between AD-related histological pathologies (i.e., SP and NFT) and the occurrence of degenerative features in microglia. Therefore, to determine whether the incidence of dystrophic microglia was higher in the proximity of extracellular deposits of Aβ proteins (senile plaques), double immunohistochemistry was performed for both Aβ (6F3D) and microglia (Ferritin or LN3). Although amyloid deposition is considered a prerequisite for the unequivocal diagnosis of AD, they also occur in the brains of non-demented individuals, albeit to a lesser degree and in a more restricted distribution (Arriagada et al. 1992). Consequently, we chose to analyze and compare the instances of dystrophic microglia near Aβ deposits in both cognitively normal (HPC) and demented (AD) individuals.

In both HPC and AD tissues, HLA-DR-positive microglia showed mostly a ramified morphology (Fig. 3-8A-B), even in close proximity to SPs (Fig. 3-8C-D). These double labeling experiments corroborated the quantitative analysis of the proportion of dystrophic microglia in

HLA-DR immunoreactive microglia (Fig. 3-3B), which indicated that only approximately 10% of HLA-DR-positive microglia in HPC and AD tissues presented signs of degeneration. The dystrophic microglia in these tissues showed predominantly morphological features of atrophy and spheroid formation. Moreover, the few dystrophic microglia that could be identified in these tissues appeared randomly distributed throughout the brain parenchyma. Thus, there was no obvious spatial correlation between HLA-DR-positive, dystrophic microglial cells and SPs.

Similarly, Ft-positive dystrophic microglia were not concentrated around SPs, but scattered throughout the brain parenchyma of both HPC and AD tissues (Fig. 3-9). Taking into consideration that the incidence of dystrophic changes is higher in Ft-IR microglia (Fig. 3-3B), most Ft-positive microglia in both AD and HPC tissues appeared morphologically aberrant irrespective of proximity to Aβ deposits. Interestingly, this result was already apparent in our quantification of dystrophic microglia in Fig. 3-3B; Aβ deposition as a common denominator between HPC and AD tissues appeared to be insufficient in promoting dystrophic changes, since only roughly half of all Ft-positive microglia in HPC tissue samples appeared dystrophic while the large majority (about 90%) of Ft-positive microglia in AD subjects showed signs of dystrophy (Fig. 3-3B). Perhaps because of the higher incidence of dystrophic changes in Ft-IR microglia compared to HLA-DR-positive microglia, nearly all Ft-positive microglia appeared dystrophic at or near SPs (Fig. 3-3C-D).

Brain Specimens Used in This Study Represent Early AD

Because we did not observe any correlation in the proximity of microglial cells exhibiting dystrophic features to Aβ deposits in both HPC and AD brain specimens, next we were interested in determining the identity of the SPs present in our brain specimens. We noticed that the 6F3D-immunoreactive SPs were prevalent mostly in the neocortical brain regions (SFG, temporal

gyrus), particularly in cortical layers III-V (Fig. 3-10A). Morphologically, the stained SPs appeared amorphous and surrounded by a well-defined outline contour, all of which are defining characteristics of diffuse SPs (Fig. 3-10B). This morphological characterization was corroborated by the finding that most microglial cells surrounding the plaques appeared ramified and not hypertrophic (Fig. 3-10C). We also attempted to stain NFTs in adjacent tissue sections using various established markers of NFTs (CNPase [Calbiochem]; PHF-Tau clone AT8 [Thermo Scientific]; RIP [BD Transduction labs]) and immunohistochemical procedures with no success, however (data not shown). The predominance of diffuse SPs in the neocortex and the absence of NFT pathology and neuritic plaques suggest that our brain specimens are staged in the early phase of the disease.

Analyses of Microglial Ferritin Immunoreactivity in Young and Aged Rats

Acute Activation of Microglial Cells Does Not Induce Ferritin Expression

Because dystrophic microglia exhibit some morphological similarities with activated microglial cells (Lopes et al. 2008; Streit 2006), namely deramification and spheroid formation (Table 3-3), we subsequently wanted to determine whether microglial activation induces Ft expression and if perhaps the appearance of dystrophic microglia is increased under injury-induced activation conditions in aged animals. To this end, we analyzed Ft immunoreactivity in microglial cells activated *in vivo* by the well-characterized FN axotomy paradigm in both young and aged rats.

To examine whether Ft immunoreactivity is upregulated in activated microglial cells, the right FN of rats was acutely injured while leaving the left FN intact to serve as an internal control. Brain sections from the axotomized rats were then immunostained for L-ferritin. No difference in staining patterns was found between the axotomized and control (contralateral)

sides of the rat FNu, regardless of the time interval following the nerve injury or the age of the animal (Figure 3-11). However, Ft immunoreactivity within the FNu increased with age,. At 3 months of age, Ft immunohistochemistry showed a light staining of both axotomized and control FNu where only a few intensely stained cells could be identified (Figure 3-11, top panel). In rats aged 30 months, there was a visible increase in Ft background staining in both sides of the FNu, which appeared to spread to adjacent areas accompanied by an increase in the number and distribution of immunoreactive cells (Figure 3-11, bottom panel).

In order to find out whether the few Ft-IR cells observed in the FNu were microglial cells, double immunofluorescence staining was performed using both Ft and microglial markers. Microglial cells were visualized by staining with OX-42, a mouse monoclonal antibody (mAb) that specifically recognizes type 3 complement receptors (CR3) expressed by both ramified and activated microglia (Ling et al. 1992; Milligan et al. 1991). Induction of microglial activation was confirmed by changes in cell morphology (hypertrophy), cell number (proliferation), and immunophenotype (upregulation of CR3 antigens) within the axotomized FNu of both young (Figure 3-12B) and aged (Figure 3-12H) rats compared to the control side (Figures 3-12A, 3-12G). This microglial activation response did not induce an upregulation of Ft, as evidenced by an equivalent number of Ft-positive cells in both sides of the FNu (Figures 3-12C-D, 3-12I-J). However, a higher number of Ft-IR cells was observed in aged rats (Figure 3-12I-J) compared to the younger group (Figure 3-12C-D) in accordance with the increased staining shown in Figure 1. In both axotomized and control FNu these Ft-IR cells did not colocalize with OX-42-IR microglia (Figures 3-12E-F, 3-12K-L), although a few did in aged animals (Figure 3-12K-L).

Although the majority of Ft-positive cells within the rat FNu did not colocalize with CR3 antigens, their identity could be resolved based on defining morphological characteristics. Ft-

positive cells had a larger and rounder nucleus than OX-42-positive microglia as well as fewer (if any) processes stained (Figure 3-13), and these morphological features identified them as oligodendrocytes by comparison with previously published oligodendroglial immunohistochemical data using L-ferritin (Cheepsunthorn et al. 1998; Cheepsunthorn et al. 2001; Koeppen and Dickson 2001; Ogawa et al. 1994).

Ferritin Immunohistochemistry Labels Predominantly Oligodendrocytes in Rat Brains

Our Ft histological studies on human brain specimens indicated that only a subset of microglial cells express L-rich ferritins (see Figs. 3-3 and 3-4). We noticed similar results in FNu sections in rats (Fig. 3-12). In order to determine the validity of our results in rats, we decided to also stain rat coronal sections that contained the hippocampus, an area previously established to contain a high number of L-Ft-positive cells (Huang and Ong 2005). Our histological analysis corroborated earlier studies in that Ft-positive cells were found predominantly in the hippocampal region of rats, irrespective of the age of the animal (Fig. 3-14). Morphological evaluation of these Ft-positive cells under high power magnification revealed cells with a darker perinuclear staining and few stained processes, all of which are suggestive of oligodendroglial phenotype (Fig. 3-14). Our histological characterization of L-Ft-positive cells in the rat hippocampus was supported by our double immunohistrochemisry findings that OX-42-positive microglia do not colocalize with L-Ft markers (Fig. 3-15). In addition, Ft-IR cells did not colabel with OX-42-positive microglia in either cortical or cerebellar regions (Fig. 3-15). Moreover, these Ft-IR cells presented a morphology different from OX-42-IR microglia, including a rounder and slightly larger perinuclear regions and fewer, punctate (thin) branches, all of which are hallmark characteristics of oligodendroglial cells.

Morphological Analyses of Microglial Senescence in the Rat Brain under Conditions of Normal Aging and Acute Injury

Accumulation of Lipofuscin Granules are Prevalent in Dystrophic Microglia of the Aging Rat Brain

Since the FN axotomy procedure performed represents a mild, reversible injury that does not lead to debris accumulation, no phagocytic activity by activated microglial cells should take place. As stated previously, microglial cells have been shown to senesce with advancing age (Flanary and Streit 2003; Streit 2006), the outcome of which remains unknown. Therefore, our next aim was to investigate whether there were any microglial cells in the aged rat brain that would exhibit an altered activation response. Since prior work had reported microglial hypertrophy in aged rats (Conde and Streit 2006), we wanted to investigate whether these enlarged microglia were expressing lysosomal proteins normally found in phagocytic cells. ED1 is a mouse mAb that recognizes a single chain glycoprotein of 110kDa expressed predominantly on the lysosomal membrane of phagocytic cells (i.e., microglia/macrophages) (Dijkstra et al. 1985). Double labeling immunofluorescence was, therefore, performed in axotomized rat brain tissues using both ED1 and ionized calcium binding adaptor molecule 1 (Iba-1) markers, the latter of which is a rabbit polyclonal antibody whose antigen is specifically expressed in microglial cells (Ito et al. 1998). As expected and confirming prior by Graeber et al. (1998), our immunofluorescence analyses revealed that ED1 immunoreactivity is absent in both the unoperated and axotomized FNu of young rats (Fig. 3-16A-B). However, in aged brain, a large fraction of Iba-1-positive microglia co-localized with ED1 in aged tissues, however (Figure 3-16C-D). Surprisingly, these ED1-IR microglia were found predominantly and more conspicuously in the control side of the FNu (Fig. 3-16C) compared to the axotomized side (Fig. 3-16D), indicating that expression of ED1 antigen was unrelated to microglial activation.

Upon closer examination of the ED1-positive microglia, we noticed that in the non-axotomized FNu these cells had shorter, less complex branches and a stout perinuclear region than ED-1-negative microglia (Fig. 3-16E). Although less ramified, there was no hypertrophy of major processes as is typical of activated microglial cells. In the axotomized FNu, the morphology of ED1-positive microglia was indistinguishable from ED1-negative microglia (Fig. 3-16F). Lastly, we noticed that ED1 antigens accumulated preferentially in the perinuclear area of the cytoplasm (Fig. 3-17). Interestingly, we also noticed that the ED1-positive signal in microglia was detectable by fluorescence microscopy across a wide spectral range (excitation: 350-580 nm; emission: 400-603 nm) (Fig. 3-18), suggesting that the ED1 positive signal was congruent with autofluorescence.

Autofluorescence refers to the intrinsic emission of light from endogenous compounds other than the fluorophore of interest. It is a common occurrence in aged tissues, due primarily to the accumulation of autofluorescent lipofuscin (LF) granules within long-lived cells (Brunk and Terman 2002; Terman and Brunck 2004). In our analyses, all ED1-positive signal in microglia coincided with autofluorescent LF granules by excitation with ultraviolet, blue, and green light as illustrated in Figure 3-18A-C (also see the merged image in Fig. 3-19A). Although LF appeared in all morphological subtypes of microglia, their intensity and size was more noticeably visible in microglial cells exhibiting signs of dystrophy (Figure 3-19A-C), namely loss of distal, and sometimes proximal, branches compared to LF-negative ramified microglia (Figure 3-19D). Most LF granules in Iba-1-IR microglia accumulated in the nuclear periphery (Figures 3-19A-B). Occasionally, we also found LF particles localized within cytoplasmic spheroids away from the perinuclear cytoplasm (Figure 3-19C). Spheroid formation in human microglia is considered a characteristic trait of dystrophy. In regards to the anatomical localization, LF-containing

microglia were found predominantly in the non-axotomized FNu of aged rats (Table 3-4), reinforcing the idea that LF accumulation occurs independent of microglial activation.

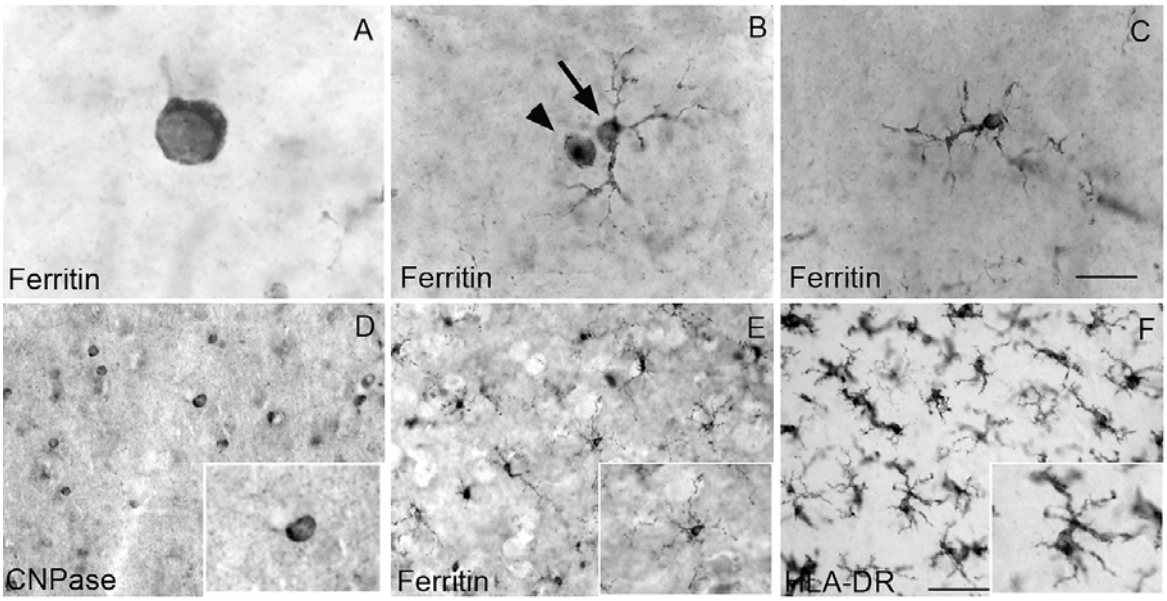

Figure 3-1. Morphological characteristics differentiate ferritin-positive microglia from ferritin-positive oligodendrocytes. Photomicrographs taken from serial SFG sections from an 85-year-old ND individual. (A) L-ferritin-positive oligodendrocytes exhibit strong perinuclear staining, few processes and a large nucleus, characteristics that facilitate the differentiation of ferritin-positive oligodendrocytes (B, arrowhead) from ferritin-positive microglia (B, arrow). In turn, ferritin-immunoreactive microglia present fine cytoplasmic ramifications and a small, rounded or irregularly shaped nucleus (C). Oligodendrocyte-like morphology in (A-B) was verified by comparison to cells immunoreactive to the oligodendrocyte-specific marker CNPase (D). Likewise, microglial morphology in (B-C) was similar to HLA-DR-positive microglia (F). In gray matter, most ferritin-positive cells present a branched morphology similar to microglia (E). Scale bar = (A-C) 10μm, (D-F) 3μm.

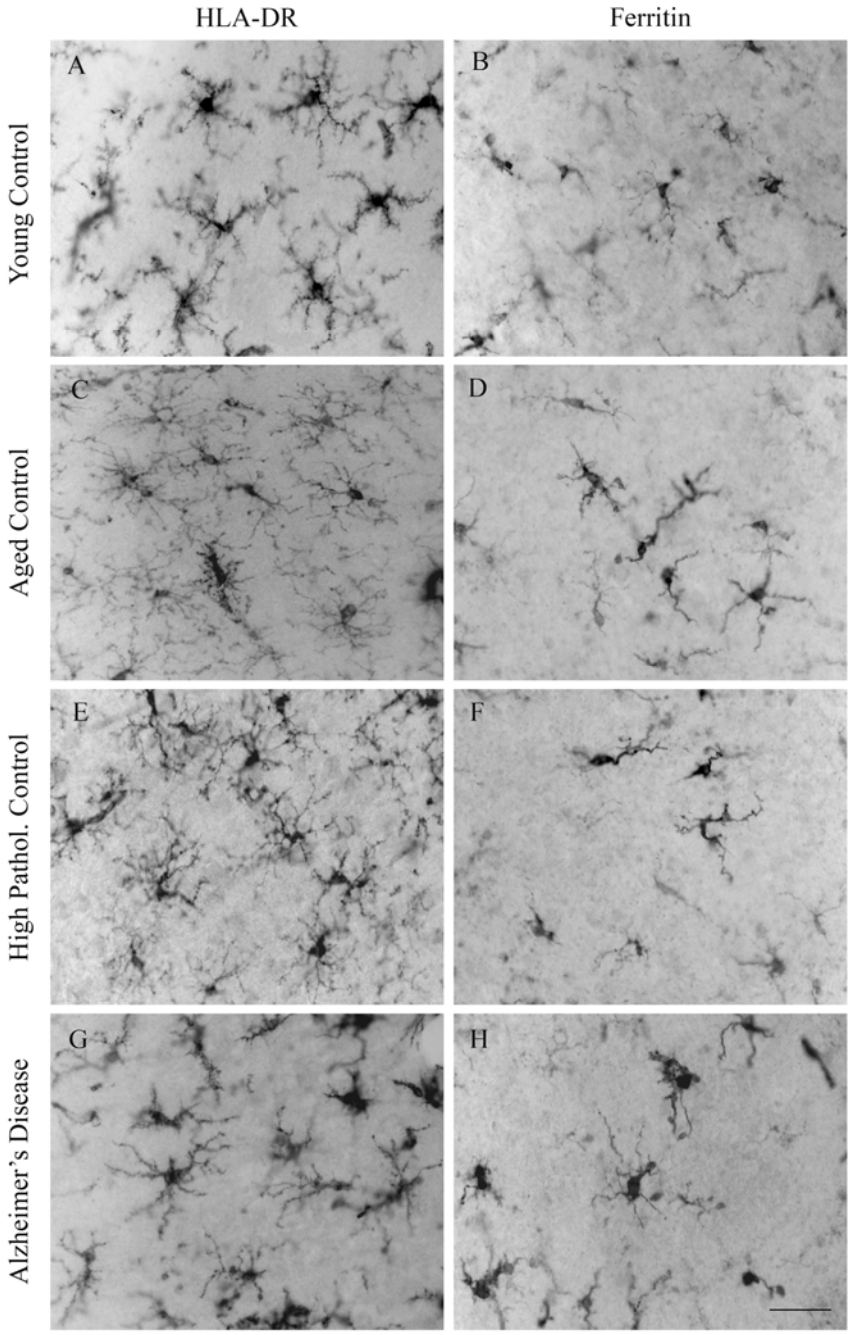

Figure 3-2. Representative photomicrographs of the number of microglia immunoreactive for either HLA-DR antigens or ferritin proteins. Microglia immunoreactive for either HLA-DR antigens (A, C, E, G) or L-ferritin proteins (B, D, F, H) in adjacent SFG sections of a 34-year-old control individual (A-B), an 81-year-old control individual (C-D), an 83-year-old HPC subject (E-F), and an 81-year-old AD subject (G-H). The photomicrographs are representative of the number of microglial cells stained with each marker. Note the extensive branched morphology of ramified microglia immunoreactive for HLA-DR. L-ferritin-positive microglia exhibit mostly a dystrophic morphology. In all groups, microglial labeling was less prominent for ferritin expression (B, D, F, H) than for HLA-DR antigen expression (A, C, E, G). Scale bar = (A-H) 20μm.

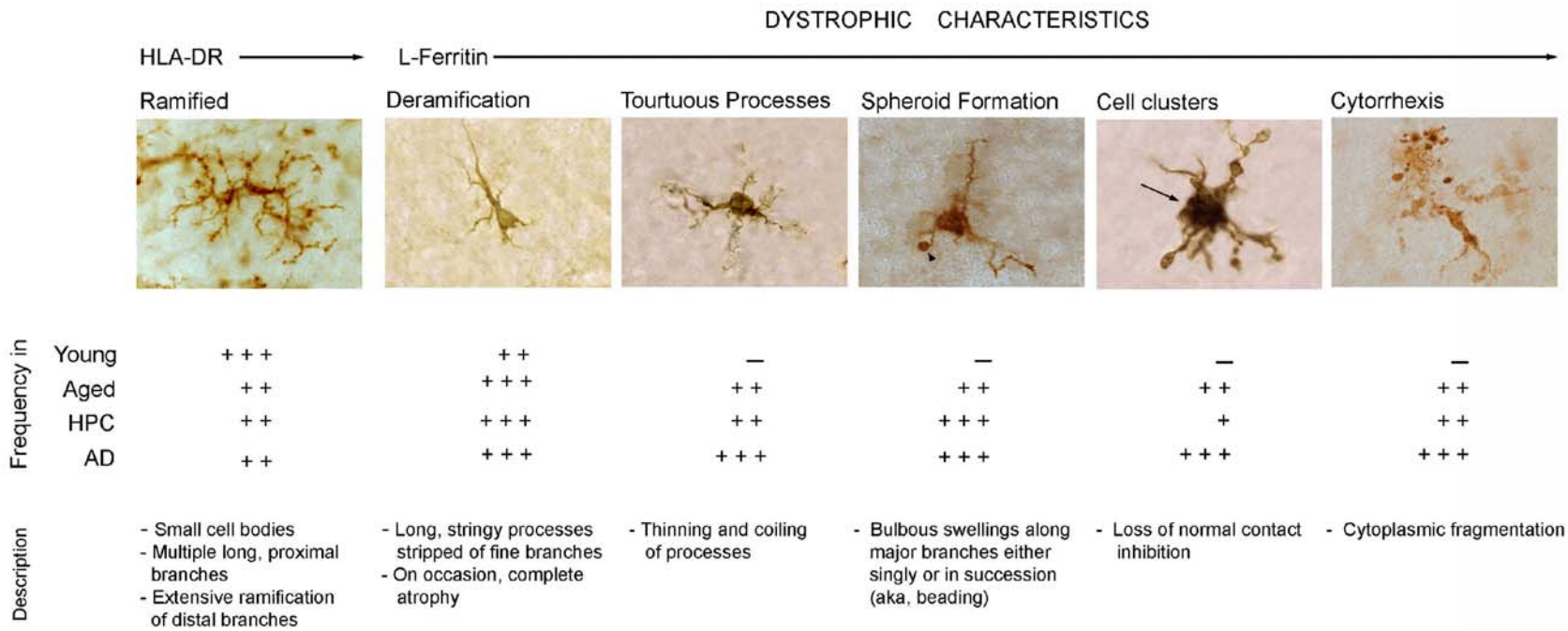

Table 3-1. Classification of microglial dystrophic characteristics based on ferritin immunohistochemistry. Microglial morphology in the temporal cortex of an 81-year-old ND individual (HLA-DR stained) and in an 81-year-old AD patient (Ferritin stained). Frequency refers to the predominance of a given morphology in each cohort under study. Symbols: -, absent; +, rare; ++, common; +++, prevalent.

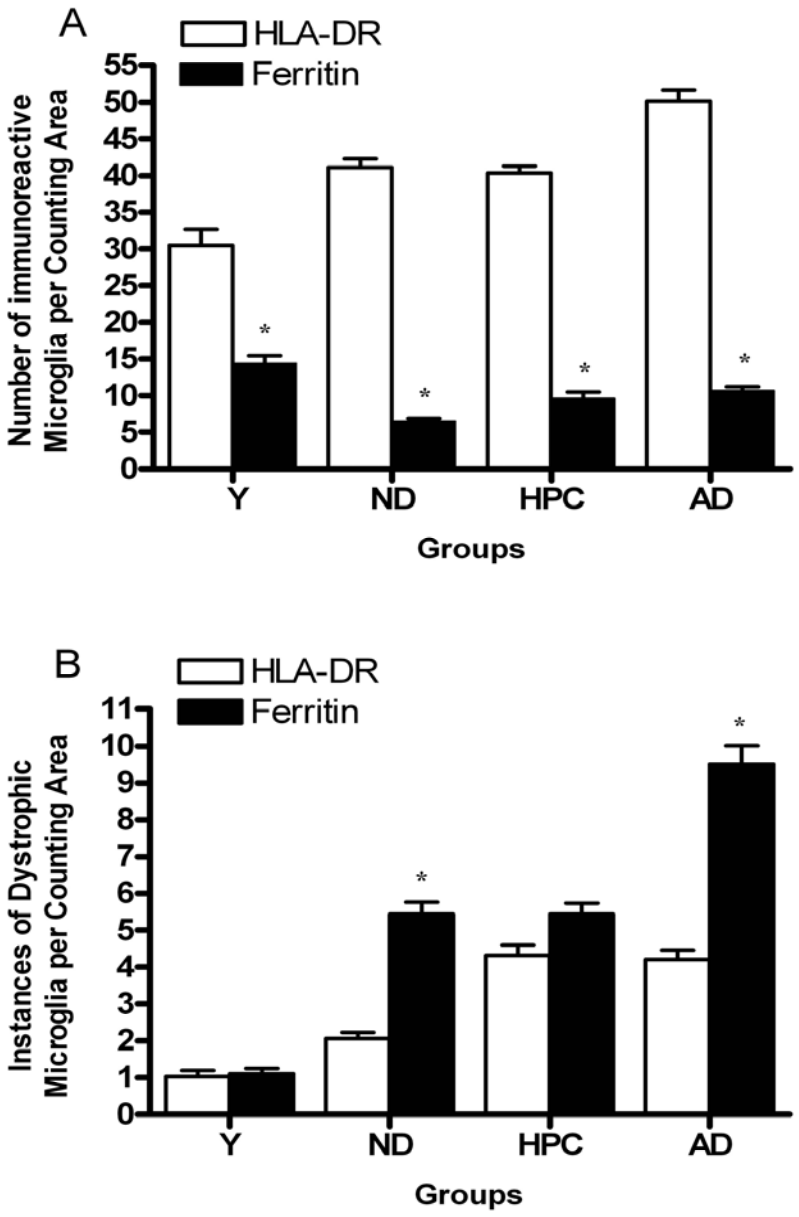

Figure 3-3. Comparison of the average number of immunoreactive (A) and dystrophic (B) microglia stained for either HLA-DR antigens (open bars) or ferritin proteins (closed bars). After scoring the number of immunoreactive microglia for each marker in (A), each immunoreactive microglial cell was evaluated qualitatively based on a predefined set of morphological criteria for dystrophic changes (B). Values are means ± SEM.
* $p < 0.05$ versus HLA-DR for each group.

Table 3-2. Proportion of HLA-DR- and ferritin-immunoreactive microglia in human brain specimens that exhibit dystrophic characteristics.

	Y	ND	HPC	AD
HLA-DR	4%	5%	11%	9%
Ferritin	8%	83%	57%	89%

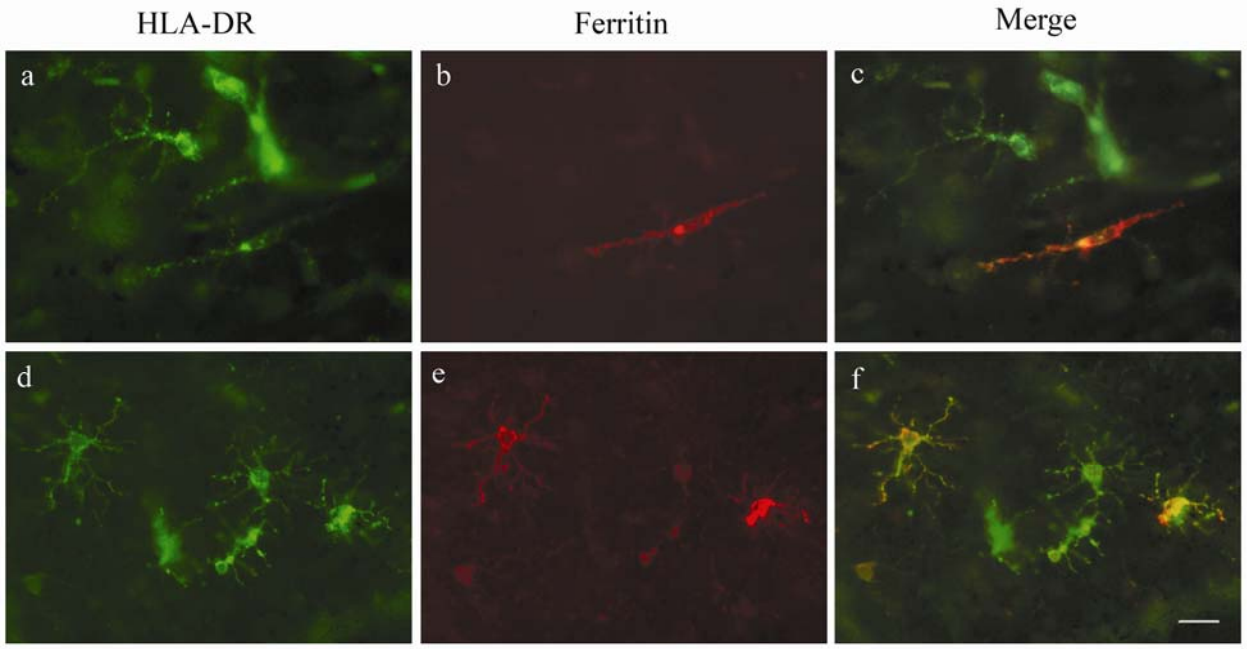

Figure 3-4. Ferritin immunoreactive microglia constitute a subpopulation of the larger HLA-DR-positive microglial pool. Immunofluorescence microscopy of microglial cells for HLA-DR (green) and ferritin (red) antigens in temporal lobe cortex of a 34-year old Y individual (a-c) and in a 77-year-old HPC subject (d-f). Merged images of both channels are included, with yellow representing overlapping signal. Note that not all microglia express ferritin proteins (b, e). Scale bar = (a-f) 20 µm.

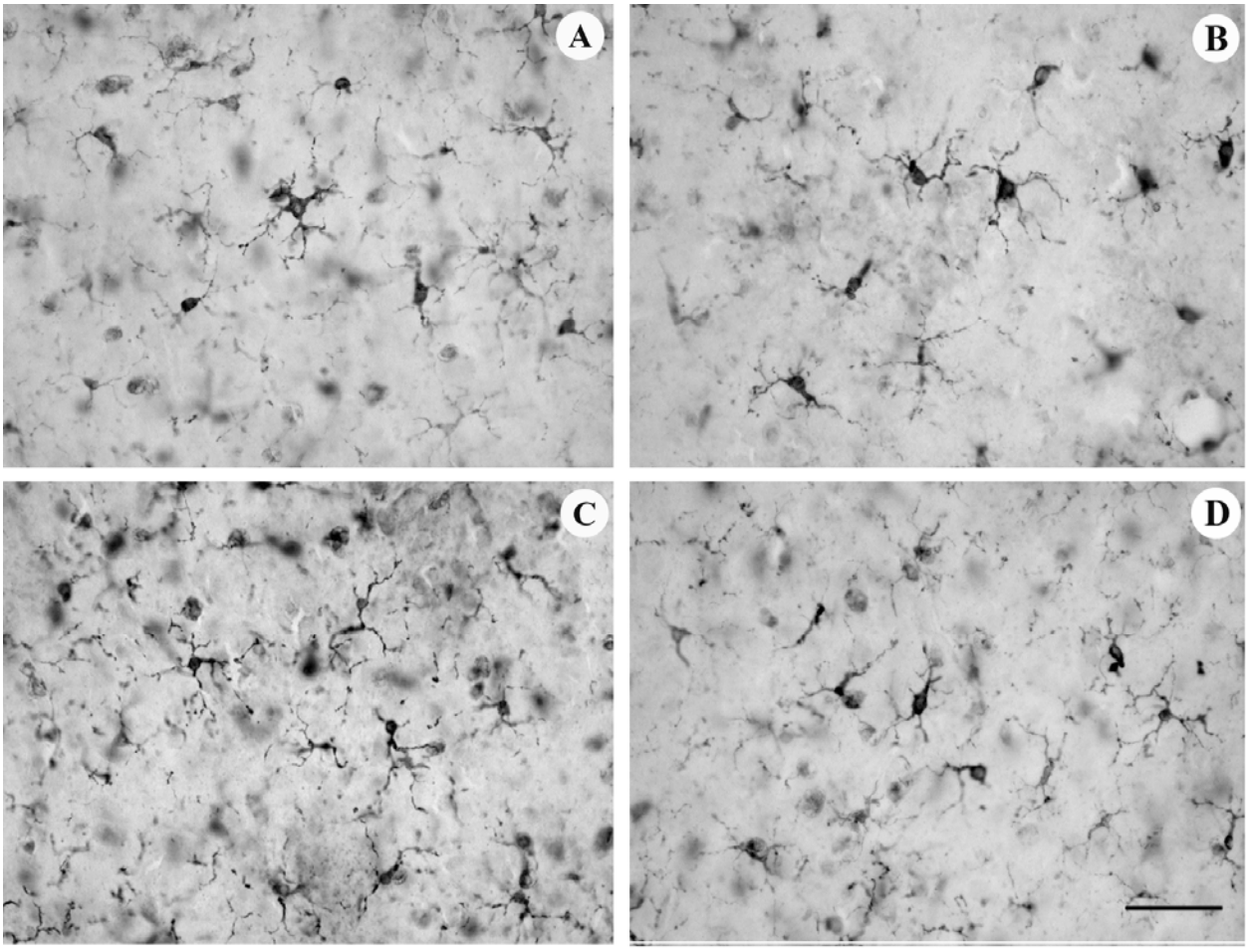

Figure 3-5. Postmortem interval study. Representative photomicrographs of L-ferritin immunoreactive microglia in cortical specimens with ascending postmortem intervals (PMIs): (A) 3 hrs, (B) 8 hrs, (C) 14 hrs, and (D) 20 hrs. No increases in the instances of microglial dystrophy were observed with increasing PMI. Scale bar = (A-D) 10μm.

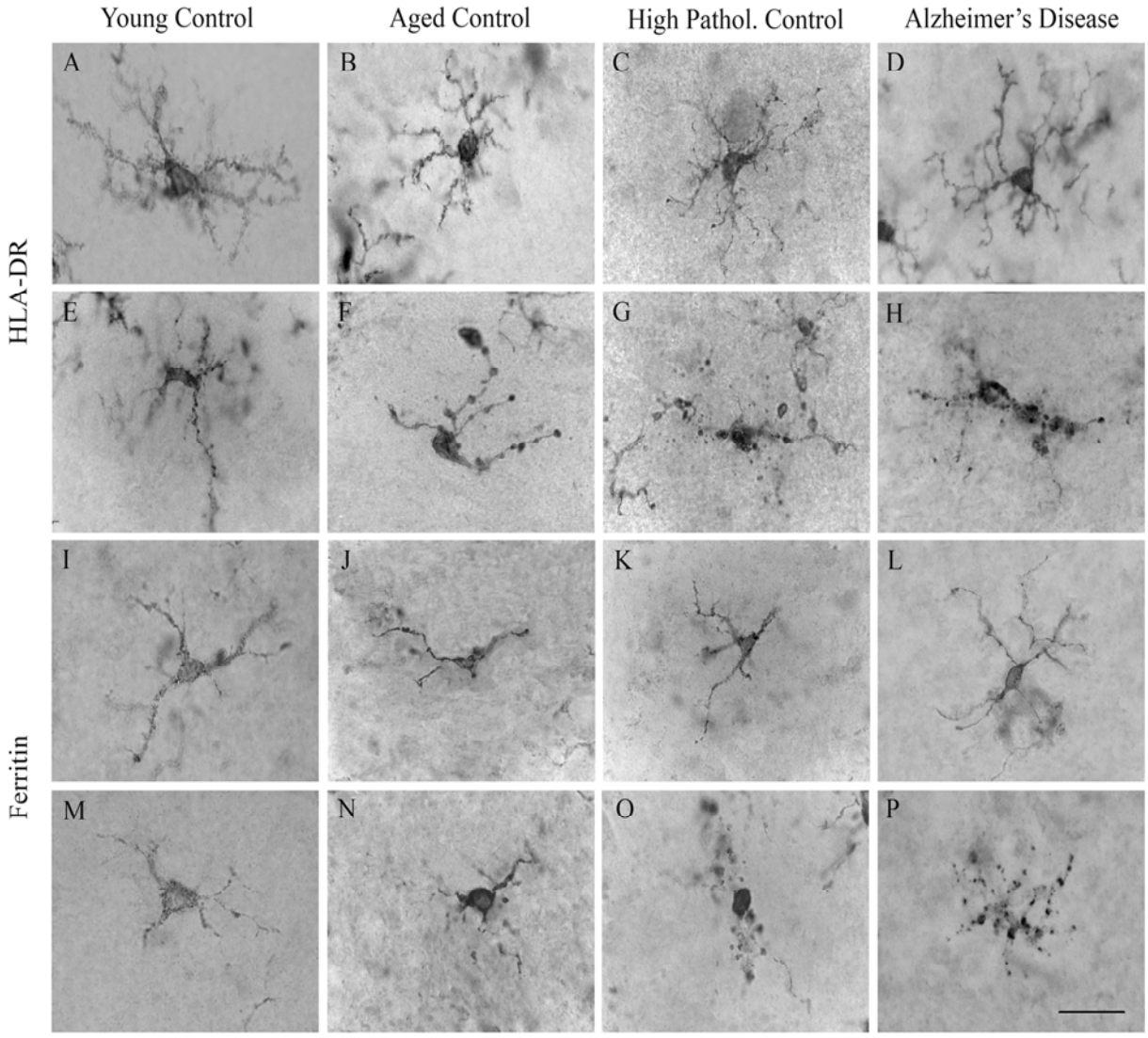

Figure 3-6. Cytorrhectic microglia are present in aged but not in young human brain tissues. Adjacent serial sections of superior frontal cortex of a 37-year old Y individual (A, E, I, M), an 85-year old ND individual (B, F, J, N), an 84-year old HPC subject (C, G, K, O), and an 85-year old AD patient (D, H, L, P) were immunohistochemically labeled for either HLA-DR (A-H) or L-ferritin antigens (I-P). Instances of ramified microglial cells were readily visible in HLA-DR-stained sections for all groups examined (A-D). A small number of HLA-DR-positive microglia presented a cytorrhectic morphological profile in all aged groups (F-H) except in young controls (E). Cytorrhexis appears to progress from thin, beaded processes (F) to overtly cytoplasmic degeneration (G-H). These HLA-DR-positive dystrophic microglia were observed scattered randomly in the brain parenchyma among ramified microglia and were relatively few in number. In contrast, ferritin-positive microglial cells never fully exhibited the highly branched morphology of ramified microglia (I-L), including in young controls (I). Cytorrhectic microglia were more numerous in ferritin-stained sections for all aged groups (N-P) except for in young controls (M), in which ferritin-positive microglia only exhibited a deramified profile. Scale bar = (A-P) 20μm.

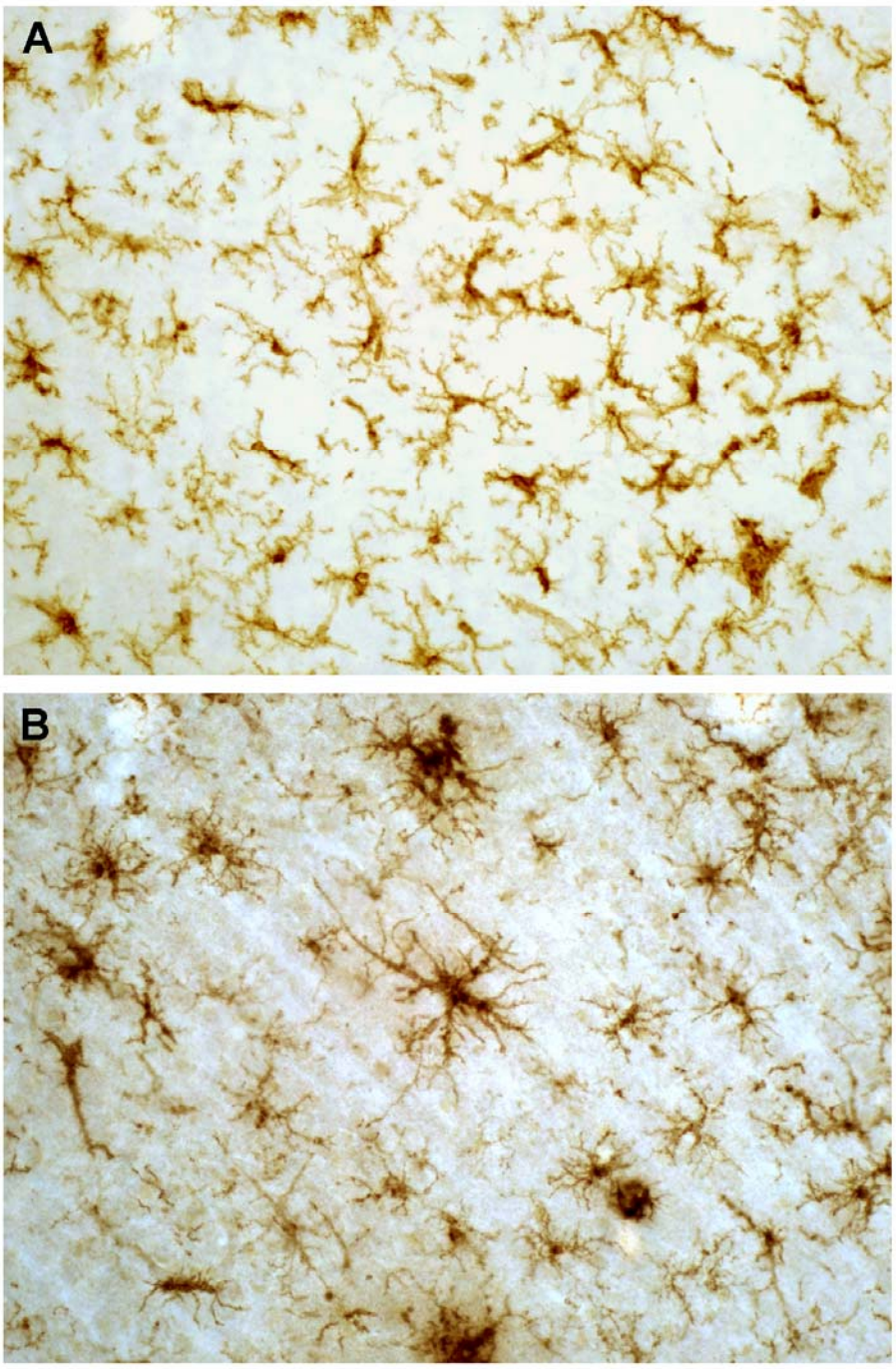

Figure 3-7. Microglial cells in AD specimens exhibit abnormal morphological features. Photomicrographs of microglial cells immunoreactive for HLA-DR antigens in the frontal cortical gray matter of a 38-year-old individual (A) and an 87-year-old AD subject (B). (A) Ramified microglial cells predominate in the tissue from younger individuals. (B) In the AD-tissue, the incidence of dystrophic microglia increases, although ramified microglial cells are still visible. Here, signs of dystrophy included deramification, formation of multicellular clusters, and spheroid formation. The higher incidence of dystrophic microglia in AD brain tissues implicates a role for microglial senescence in AD pathogenesis. Scale bar: (A-B) 100μm.

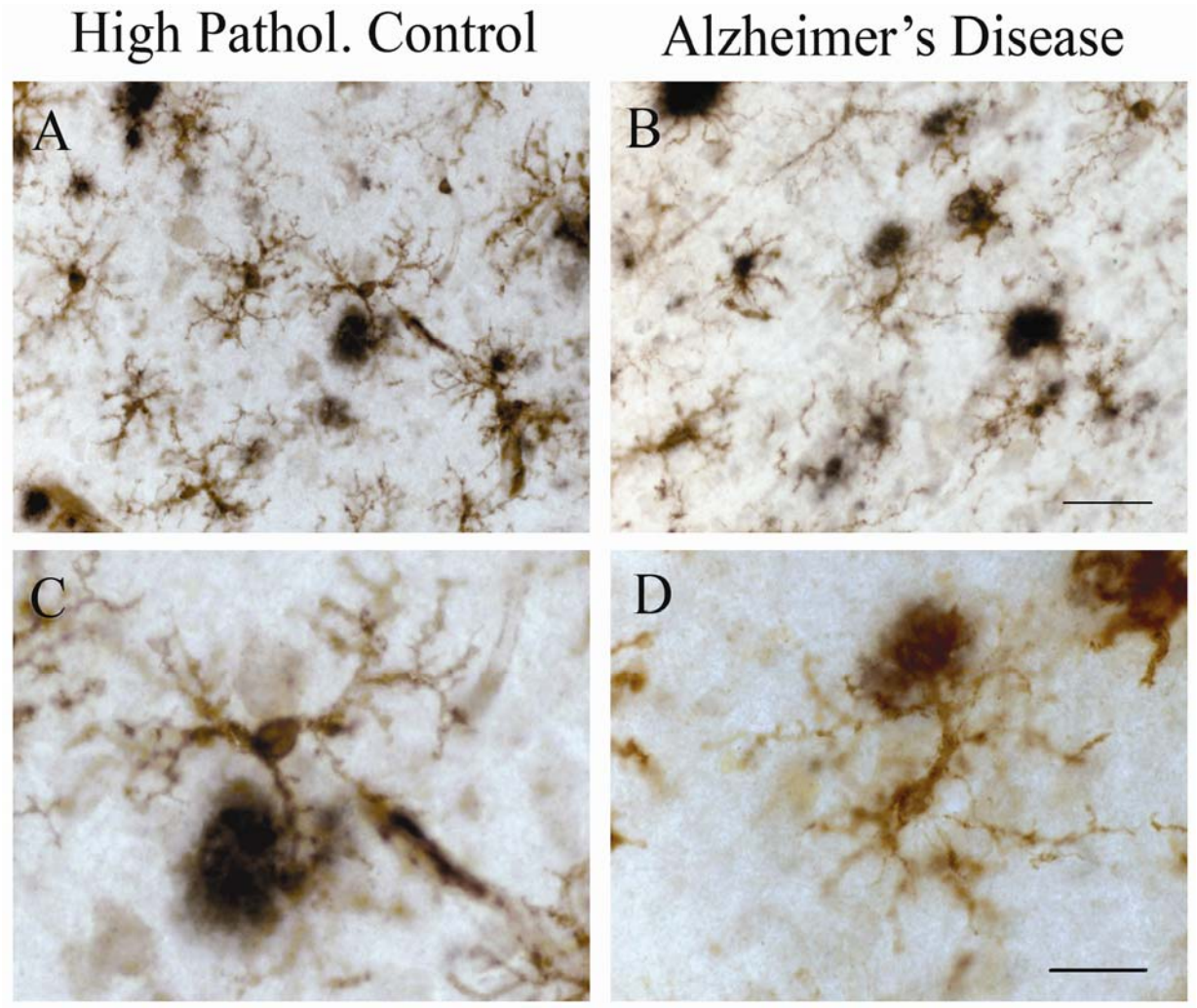

Figure 3-8. HLA-DR-positive microglia (brown) in the vicinity of senile plaques (black) present mostly a ramified morphology in both HPC and AD tissues. Nearly all HLA-DR immunoreactive microglia around senile plaques exhibited a ramified morphology in the temporal cortex of an 89-year old HPC individual (A,C) and in an 87-year old AD subject (B,D). A few dystrophic microglial cells could be identified in these tissues and they were for the most part scattered randomly in the brain parenchyma irrespective of the location of amyloid deposition. Scale bar = (A,B) 10μm; (C,D) 20μm.

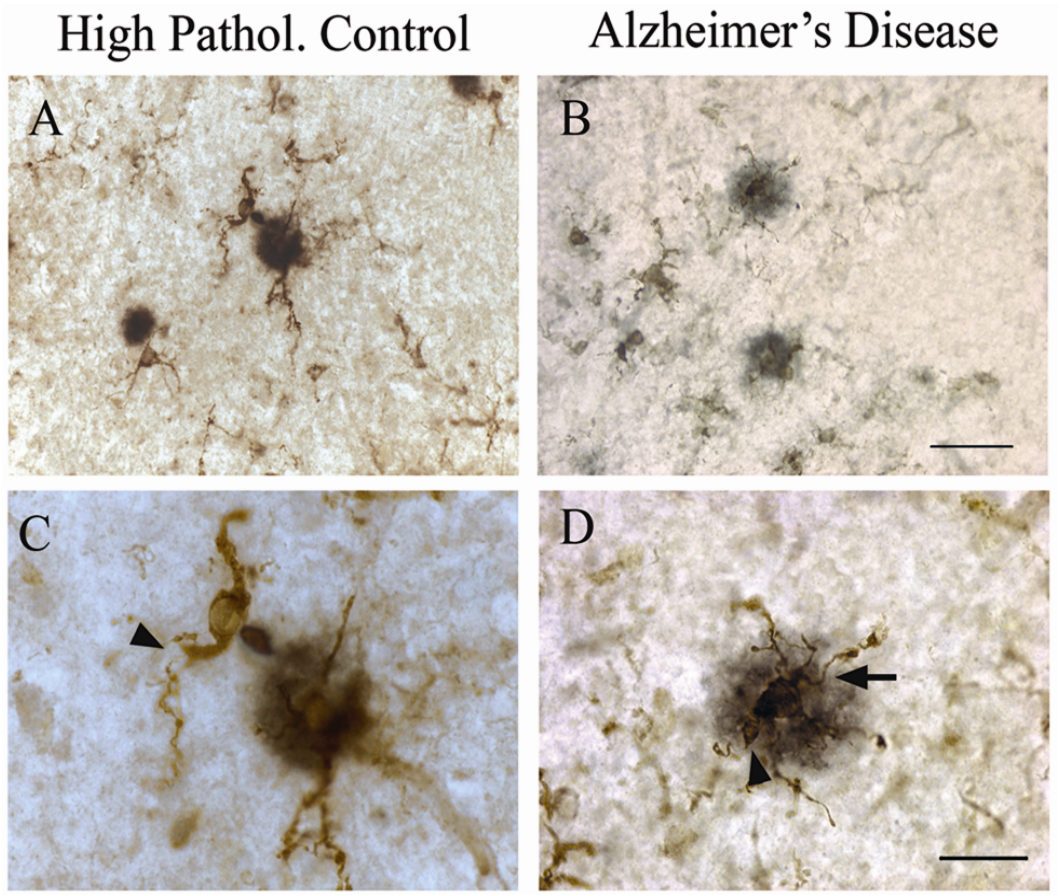

Figure 3-9. Ferritin-positive microglia (brown) present mostly a deramified profile in both HPC and AD tissues irrespective of the vicinity of senile plaques (black). Adjacent serial sections labeled for HLA-DR antigens in Figure 7 were labeled for ferritin proteins in the 89-year old HPC (A,C) and 87-year old AD (B,D) subjects. Dystrophic microglial cells could be readily identified in these tissues. They were distributed randomly in the brain parenchyma, occurring both near and away of amyloid deposits. Ferritin-positive dystrophic microglia within senile plaques often exhibited gnarling and deramification of processes (C) as well as thin, tortuous, beaded processes (D). Scale bar = (A,B) 10μm; (C,D) 20μm.

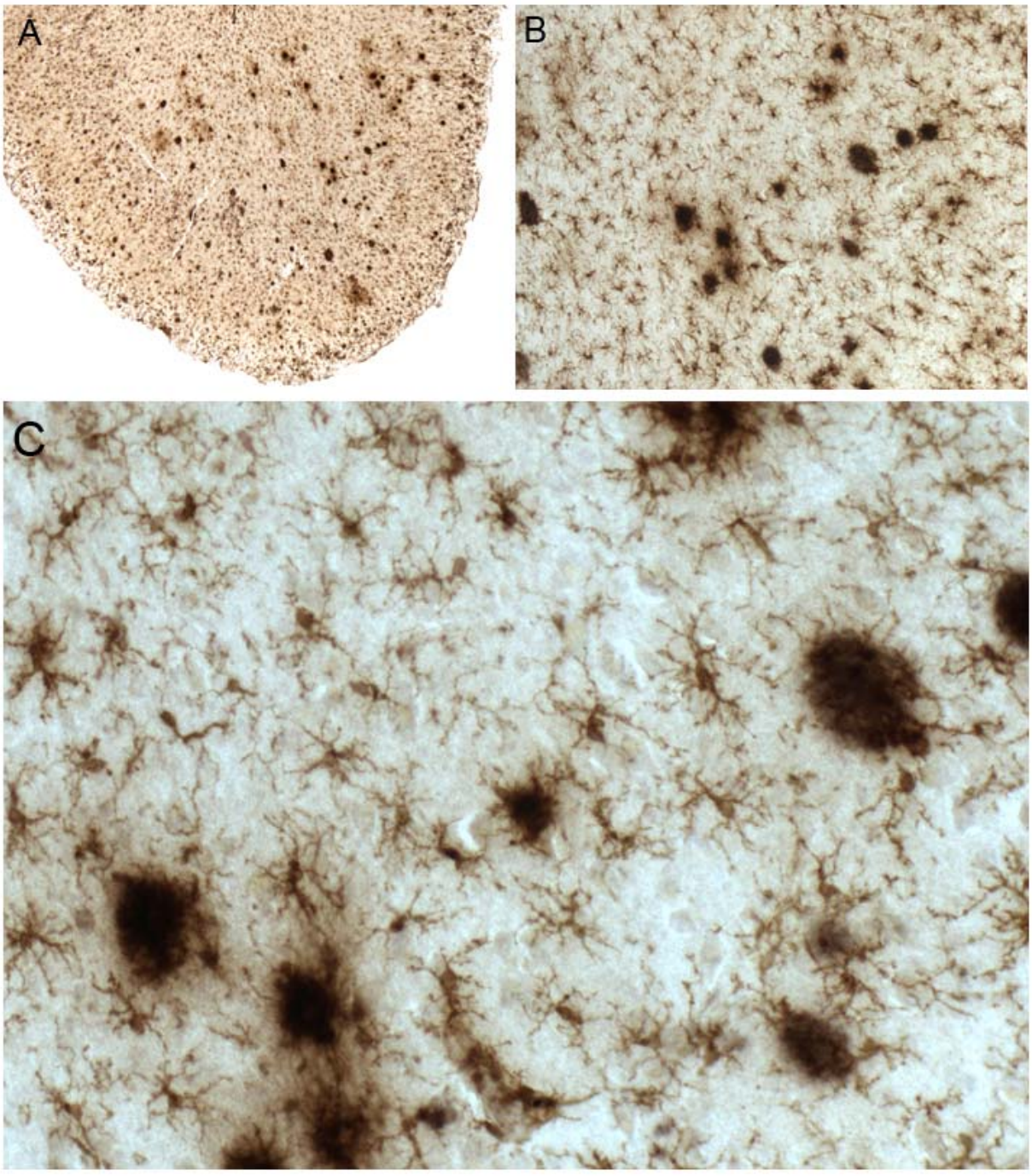

Figure 3-10. Morphological characteristics of senile plaques in the AD brain specimens under study. These photomicrographs were taken from the SFG of a 85 year old AD patient and are representative of other specimens within the AD cohort. (A) Senile plaques immunoreactive for 6F3D (black) concentrate in cortical gray matter. (B) These plaques appear homogeneous and with a sharply defined rim, all of which are characteristics of 'diffuse' plaques. (C) HLA-DR-positive microglia (brown) maintain a ramified morphology in the proximity (and even within) the plaques. All of these characteristics pinpoint an early stage for the AD brain specimens under study.

Table 3-3. Morphological Characteristics of Activated and Dystrophic Microglia

	Dystrophic Microglia	Activated Microglia
Hypertrophy	±	+ + +
Atrophy	±	–
Deramification	+ + +	±
Beading	+ +	–
Spheroids	+ +	±
Fragmentation	+	–

Symbols: –, absent; ±, less pronounced; + present; + + often present; + + +, always present.

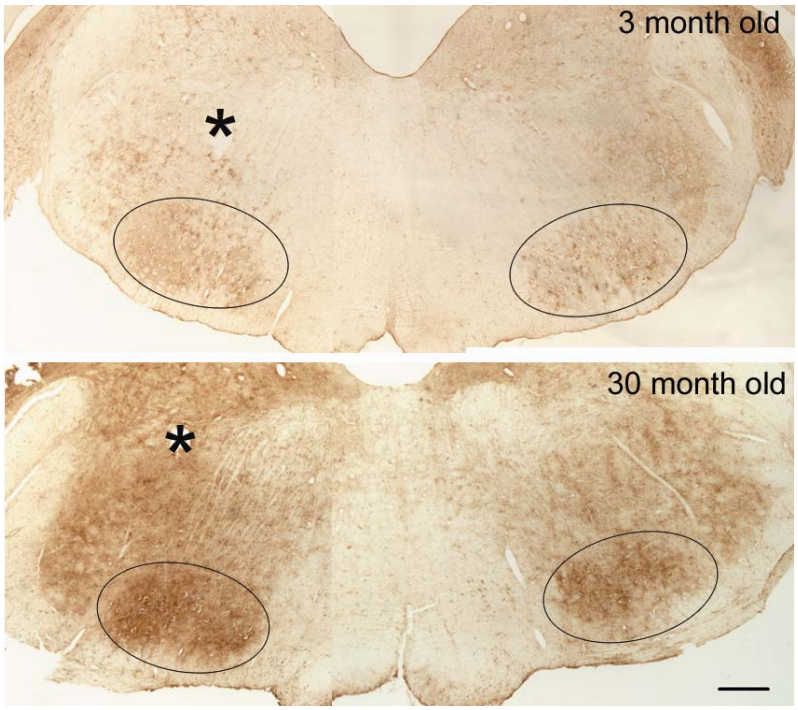

Figure 3-11. Ferritin protein levels increase with age in the rat. Ferritin immunohistochemistry through the brainstem containing the facial nucleus (outlined area) of a 3-month-old (top panel) and a 30-month-old (bottom panel) rat at 3 days postaxotomy. Light ferritin staining in younger tissues increased in intensity and size with age. No difference in ferritin immunoreactivity was observed between control (asterisk) and axotomized sides of rat facial nucleus. Scale bar = 500 μm applies to both panels.

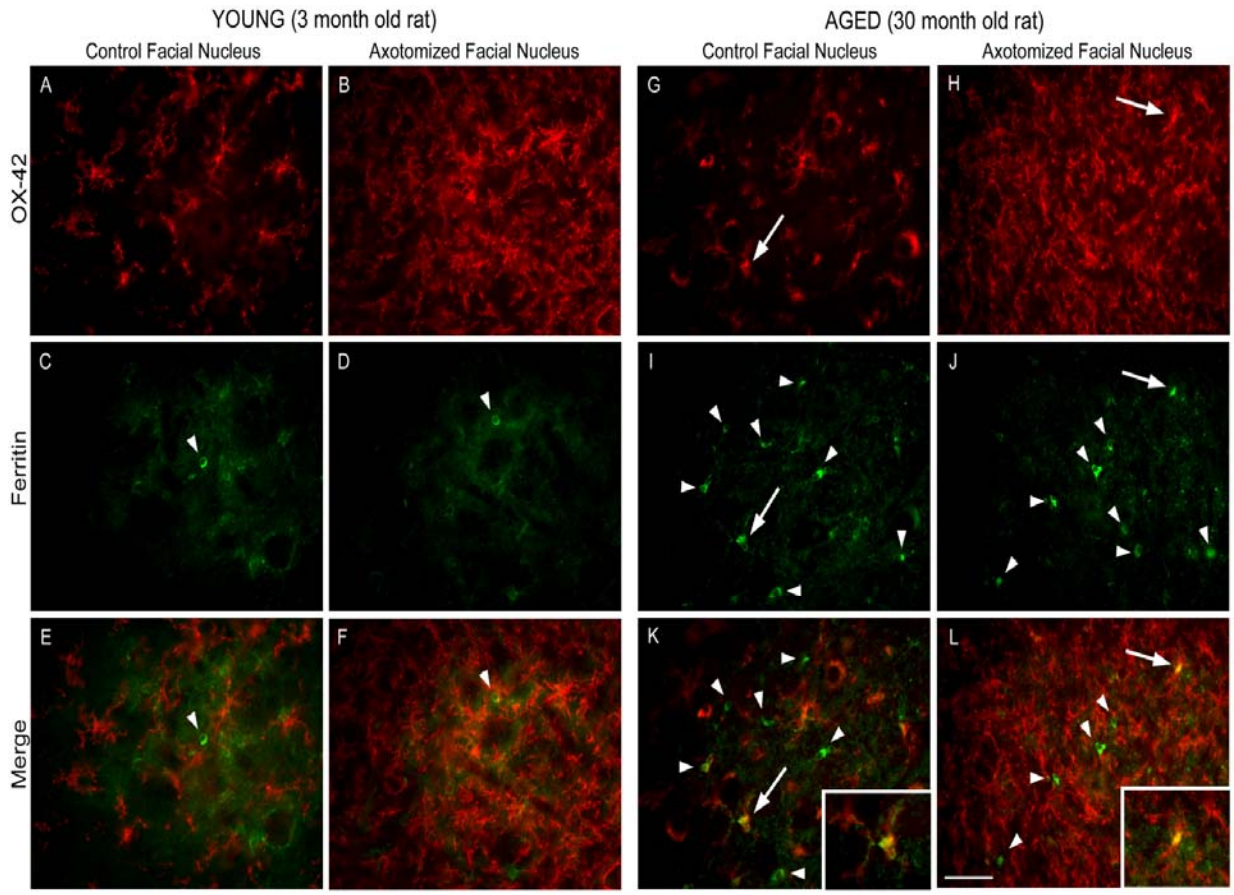

Figure 3-12. L-ferritin expression is induced by the aging process in microglial cells and not by acute activation conditions. Double-immunofluorescence staining of the facial nucleus region of both young (A-F) and aged (G-K) rats using the microglial marker OX-42 (red) and ferritin (green). OX-42-immunoreactive microglia in the unoperated side of the facial nucleus appear ramified and evenly distributed both in young (A) and aged (G) rats. Within the axotomized facial nucleus, OX-42-positive microglia are more numerous and hypertrophic (B, H). Few ferritin-positive cells were identified in the rat facial nucleus, irrespective of whether or not motoneurons were injured (arrowheads in C-D, I-J). Most of these ferritin-positive cells did not co-localize with the microglial marker (E-F, K-L) although some colocalization was apparent but in aged tissues only (K-L, arrows). Yellow color in merged images (K-L) defines co-expression. Insets show a higher magnification view of the double labeled cells. Scale bar= 10μm (A-L).

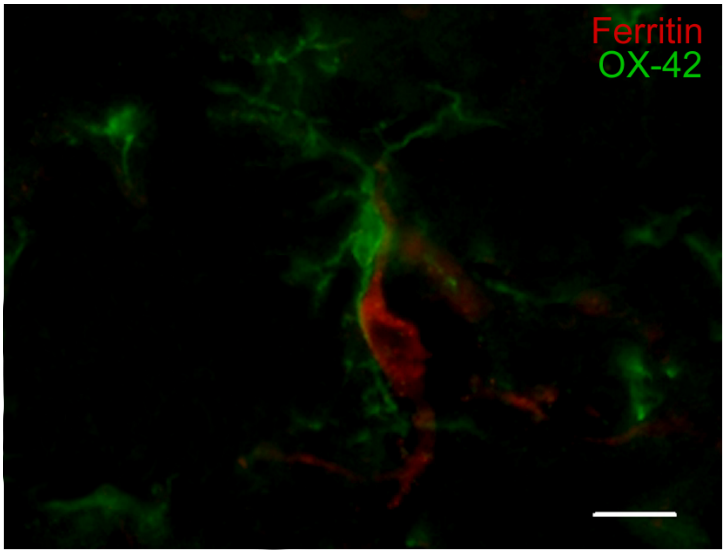

Figure 3-13. Cellular characterization of ferritin-positive (red) and OX-42-positive (green) cells within the rat facial nucleus. The majority of ferritin-immunoreactive cells did not co-localize with the microglial marker OX-42. Moreover, these cells had a larger cell nucleus and fewer processes compared to OX-42-positive microglia, fitting the morphological appearance of oligodendrocytes. Scale bar= 10μm

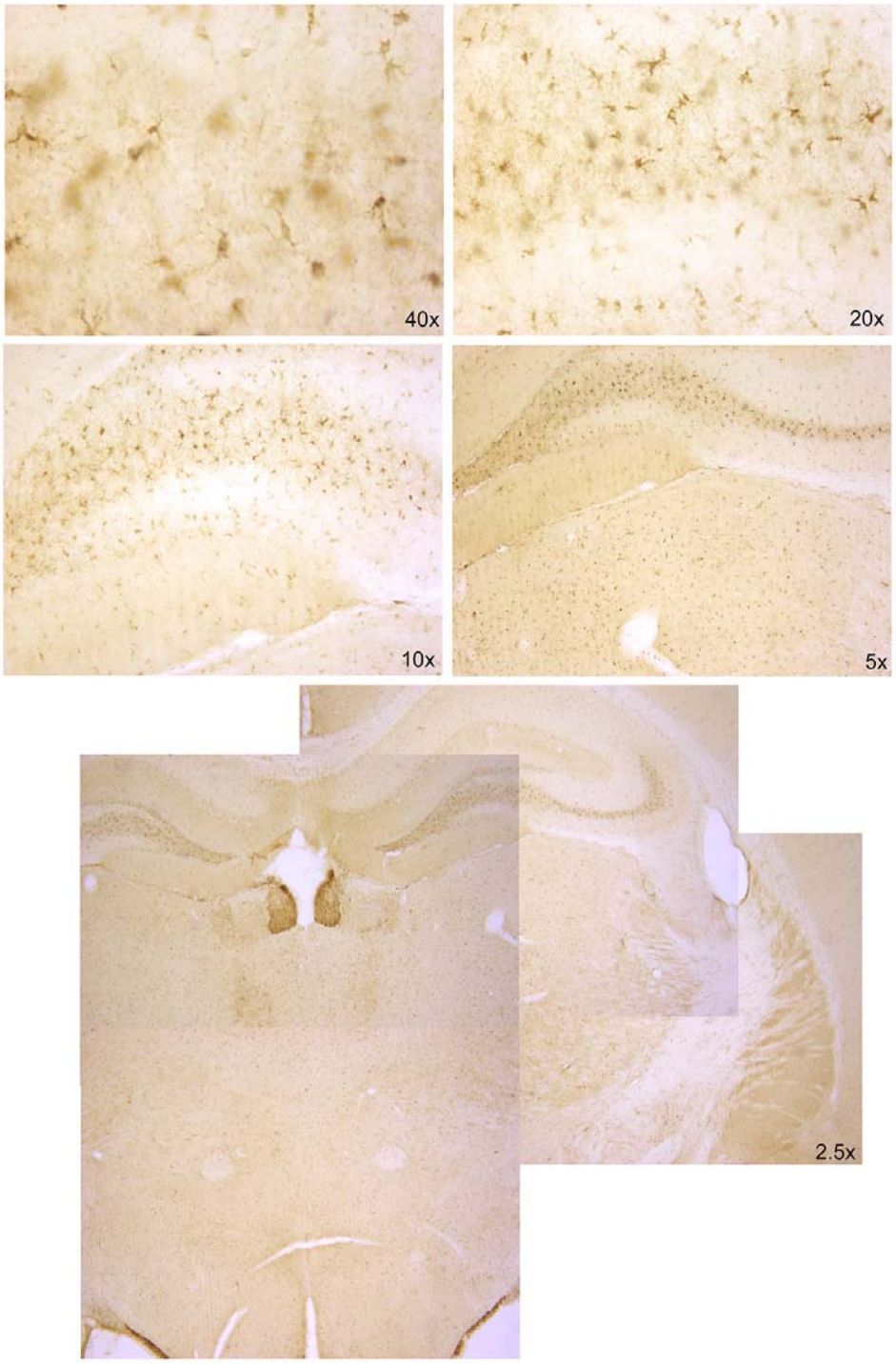

Figure 3-14. Ferritin positive cells are prevalent in the rat hippocampus. Ferritin immunohistochemistry on a coronal section of a 3-month-old rat at the level of the hippocampal formation. Composite of low magnification images (2.5x objective lens) show that the highest density of ferritin-positive cells are concentrated in the CA3 region of the hippocampus. At higher magnification, the morphology of these cells become apparent as that of microglia, with small cell bodies and numerous processes.

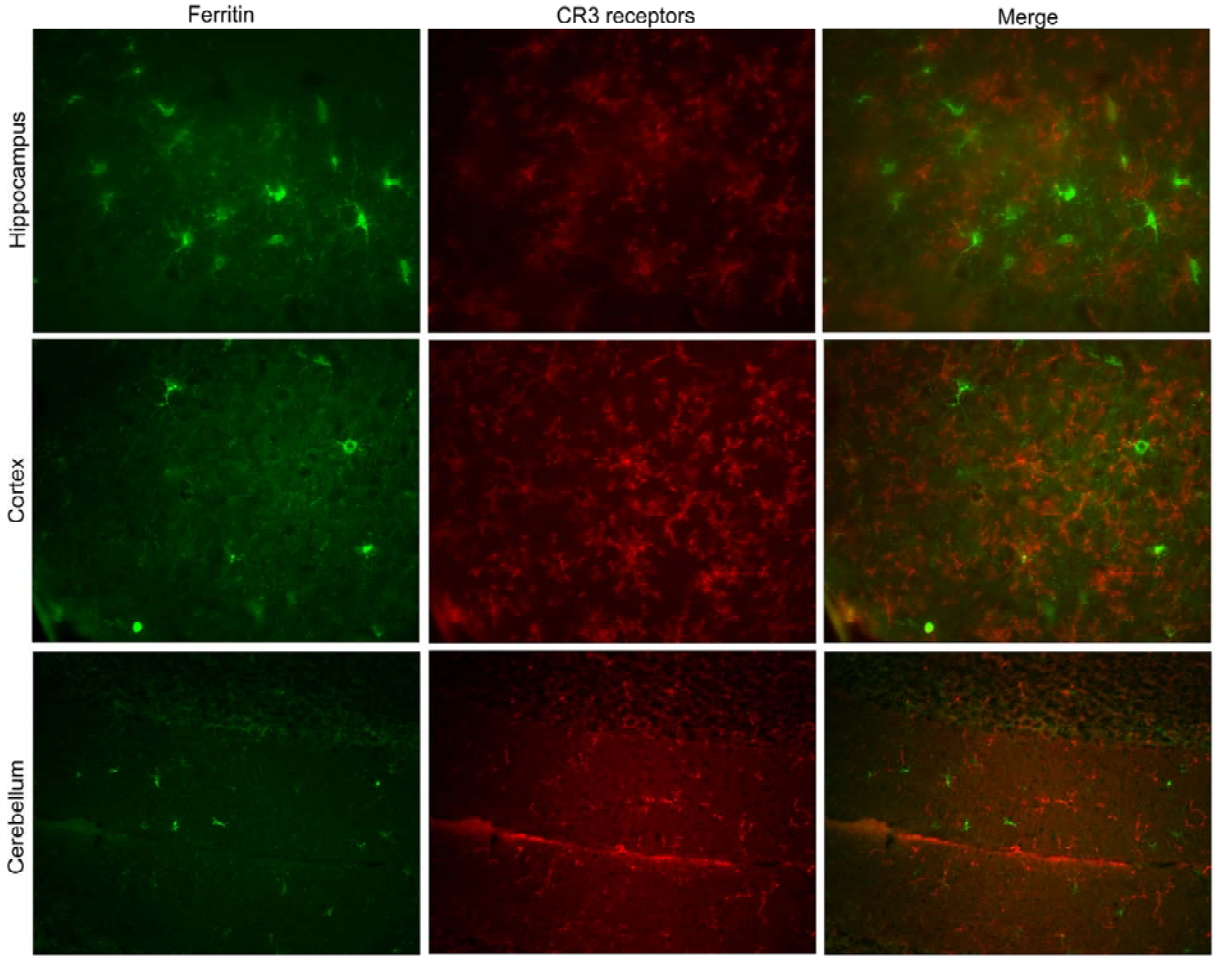

Figure 3-15. Double immunofluorescence staining for ferritin and CR3 receptors in the hippocampal, cortical, and cerebellar regions of a 30-month-old rat. L-ferritin-imunoreactive cells (green) do not colocalize with CR3-positive microglia (red) as shown in merged images. Ft-IR cells exhibit a larger and more densely stained perinuclear regions and fewer IR processes compared to OX-42-labeled microglia.

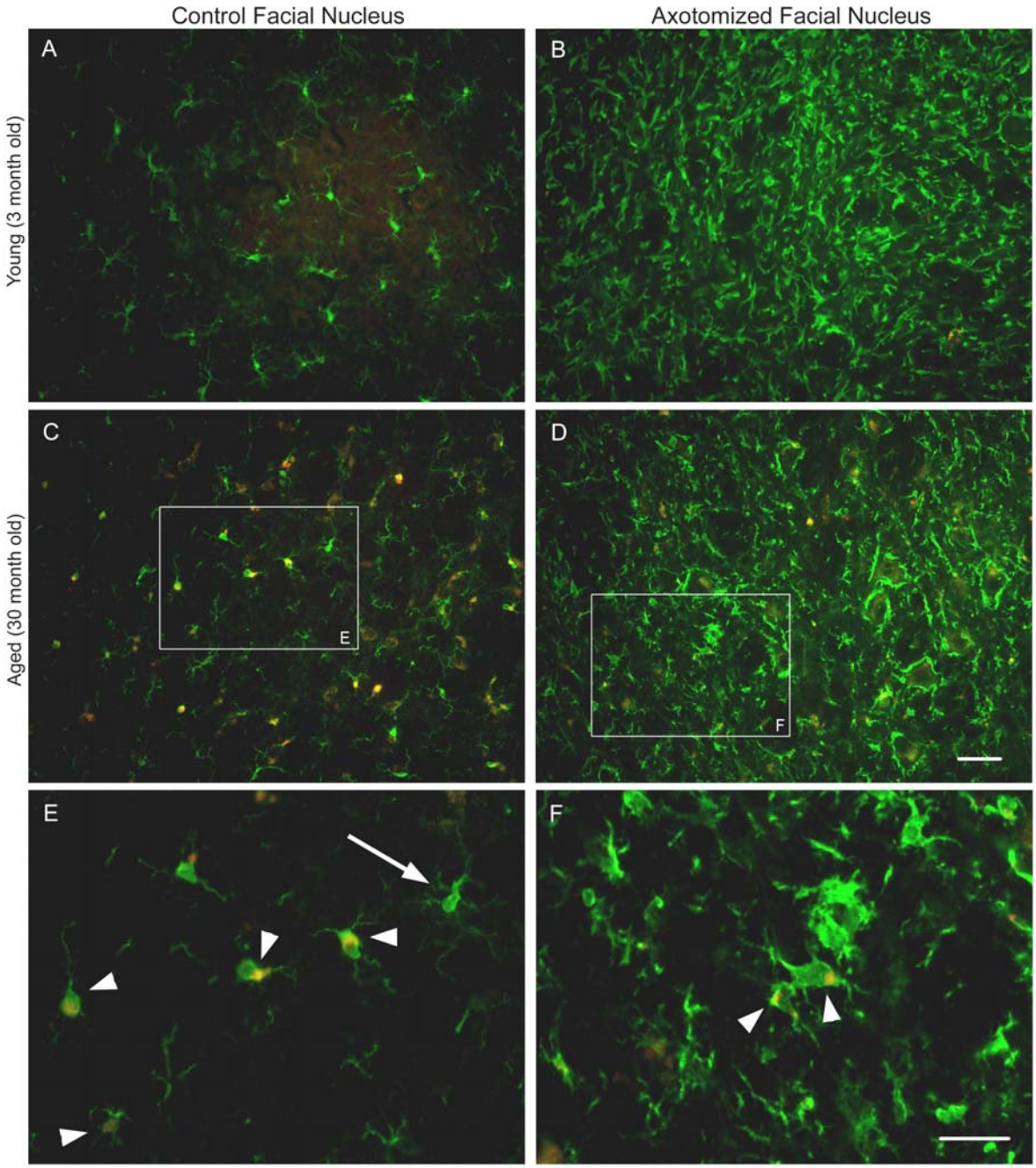

Figure 3-16. Immunofluorescence staining using Iba-1 (green) and ED1 (red) in the control (A, C) and axotomized (B, D) facial nuclei of a 3-month-old rat (A-B) and a 30-mo old rat (C-D) 10 days postaxotomy. There is no co-labeling between Iba-1 and ED1 immunoreactive microglia in younger brains (A-B). However, colocalization of the markers is readily visible (yellow) in aged tissues (C-D). (E-F), higher magnification of boxes in C-D. Note that ED1 immunoreactivity (red) is confined to the perinuclear region of OX-42 positive microglia (green). (E) ED1-positive microglia exhibit a dystrophic morphology (arrowhead) in the control facial nucleus compared to ED1-negative microglia (arrow). (F) The morphology of ED1-positive microglia in the axotomized FN (arrowhead) is indistinguishable from that of ED1-negative microglia. Scale bar = 100 μm (A-D), 20μm (E-F).

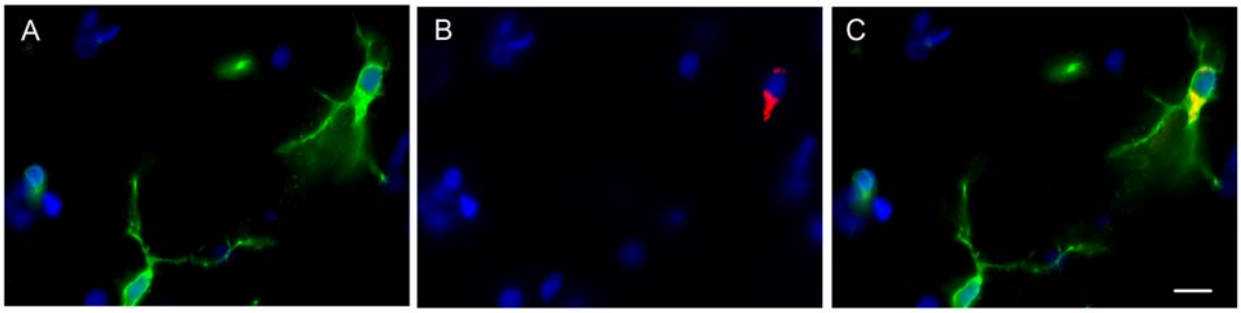

Figure 3-17. ED-1 immunoreactivity (red) is limited to the perinuclear region (B) of Iba-1-positive microglia (green; A). Yellow color in (C) indicates co-localization. DAPI-positive nuclear DNA is depicted in (A-C). Scale bar = 10 μm (A-C).

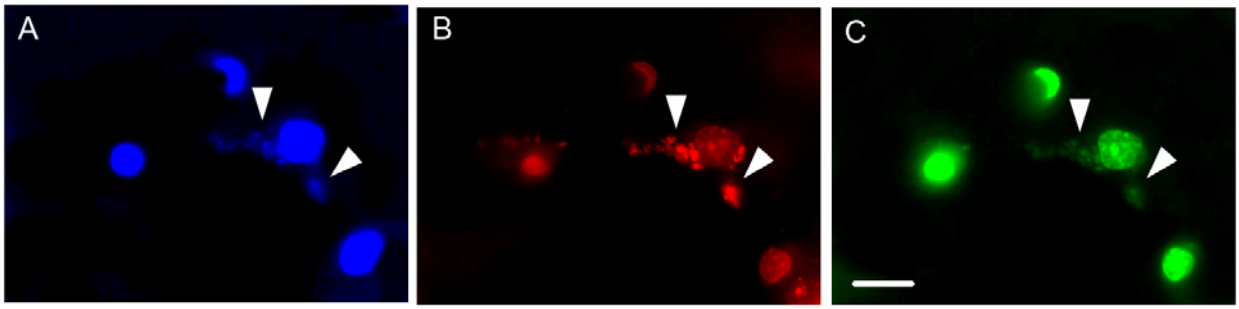

Figure 3-18. Autofluorescence of lipofuscin particles using ultraviolet (A), green (B), and blue (C) excitation lights (360-460, 490-570, and 440-490 nm, respectively). Scale bar= 20 μm (A-C). Lipofuscin granules (arrowhead) can be seen with various wavelengths of light in the same cell. Scale bar= 20 μm (A-C).

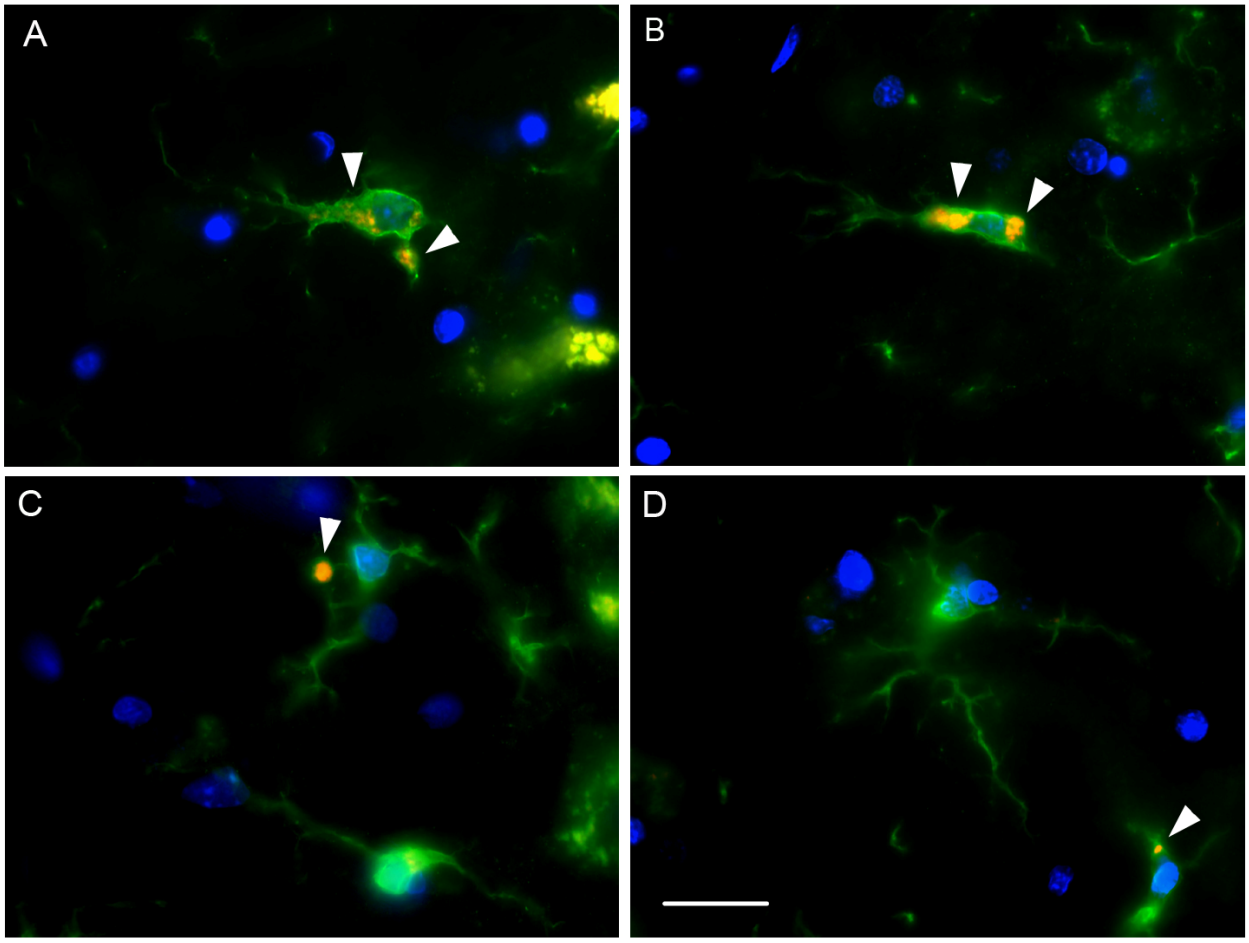

Figure 3-19. Lipofuscin granules accumulate in senescent dystrophic microglia of aged rats. Fluorescence staining using Iba-1 (green) and ED1 (red) immunohistochemical markers in the non-axotomized facial nucleus of a 30-month-old rat. Photomicrographs represent merged images taken with ultraviolet, green, and blue excitation lights. Cell in (A) is the merged image depicted in Fig. 3-18A-C. The majority of Iba-1 immunoreactive microglia (green) that exhibit signs of dystrophy are double labeled for lipofuscin (red), which appears yellow in merged images (A-C). Dystrophic morphologies in these cells include an abnormal enlargement of the perinuclear region (arrowhead in A-B), which often occurs in severely deramified microglia, and spheroid formation (C) at distal branches. (D) Representative image of the ramified morphology of lipofuscin-negative, OX-42-positive (green) microglia. DAPI-positive nuclear DNA is depicted in (A-D). Scale bar= 10 μm (A-D).

Table 3-4. Cell counts of immunoreactive microglia in the unoperated and axotomized facial nucleus†

	Young Group		Aged Group	
	Control F.N.	Axotomized F.N.	Control F.N.	Axotomized F.N.
Iba-1	10.05 ± 0.7	30.83 ± 10.6*	10.55 ± 0.13	30.70 ± 7.73*
Lipofuscin	0.3 ± 0.2	0.20 ± 0.11	2.28 ± 0.49**	1.68 ± 0.13**

† Values are expressed as the mean ± S.E.M. Symbols: F.N., facial nucleus; * $p < 0.05$ compared with the corresponding numbers in the unoperated facial nucleus; ** $p < 0.001$ compared with the corresponding numbers in younger animals.

CHAPTER 4
DISCUSSION AND CONCLUSION

Overview of Findings

The primary aim of this investigation was to compare and contrast degenerative morphological traits in microglial cells of both human and rodent brains. Our histological analyses provide evidence that although microglial degeneration is not a unique phenomenon to humans, the degree of structural deterioration that microglia undergo as a function of senescence in aging brains differs between humans and rats (see Table 4-1). In humans, microglial dystrophy appears to be an elaborated process commencing with thinning and deramification of distal processes followed by the formation of bulbous swellings along remaining branches, atrophy, and finally complete degeneration of the microglial cytoplasmic structure. We found that the end-stage of degeneration (cytorrhexis) is particularly widespread in cortical gray matter microglia of the early-stage Alzheimer's disease brain. In turn, dystrophic microglia of aged rats do not develop as many stages and/or severity of degeneration. Furthermore, ostensibly degenerative microglia in rodents exhibit a considerable enlargement of the cytoplasmic regions immediately adjacent to the cell's nucleus, the principal location for many organelles, including lysosomes. These so-called "pot bellies" are absent in dystrophic microglia of human brains. In regards to similarities, we noticed that dystrophic microglia in both human and rodent brains present primarily a deramified morphology. In some instances, spheroid-like structures along the remaining stripped-down processes can be found in both species.

In this chapter, I will address and interpret our findings taking into account the possibility that overtly dystrophic microglia of aged human brains may facilitate the pathogenicity of age-dependent neurodegenerative disorders, such as AD. In light of the differences we found between dystrophic microglia in human versus rat brains (Table 4-1), it seems worthy of note

that although rodents are also affected by deterioration of cellular and systemic functions that are associated with the normal aging process, no neurodegenerative disorder has ever been shown to occur spontaneously in rodents. Subsequently, I will consider here the possibility that one of the reasons why rodents do not develop neurodegenerative diseases is related to their lack of overtly dystrophic microglia. Moreover, the findings reported herein underscore the importance of a thorough evaluation of the microglial morphological status in order to appropriately assess their contribution to age-related neurodegeneration and neurodegenerative diseases. As a final point, our immunohistochemical analyses of senescent microglia also reduced the listing of potential causes of cytoplasmic degeneration by providing evidence that microglia immunoreactive for the iron storage protein ferritin are significantly more likely to exhibit dystrophic traits with aging than ferritin-negative microglia. The implication here is that the degeneration of microglial cytoplasmic structure may be the outcome of iron-mediated free-radical reactions.

Only a Subset of Microglial Cells Express L-rich Ferritin Proteins

It has long been known that microglial cells form a heterogeneous cell population within the CNS, both in terms of morphological features and present functional status. More recently, subsets of microglia that selectively express certain antigens have further increased our knowledge of the complexity of the parenchymal microglial pool. For instance, expression of such epitopes as the 5D4 keratan sulfate proteoglycan (Bertolotto et al. 1998), the membrane-bound scavenger receptor CD163 (Roberts et al. 2004), the leukocyte chemotactic factor and the leukocyte common antigen (Mittelbronn et al. 2001) as well as the hematopoietic stem cell marker CD34 (Wirenfeldt et al. 2005) have all been shown to identify a subpopulation of microglial cells in the normal, diseased, and injured CNS. The immunohistochemical results we report herein support the concept of microglial cells as a specialized cell population of the CNS

by showing that only a subset of microglia participate in long-term iron storage via the expression of L-rich ferritin proteins. We hypothesize that the reason only a subset of microglial cells participate in prolonged iron storage is to minimize the potential for iron-dependent oxidative damage in ferritin-positive microglia.

Potential Link between Iron Storage, Senescence and Microglial Dystrophy

In our immunohistochemical analyses of human brain specimens from elderly and AD subjects, we found that microglial degeneration appears to be associated with iron-mediated oxidative stress by providing evidence that L-ferritin immunoreactive microglia are particularly susceptible to dystrophic changes, especially in the aged brain where more than 60% of L-Ft-positive microglia exhibited signs of cytoplasmic deterioration. Similar findings were obtained in tissue specimens from HD patients and the r6/2 mouse model of HD (Simmons et al. 2007). From these results we concluded that both long-term iron storage and cell senescence contribute to microglial dystrophy.

One potential mechanism by which iron storage and senescence may interact relates to the age-related increase in ferritin-to-iron ratio. In young animals, when iron levels are relatively low, ferritin expression efficiently maintains iron in a non-reactive form due to the high ferritin-to-iron ratio, but as the brain ages and accumulates iron, ferritin becomes overloaded with iron and increased ferritin levels may not be sufficient to contain the elevated iron concentrations (Kaur et al., 2007). The iron saturation of ferritin proteins in older animals would likely enhance the risk of iron release during ferritin turnover (Kaur et al., 2007), thus increasing the probability of iron-induced oxidative damage. On the other hand, microglial dystrophy may be the consequence of improper cellular functioning due to intrinsic senescence mechanisms in ferritin-positive microglia. As reported earlier, microglia undergo age-related changes in metabolic

activity, including a decrease in proteolytic activity and a higher production of ROS (Streit et al. 2008). An extension of this premise in the context of the current study is the possibility that senescent microglia gradually lose their ability to maintain viable ferritin-bound iron stores and to fight extracellular and intracellular stressors, all of which could result in greater vulnerability to degeneration and/or death.

The microtubule network is probably the first to be affected by the unwanted release of iron from ferritin proteins due primarily to two factors: 1) Ferritin molecules bound to microtubules contain twice as many iron atoms compared to unbound ferritin (Hasan et al., 2006); and 2) $OH^{\bullet}$ generated by the reaction of labile Fe^{2+} with H_2O_2, which is controlled in large part by microglia, is the most reactive and short-lived ROS, capable of near instant oxidation of nearby molecules (Kruszewski 2003). Thus, the high iron concentration of microtubule-bound ferritin proteins and their close proximity to microtubules increase the susceptibility of the microtubule network to iron-catalyzed oxidative stress reactions**.** This premise may account, at least in part, for the degenerative changes observed in microglial cytoplasmic structure, of which their microtubule-rich processes seem to be the most vulnerable.

Microglial Cells are Vulnerable to Oxidative Stress Reactions in Aged Brains

Because oxidative stress is the outcome of an inadequate balance between production and elimination of ROS, a diminished microglial antioxidant capacity may be necessary in order for microglial dystrophy to occur. Immunocytochemical studies of the antioxidative capacity of microglial cells have revealed that among other neural cells microglia are strongly immunoreactive for glutathione peroxidase (GPx), an enzyme that uses glutathione to reduce H_2O_2 to water (Hirrlinger et al. 2000; Lindenau et al. 1998). The predominance of this antioxidant system in microglia pinpoints the potentially deleterious effects of iron-mediated

oxidative stress and the need for endogenous protective mechanisms. It is not yet known whether microglial GPx potential is maintained at sufficient levels in the aged brain to account for the age-related increase in brain iron levels.

Despite the lack of evidence for an altered microglial antioxidative potential with aging, oxidative stress markers have been identified in microglia. Specifically, the reactive carbonyl crotonaldehyde, which is generated during lipid peroxidation, localizes in microglial cells in the AD brain (Kawaguchi-Niida et al. 2006). Moreover, striatum microglia of aged (> 11 weeks), but not young, R6/2 mice (a mouse model of Huntington's disease) was found to be immunoreactive for 8-OHdG, a DNA base oxidized in free radical reactions by $^{\bullet}OH$ (Simmons et al. 2007). Taken together, these findings suggest that the microglial antioxidative capacity may be insufficient in neutralizing ROS within the aging brain, where senescence microglia prevail.

In general, every antioxidative protective biomolecule (e.g., GPx) has at least one target oxidant molecule (e.g., H_2O_2), thus providing an efficient means for ROS detoxification. The exception to this is $^{\bullet}OH$, which is produced from the interaction of Fe^{2+} with H_2O_2 and is extremely reactive. Mitochondrial reactions are the main cellular sites of H_2O_2 production and dystrophic microglia have been shown to contain degenerated mitochondria (Wierzba-Bobrowicz T et al. 2004). Activated microglial cells are also capable of producing H_2O_2 by the activity of the enzyme NADPH oxidase at the cell membrane (Twig et al. 2001). As a nonpolar molecule, H_2O_2 is able to diffuse across membranes. Hence, chronic microglial activation may lead to increased H_2O_2 exposure intracellularly. Taken together, these observations suggest that L-ferritin-positive microglia are highly dependent on iron and H_2O_2 homeostasis to prevent iron-induced oxidative damage.

Hallmarks of Microglial Degeneration in Human and Rodent Brains

Our meticulous morphological analyses of immunoreactive microglia under the light microscope revealed important characteristics between dystrophic microglia in human and rodent brains. These findings, which have been previously described, are summarized in Table 4-1. Here, I will place emphasis on the defining characteristics that distinguish dystrophic microglia in human brains from dystrophic microglia in rodents. In both species, cytorrhexis, or the fragmentation of the cell's cytoplasm into two or more parts, appears to be the most severe form of cytoplasmic degeneration. Whereas cytorrhectic microglia are rare in rodents of all ages and in tissue specimens from young human adults, they are prevalent in aged human brains, especially in AD patients. Cytorrhexis in microglia range in severity from a relatively small nick on a distal process to nearly complete obliteration of the cell's cytoplasmic structure as shown in Fig. 3-6. The blatantly abnormal morphology of these cells suggests that they are in the process of degeneration, though the underlying mechanisms by which cytorrhectic microglia execute cellular demise are not presently known.

Typically, pathways leading to cell death are discussed as discrete, independent entities that are separated dichotomously into either apoptosis or necrosis. Just like the initial morphological characterization of cytorrhexis reported herein, the detection of apoptotic and necrotic cell death mechanisms were initially based on cell morphology by using light and electron microscopy (Kerr et al. 1972). Nowadays, morphological features that distinguish apoptosis from necrosis as well as their biochemical and physiological characteristics are well-characterized. Apoptosis is a form of caspase-mediated cell death that exhibit, among other features, chromatin condensation and cytoplasmic fragmentation into apoptotic vesicles (see Table 4-2). Apoptotic cells are readily recognized and phagocytosed by tissue macrophages resulting in an anti-inflammatory outcome. Necrosis, on the other hand, describes the

postmortem observation of dead cells that have lost membrane integrity from cell swelling and subsequent lysis (Table 4-2). *In vivo* necrotic cell death is often associated with extensive tissue damage resulting in intense inflammatory reaction.

Although dystrophic microglia share some features with apoptotic cells and necrotic cells (as summarized in Table 4-2), they do not wholly conform to either cell death pathway. In particular, cytorrhexis (i.e., end-stage dystrophy) affect individual microglial cells (akin to apoptosis) but do not form apoptotic cell bodies (unlike apoptosis). Moreover, preliminary immunohistochemical studies using the terminal deoxynucleotidyl transferase-mediated dUTP nick end labeling (TUNEL) method to visualize DNA fragmentation in individual nuclei, which is often used as a defining characteristic of apoptotic cells, yielded only negative results in previous histological preparations from our laboratory (data not shown). Notably, although tissue debris resulting from either apoptosis or necrosis is phagocytosed by macrophages, no evidence of activated microglia and/or macrophages are observed in the vicinity of dystrophic microglia. In all, because so little is currently known about the biochemical pathways leading to microglial cytorrhexis, it seems unreasonable to classify cytorrhectic microglia into a specific mode of cell death just yet.

Despite the widespread use of a dichotomous classification of cell death into either apoptosis or necrosis, recent observations suggest that the true biological spectrum of cell death is much more diverse than initially appreciated. Other pathways of cell death identified thus far include autophagy, oncosis, and pyroptosis, among others. Today it is also evident that the molecular processes that mediate cell death may actually overlap considerably in dying cells. Futher investigations into molecular and biochemical alterations in dystrophic microglia is likely

to aid in the elucidation of whether dystrophic microglia are degenerating based on yet unidentified pathways or on a combination of known cell death programs.

In the aged rodent brain, cytorrhectic microglia are infrequent. Instead, overtly dystrophic microglia in aged rats exhibit a gross enlargement of their perinuclear region, which under fluorescence microscopy has been determined to contain autofluorescent LF granules. In turn, in our immunohistochemical analyses no LF-positive microglia were detected in human brains. It is not yet known what the cellular and physiological relevance of this discrepancy is. Labile iron acts as a catalyst in LF formation and accumulation within the lysosomal compartment of senescence cells (Jolly et al. 1995; Terman and Brunck 2004), the same site of normal Ft turnover. It is possible, therefore, that senescent microglia become inadequate in maintaining their intracellular ferritin-to-iron homeostasis, probably due to an impairment of their degradative pathways (Stolzing and Grune 2003) that terminates in labile iron incidence within lysosomes.

For yet unknown reasons, it is possible that rats have a propensity to accrue lipid-laden LF particles, and the resulting labile iron from lysosomes may catalyze LF-formation instead of Fenton-type reactions, which is thought to occur in humans. This hypothesis would provide a basis as to why cytorrhectic (i.e., degenerating) microglia are found primarily in humans while LF-positive microglia are predominant in rodents. Altogether, it seems that even though the morphological features of dystrophic microglia differ somewhat between humans and rats, they are still interlinked by their association with iron chemistry.

Microglial Dystrophy Is Not Due to Postmortem Tissue Autolysis

Our immunohistochemical analyses revealed that the morphological signs of microglial degeneration in L-ferritin positive microglia were manifested by shortening, thinning, twisting,

and fragmentation of processes. These changes were in accordance with previous reports of microglial degeneration cited in the literature (see Table 1-2). In order to determine whether these aberrant morphological characteristics could actually be an artifact of postmortem tissue autolysis, we compared the morphology of ferritin-positive microglia in tissues with PMI ranging from 3 to 20 hours. Our investigation provided no correlation between microglial dystrophy and increased postmortem delay, supporting the idea that microglial degeneration is a true pathophysiological event. Additional support for this notion is derived from our recent observations in an animal model of amyotrophic lateral sclerosis (where autolysis is not an issue) demonstrating widespread microglial dystrophy in areas undergoing motoneuron degeneration (Fendrick et al. 2007).

Dystrophic Microglia Are Most Prevalent in the Alzheimer's Disease Brain Than in Age-Matched Non-Demented Control Tissues

In our immunohistological characterization of dystrophic microglia, it became readily apparent that the incidence and severity of microglial dystrophy was considerably greater in AD tissues compared to young and even age-matched controls. Why dystrophic microglia are preferentially localized in the AD brain is presently unknown, however. The predominance of specific dystrophic morphologies (i.e., formation of spheroid-like protuberances [bulbous swellings] along major processes and multicellular clusters) in brain tissues that have extracellular Aβ aggregates in common (HPC and AD tissues), raised the possibility that the proximity to histopathological hallmarks of AD played a contributory role in the demise of microglial cells. To address this question, we first investigated whether these dystrophic changes could be linked to the amyloid-β deposition that is present in both of these tissues.

Although both HPC and AD tissues contained Aβ deposits, the incidence of L-Ft-positive dystrophic microglia was significantly higher in AD tissues, which suggests that Aβ deposition alone does not seem to predispose microglial cells to degeneration. Furthermore, we found no correlation between dystrophic changes and proximity to SPs for both HLA-DR- and ferritin-positive microglia. Taken together, it seems likely that an altered homeostatic milieu, instead of SP accumulation *per se*, may play a more significant role in the occurrence of dystrophic microglia. Of interest, changes in calcium and iron homeostasis, as well as higher indices of oxidative stress markers have been reported in AD brains (Selkoe 2004), the significance of which to microglial dystrophy remains unknown. On one side, it is possible that senescent microglia contribute to the altered brain homeostasis that occurs in AD tissues due to altered microglial functioning. Alternatively, senescent microglia may be particularly vulnerable to such changes, which may then predispose this subset of older microglia to degeneration secondarily.

In regards to the relationship between NFTs and dystrophic microglia, our analysis was hindered by the fact that no positive immunohistochemical signal was obtained for NFTs in any of the tissues used in this study. These negative data was corroborated by evaluating the morphological characteristics of the 6F3D-positive senile plaques. In all tissues examined, both HPC and AD, we found that the SPs had a diffuse morphology and were distributed primarily in the gray matter region of the SFG. Additionally, we were unable to stain these SPs with Congo Red. In all, these findings suggest that the AD tissues under study can be situated in the early stages of the disease (see Tables 1-3 and 1-4).

Since dystrophic microglia are prevalent in early AD, it is possible that microglial degeneration actually contributes to AD pathogenesis and/or progression. Further studies are necessary to delineate the precise effect of degenerating microglia in AD brains. Since AD

dementia is best correlated with loss of synapses rather than the accumulation of protein aggregates (DeKosky and Scheff 1990), it is possible that with aging and the ensuing progressive accumulation of dystrophic microglia in the brain parenchyma, results in more and more widespread malnourishment of neurons, which could first have an effect on the maintenance of synapses and subsequently on the well-being of neurons themselves.

The current findings offer additional evidence for the microglial dysfunction hypothesis of AD (Streit 2004) by demonstrating a direct relationship between microglial dystrophy and the expression of L-rich ferritin proteins. The dysfunction hypothesis states that a principal cause for development for aging-associated neurodegeneration is found in an age-related decline in microglial neuroprotection which occurs because microglial cells themselves are subject to cellular senescence, as evidenced primarily by the increased incidence of dystrophic microglia in aged brains. The current findings offer a possible mechanism as to why dystrophic changes occur in microglia, namely, that dystrophy is a result of iron-mediated oxidative damage.

Dystrophic Microglia are Associated with Aging and Not Injury Conditions in Aged Rats

Axotomy by brief constriction of fibre tracts of FMNs produces a mild neuronal injury that induces a transient microglial activation response within the FNu (Graeber et al. 1988a; Graeber et al. 1988b; Moran and Graeber 2004). Because there is no cell death (i.e., injured motoneurons regenerate their peripheral axons), activated microglial cells normally do not reach the advanced phagocytic stage of activation (Streit et al. 2000). In order to determine whether the degree of microglial activation to such reversible neuronal injury is disregulated in dystrophic microglia of aged rats, we analyzed microglial immunoreactivity to the macrophage-specific marker ED1 in FNu sections from axotomized young and aged rats. The antigen recognized by ED1, which is the rat homologue of human CD68, is expressed on the lysosomal membranes of

phagocytic (i.e. myeloid) cells and is often used as a marker of phagocytic activity (Dijkstra et al. 1985; Flaris and Hickey 1992). Macrophages (constitutively ED-1-positive) and microglia (facultatively ED1-positive) are functionally and developmentally related, expressing a similar repertoire of genes (Sedgwick and al. 1991).

First, we noticed occasional ED1-immunoreactive cells but mostly in the control FNu of aged rats (not the axotomized side as expected). Aging appears to promote ED1 immunoreactivity in rats after cortical stab injury (Kyrkanides et al. 2001) and stroke (Badan et al. 2003a; Badan et al. 2003b). However, since in the rodent FN axotomy model there is no disruption of the BBB (Moran and Graeber 2004), it seemed unlikely that ED1-positive cells would be present in the axotomized FNu, especially in the uninjured side. The possibility that the rapid microgliosis observed in the lesioned FNu is dependent on the recruitment of blood-borne progenitors (i.e., ED1-positive macrophages) has been recently dismissed in a study using chimeric animals obtained by parabiosis (Ajami et al. 2007). More specifically, the authors reported that although rare ED-1-positive cells were present in the axotomized FNu area, they were located inside blood vessels and not in the brain parenchyma (Ajami et al. 2007).

Upon closer examination of the ostensibly ED1 immunoreactive microglia present in aged rat tissue sections, it was noticeable that immunofluorescence was achieved irrespective of the fluorophore used, raising the possibility that the positive signal was in fact derived from autofluorescence. Instead of disregarding these data as artifact, we analyzed the characteristics of these seemingly autofluorescent microglia. Based on spectral properties and cellular localization, it was determined that the autofluorescent material was derived from intracellular LF granules. Lipofuscin, or age pigment, is a heterogeneous nondegradable lipophilic material that accumulate within lysosomal compartments as residual bodies (Brunk and Terman 2002; Terman

and Brunk 2004). We concluded, therefore, that the combined effect of staining lysosomal membrane proteins with the autofluorescent signal from lysosomal LF particles led to our conspicuous detection of LF material in microglial cells of aged rats.

Our in-depth analysis of these 'autofluorescent' microglia also led to the discovery that lipofuscin-positive microglia, observed primarily in the non-axotomized FNu of aged rats, exhibit dystrophic morphological characteristics. In particular, LF-positive microglia presented deramification of distal processes, an abnormal swelling of the perinuclear region and spheroid-formation, all of which were readily noticeable in the control FNu. Because the axotomized FNu is populated by hypertrophic microglia, which also exhibit deramification patterns and an enlargement of the cell body, the differentiation between dystrophic and activated microglia was significantly more difficult to achieve. Nonetheless, the finding of LF particles in microglial cells seems to be in itself a strong enough indicator of microglial dystrophy in aged rats as highlighted below.

Lipofuscin accumulates progressively with advancing age, which explains why autofluorescent LF signals were absent in young rat brain tissues. Interestingly, we observed only a neglibible number of LF-positive microglia in the axotomized FNu of aged rats. Because LF accumulation is usually seen in cells that have reached a postmitotic phase (Brunk and Terman 2002), our results can be interpreted as a sign that LF-positive microglial cells are, in fact, senescent cells. That is, the low numbers of LF-positive microglia in the axotomized FNu may stem from the fact that upon activation conditions that demand cell proliferation (e.g., FN axotomy), LF-positive microglia, which are incapable of undergoing cell proliferation, are outnumbered by mitotic LF-negative microglia. Altogether, our findings suggest that senescent, dystrophic microglia in aged rats are manifested predominantly as LF-positive microglia. LF

granules has been previously shown to accumulate in aging microglia from rodent brains (Sierra et al. 2007; Xu et al. 2008), although this study is the first known account of the probable association between LF accumulation with microglial senescence and dystrophy.

Ferritin Immunoreactivity Is Not Upregulated in Activated Microglial Cells

Because Ft immunohistochemistry has been used in the past to identify activated microglial cells (Grundke-Iqbal et al. 1990; Kaneko et al. 1989) and activated microglia share some morphological similarities with dystrophic microglia, namely atrophy of distal branches (Table 4-1;(Lopes et al. 2008; Streit 2006), a secondary goal of this thesis was to investigate whether microglial activation induces Ft expression. To answer this question we utilized the FN axotomy paradigm, since the microglial activation response in this model is well-characterized (Graeber et al. 1988a; Graeber et al. 1988b; Moran and Graeber 2004; Streit et al. 2000).

Previously, the rat FNu has been shown to express very low levels of L-Ft mRNA (Han et al. 2002), while to our knowledge the present study is the first to report on L-Ft protein levels in the rat FNu. We hypothesized that if Ft immunoreactivity is indeed supposed to specifically label activated microglial cells, Ft expression should be upregulated during activation conditions. Our histological analysis revealed that microglial Ft expression is not affected by injury-induced activation conditions by comparison of Ft-staining patterns between axotomized and uninjured sides of the FNu from both young and aged rats. The only difference found was a higher level of Ft immunoreactivity in aged animals. We also noticed that the majority of Ft-IR cells found in either side of the rat FNu exhibited morphological characteristics of oligodendrocytes, while only occasionally Ft-positive microglial cells were identified in the aged rat FNu.

Several observations can account for such findings. First, cellular Ft expression is regulated primarily by iron availability at the posttranslational level, with high iron levels

inducing Ft upregulation (Hentze et al. 2004). Since brain iron levels increase steadily with advancing age (Benkovic and Connor 1993; Focht et al. 1997), the increase in Ft expression with aging is attributed to ferritin's role as an intracellular scavenger of excess iron (Focht et al. 1997). Second, it is possible that in the rat FNu most L-Ft proteins are expressed primarily by oligodendrocytes instead of microglial cells due to an intrinsic region- and species-specific Ft subunit distribution (Benkovic and Connor 1993; Connor et al. 1994). Third, axotomy of the FN has been shown to upregulate the expression of TfR, which are responsible for an increased cellular iron uptake in regenerating FMNs (Graeber et al. 1989). TfR expression is inversely related to Ft expression, that is TfR levels increase in conditions of low iron availability (Harrison and Arosio 1996), thus providing another explanation for the low levels of Ft immunoreactivity in the rat FNu observed in the present study. Overall, we observed that activation conditions were insufficient to upregulate Ft expression levels in microglia. Aging and the resulting increase in brain iron levels, on the other hand, appeared to promote microglial Ft expression within the rat FNu. In all, our data suggests that ferritin immunoreactivity is a poor indicator of activated microglial cells.

Concluding Remarks

In summary, although ferritin immunohistochemistry has been known for its use as a generic microglial marker (Grundke-Iqbal et al. 1990; Kaneko et al. 1989), our current results suggest that ferritin immunoreactivity could be used more specifically as a selective marker of those microglial cells that are in danger of being lost. An extension of the current findings suggest a possible mechanism as to why dystrophic changes occur in microglia, namely, that dystrophy is a result of iron-mediated oxidative damage.

In our morphological analyses of microglial cells in the normal and diseased human brain, we found that ferritin-positive dystrophic microglia predominated in the aged brain, particularly in postmortem tissue from Alzheimer's disease brains. Because microglial degeneration is widespread in tissues undergoing age-related neurodegeneration associated with disease conditions (i.e., AD), it is speculated that dystrophic microglia may participate in the disease process. This hypothesis is based on the probability that the morphological abnormalities that characterize dystrophic microglia likely reflect aberrant functional states. More specifically, degeneration of the microglial cytoplasmic structure would clearly be an impediment to the normal surveillance functions of these cells, particularly by affecting the structural identity of ramified microglia and consequently impairing constitutive neuroprotective functions in such dystrophic microglia.

A secondary aim of this thesis was to determine whether the graded repertoire of microglial activation is misregulated in aged animals to permit activated microglia to reach the phagocytic stage, which should not occur in response to such a reversible neuronal injury. In this study, we also provided evidence that neither Ft nor ED1 immunoreactivity is affected by mildly acute activation conditions in microglial cells of either young or aged rats. On the other hand, we report on the discovery of lipid-laden autofluorescent granules (i.e., lipofuscin) in predominantly dystrophic microglia of aged rats.

Collectively, our findings provide a theoretical basis on which to probe the specific molecular mechanisms that contribute to microglial senescence. More specifically, iron dyshomeostasis emerged as a potential culprit in the degenerative potential of microglial cells in both aged human and rodent brains. Further studies are required to investigate the extent to which alterations in ferritin and iron homeostasis may correlate with microglial dystrophy.

Table 4.1. Comparison of dystrophic morphological characteristics between humans and rodents

DYSTROPHIC MORPHOLOGIES	HUMAN	RODENT
Deramification	+	+
Thinning/Tortuous Processes	+	–
Spheroid Formation	+	±
Cell Clusters	+	–
Cytorrhexis	+	–
Lipofuscin Accumulation	–	+
Enlargement of perinuclear cytoplasm	±	+

Symbols: –, absent; ±, sometimes present; +, common.

Table 4.2. Differential features between dystrophy, apoptosis, and necrosis

Microglial Dystrophy	Apoptosis	Necrosis
- No loss of membrane integrity	- Membrane blebbing, but no loss of membrane integrity	- Loss of membrane integrity
- Begins with decrease in arborization and volume of cell processes	- Begins with shrinking of cytoplasm	- Begins with swelling of cytoplasm and mitochondria
- Ends with random fragmentation of the cytoplasm (cytorrhexis)	- Ends with fragmentation of cells into smaller cell bodies	- Ends with total cell lysis
- No vesicle formation	- Formation of membrane-bound vesicles (apoptotic bodies)	- No vesicle formation, complete lysis
- Chromatin condensation: Unknown	- Chromatin condensation	- No chromatin condensation
- Intact Nucleus	- Non-random DNA fragmentation	- Random DNA fragmentation
- Degenerating mitochondria reported	- Mitochondria becomes leaky due to pore formation involving proteins of the bcl-2 family	- Disintegration (swelling) of organelles, including mitochondria
- Caspase-independent	- Caspase-dependent	- Caspase-independent
- Affects individual cells	- Affects individual cells	- Affects groups of contiguous cells
- Unknown if dying cells are phagocytosed	- Phagocytosis by macrophages	- Phagocytosis by macrophages
- Unknown if energy is required	- Energy (ATP)-dependent	- Energy (ATP)-independent
- Anti-inflammatory	- Anti-inflammatory	- Pro-inflammatory

LIST OF REFERENCES

Ajami B, Bennett JL, Krieger C, Tezlaff W, Rossi FMV. 2007. Local self-renewal can sustain CNS microglia maintenance and function throughout adult life. Nat Neurosci 10(12):1538-1543.

Arriagada PV, Marzloff K, Hyman BT. 1992. Distribution of Alzheimer-type pathologic changes in nondemented elderly individuals matches the pattern in Alzheimer's disease. Neurology 42:1681-1688.

Badan I, Buchhold B, Hamm A. 2003a. Accelerated glial reactivity to stroke in aged rats correlates with reduced functional recovery. J Cereb Blood Flow Metab 23:845-854.

Badan I, Platt D, Kessler C. 2003b. Temporal dynamics of degenerative and regenerative events associated with cerebral ischemia in aged rats. Gerontology 49:356-365.

Bali P, Zak O, Aisen P. 1991. A new role for the transferrin receptor in the release of iron from transferrin. Biochemistry 30:324-328.

Bartzokis G, Beckson M, Hance D, Marx P, Foster J, Marder S. 1997. MR evaluation of age-related increase of brain iron in young adult and older normal males. Magn Reson Imaging 15(29):35.

Bartzokis G, Cummings J, Perlman S, Hance DB, Mintz J. 1999. Increased basal ganglia iron levels in Huntington's disease. Arch Neurol 56(5):569-74.

Ben-Porath I, Weinberg RA. 2005. The signals and pathways activating cellular senescence. Int J Biochem Cell Biol 37:961-76.

Benkovic SA, Connor JR. 1993. Ferritin, transferrin, and iron in selected regions of the adult and aged rat brain. J Comp Neurol 338:97-113.

Bertolotto A, Agresti C, Castello A, Manzardo E, Riccio A. 1998. 5D4 keratan sulfate epitope identifies a subset of ramified microglia in normal central nervous system parenchyma. J Neuroimmunol 85:69-77.

Blinzinger K, Kreutzberg G. 1968. Displacement of synaptic terminals from regenerating motoneurons by microglial cells. Z Zellforsch 85:145-157.

Bodles AM, Barger SW. 2004. Cytokines and the aging brain - what we don't know might help us. Trends Neurosci 27:621-626.

Braak H, Braak E. 1991. Neuropathological staging of Alzheimer-related changes. Acta Neuropathol 82:239-259.

Brunk UT, Terman A. 2002. Lipofuscin: mechanisms of age-related accumulation and influence on cell function. Free Rad Biol Med 33(5):611-619.

Buckwalter MS, Wyss-Coray T. 2004. Modelling neuroinflammatory phenotypes in vivo. J Neuroinflamm 1:10.

Carpenter AF, Carpenter PW, Markesbery WR. 1993. Morphometric analysis of microglia in Alzheimer's disease. J Neuropath Exp Neurol 52(6):601-608.

Cheepsunthorn P, Palmer C, Connor JR. 1998. Cellular distribution of ferritin subunits in postnatal rat brain. J Comp Neurol 400:73-86.

Cheepsunthorn P, Palmer C, Menzies S, Roberts RL, Connor JR. 2001. Hypoxic/ischemic insult alters ferritin expression and myelination in neonatal rat brains. J Comp Neurol 431:382-396.

Conde JR, Streit WJ. 2005. Effect of aging on the microglial response to peripheral nerve injury. Neurobiol Aging. 27(10):1451-61.

Conde JR, Streit WJ. 2006. Microglia in the aging brain. J Neuropathol Exp Neurol 65(3):199-203.

Connor JR, Boeshore KL, Benkovic SA, Menzies SL. 1994. Isoforms of ferritin have a specific cellular distribution in the brain. J Neurosci Res 37:461-465.

Connor JR, Menzies SL. 1995. Cellular management of iron in the brain. J Neurol Sci 134 (Suppl):33-44.

Connor JR, Menzies SL, St Martin SM, Mufson EJ. 1990. Cellular distribution of transferrin, ferritin and iron in normal and aged brain. J Neurosci 27:595-611.

Connor JR, Snyder BS, Arosio P, Loeffler DA, LeWitt P. 1995. A quantitative analysis of isoferritins in select regions of aged, parkinsonian, and Alzheimer's disease brains. J Neurochem 65:717-724.

Crisby M, Ralman SM, Sylven C, Winblad B, Schultzberg M. 2004. Effects of high cholesterol diet on gliosis in apolipoprotein E knockout mice. Implications for Alzheimer's disease and stroke. Neurosci Lett 369(2):87-92.

Cummings JL, Cole G. 2002. Alzheimer disease. J Am Med Assoc 287:2335-2338.

Davalos D, Grutzendler J, Yang G, Kim JV, Zuo Y, Jung S, Littman DR, Dustin ML, Gan WB. 2005. ATP mediates rapid microglial response to local brain injury in vivo. Nature Neuroscience 8(6):752-758.

DeKosky ST, Scheff SW. 1990. Synapse loss in frontal cortex biopsies in Alzheimer's disease: correlation with cognitive severity. Ann Neurol 27:457-464.

Dexter DT, Carayon A, Javoy-Agid F, Wells FR, Daniel SE, Lees A, Jenner P, Marsden CD. 1991. Alterations in levels of iron, ferritin and other trace metals in Parkinson's disease and other neurodegenerative diseases affecting the basal ganglia. Brain 114:1953-1975.

Dijkstra CD, Dopp EA, Joling O, Kraal G. 1985. The heterogeneity of mononuclear phagocytes in lymphoid organs: distinct macrophage subpopulations in the rat recognized by monoclonal antibodies ED1, ED2 and ED3. Immunology 54(3):589-599.

Dipatre PL, Gelmann BB. 1997. Microglial cell activation in aging and Alzheimer's disease: partial linkage with neurofibrillary tangle burden in the hippocampus. J Neuropathol Exp Neurol 56:143-149.

Fendrick SE, Xue Q-S, Streit WJ. 2007. Formation of multinucleated giant cells and microglial degeneration in rats expressing a mutant Cu/Zn superoxide dismutase gene. J Neuroinflamm 4:9.

Ferraro A. 1931. The origin and formation of senile plaques. Arch Neurol Psychiatry 25:1042-1062.

Flanary BE, Sammons NW, Nguyen C, Walker D, Streit WJ. 2007. Evidence that aging and amyloid promote microglial cell senescence. Rejuv Res 10(1):61-74.

Flanary BE, Streit WJ. 2003. Telomeres shorten with age in rat cerebellum and cortex in vivo. J Anti Aging Med 6:299-308.

Flanary BE, Streit WJ. 2004. Progressive telomere shortening occurs in cultured rat microglia, but not astrocytes. Glia 45:75-88.

Flaris NA, Hickey WF. 1992. Development and characterization of an experimental model of brain abscess in the rat. Am J Pathol 141:1299-1307.

Fleming MD, Romano MA, Su MA, Garrick LM, Garrick MD, Andrews NC. 1998. Nramp2 is mutated in the anemic Belgrade (b) rat: Evidence of a role for Nramp2 in endosomal iron transport. Proc Natl Acad Sci USA 95:1148-1153.

Focht SJ, Snyder BS, Beard JL, van Gelder W, Williams LR, Connor JR. 1997. Regional distribution of iron, transferrin, ferritin, and oxidatively-modified proteins in young and aged Fisher 344 rat brains. Neuroscience 79:255-261.

Gary DA, Woulfe J. 2005. Lipofuscin and aging: a matter of toxic waste. Sci Aging Knowledge Environ:re1.

Godbout JP, Chen J, Abraham J, Richwine AF, Berg BM, Kelley KW, Johnson RW. 2005. Exaggerated neuroinflammation and sickness behavior in aged mice following activation of the peripheral inate immune system. FASEB J 19:1329-1331.

Graeber MB, Raivich G, Kreutzberg GW. 1989. Increase of transferrin receptors and iron uptake in regenerating motor neurons. J Neurosci Res 23(3):342-345.

Graeber MB, Streit WJ, Kreutzberg GW. 1988a. Axotomy of the rat facial nerve leads to increased CR3 complement receptor expression by activated microglial cells. J Neurosci Res 21(1):18-24.

Graeber MB, Tetzlaff W, Streit WJ, Kreutzberg GW. 1988b. Microglial cells but not astrocytes undergo mitosis following facial nerve axotomy. Neurosci Lett 85:317-321.

Graeber MB, Lopez-Redondo F, Ikoma W, Ishikawa M, Imai Y, Nagajima K, Kreutzberg GW, Kohsaka S. 1998. The microglia/macrophage response in the neonatal rat facial nucleus following axotomy. Brain Res 813:241-253.

Grundke-Iqbal I, Fleming J, Tung YC, Lassmann H, Iqbal K, Joshi JG. 1990. Ferritin is a component of the neuritic (senile) plaque in Alzheimer dementia. Acta Neuropathol 81:105-110.

Hallgren B, Sourander P. 1958. The effect of age on the non-heme iron in the human brain. J Neurochem 3:41-51.

Han J, Day JR, Connor JR, Beard JL. 2002. H and L ferritin subunit mRNA expression differs in brains of control and iron-deficient rats. J Nutr 132:2769-2774.

Hanisch UK, Kettenmann H. 2007. Microglia: active sensor and versatile effector cells in the normal and pathologic brain. Nat Neurosci 10(11):1387-94.

Harrison PM, Arosio P. 1996. The ferritins: molecular properties, iron storage function and cellular regulation. Biochim Biophys Acta 1275:161-203.

Hentze MW, Muckenthaler MU, Andrews NC. 2004. Balancing acts: molecular control of mammalian iron metabolism. Cell 117:285-297.

Heppner FL, Roth K, Nitsch R, Hailer NP. 1998. Vitamin E induces ramification and downregulation of adhesion molecules in cultured microglial cells. Glia 22:180-188.

Hirrlinger J, Gutterer JM, Kussmaul L, Hamprecht B, Dringen R. 2000. Microglial cells in culture express a prominent glutathione system for the defense against reactive oxygen species. Dev Neurosci 22:384-92.

Hoffbrand AV, Ganeshaguru K, Hooton JW, Tattersall MH. 1976. Effect of iron deficiency and desferrioxamine on DNA synthesis in human cells. Brit J Haematol 33:517-526.

Huang E, Ong W-Y. 2005. Distribution of ferritin in the rat hippocampus after kainate-induced neuronal injury. Exp Brain Res 161:502-511.

Ito D, Imai Y, Ohsawa K, Nakajima K, Fukuuchi Y, Kohsaka S. 1998. Microglia-specific localization of a novel calcium binding protein, Iba1. Brain Res Mol Brain Res 57(1):1-9.

Jolly RD, Douglas BV, Davey PM, Roiri JE. 1995. Lipofuscin in bovine muscle and brain: A model for studying age pigment. Gerontology 41(Suppl 2):283-295.

Kaneko Y, Kitamoto T, Tateishi J, Yamaguchi K. 1989. Ferritin immunohistochemistry as a marker for microglia. Acta Neuropathol 79:129-136.

Kaur D, Rajagopalan S, Chinta S, Kumar J, Di Monte D, Cherny RA, Andersen JK. 2007. Chronic ferritin expression within murine dopaminergic midbrain neurons results in a progressive age-related neurodegeneration. Brain Res 1140:188-194.

Kawaguchi-Niida M, Shibata N, Morikawa S, Uchida K, Yamamoto T, Sawada T, Kobayashi M. 2006. Crotonaldehyde accumulates in glial cells of Alzheimer's disease brain. Acta Neuropathol 111:422-9.

Kerr JF, Wyllie AH, Currie HR. 1972. Apoptosis: a basic biological phenomenon with wide ranging implications in tissue kinetics. Br J Cancer 26:239-257.

Kim HY, LaVaute T, Iwai K, Klausner RD, Rouault TA. 1996. Identification of a conserved and functional iron-responsive element in the 5-untranslated region of mammalian mitochondrial aconitase. J Biol Chem 271:24226-24230.

Koeppen AH, Dickson AC. 2001. Iron in the Hallervorden-Spatz syndrome. Pediatr Neurol 25(2):148-155.

Korotzer AR, Pike CJ, Cotman CW. 1993. beta-Amyloid peptides induce degeneration of cultured rat microglia. Brain Res 624(1-2):121-125.

Kreutzberg GW. 1996. Microglia: a sensor for pathological events in the CNS. Trends Neurosci 19(8):312-318.

Kruszewski M. 2003. Labile iron pool: the main determinant of cellular response to oxidative stress. Mutat Res 531:81-92.

Kyrkanides S, O'Banion MK, Whiteley PE. 2001. Enhanced glial activation and expression of specific CNS inflammation-related molecules in aged versus young rats following cortical stab injury. J Neuroimmunol 119:269-275.

Lawson DM, Treffry A, Artymiuk PJ, Harrison PM, Yewdall SJ, Luzzago A, Cesareni G, Levi S, Arosio P. 1989. Identification of the ferroxidase center in ferritin. FEBS Letters 254:207-210.

Lawson LJ, Perry VH, Gordon S. 1992. Turnover of resident microglia in the normal adult-mouse brain. Neuroscience 48:405-15.

Le NT, Richardson DR. 2002. The role of iron in cell cycle progression and the proliferation of neoplastic cells. Biochim Biophys Acta 1603:31-46.

Lemstra AW, Groen in't Woud JCM, Hoozemans JJM, van Haastert ES, Rozemuller AJM, Eikelenboon P, van Gool WA. 2007. Microglia activation in sepsis: a case-control study. J Neuroinflamm 4:4.

Lieu PT, Heiskala M, Peterson PA, Yang Y. 2001. The roles of iron in health and disease. Mol Aspects Med 22(1-2):1-87.

Lindenau J, Noack H, Asayama K, Wolf G. 1998. Enhanced cellular glutathione peroxidase immunoreactivity in activated astrocytes and in microglia during excitocin induced neurodegeneration. Glia 24:252-6.

Ling E, Kaur C, Wong W. 1992. Expression of major histocompatibility complex antigens and CR3 complement receptors in activated microglia following an injection of ricin into the sciatic nerve in rats. Histo Histopathol 7(1):93-100.

Lopes KO, Sparks DL, Streit WJ. 2008. Degeneration of microglial cells in the aged and Alzheimer's disease brains is associated with ferritin immunoreactivity. Glia 56(10):1048-60.

Luber-Narod J, Rogers J. 1988. Immune system associated antigens expressed by cells of the human central nervous system. Neurosci Lett 94(1-2):17-22.

Ma L, Morton AJ, Nicholson LFB. 2003. Microglia density decreases with age in a mouse model of Huntington's disease. Glia 43:274-280.

Masliah E, Terry RD, DeTeresa RM, Hansen LA. 1989. Immunohistochemical quantification of the synapse-related protein synaptophysin in Alzheimer disease. Neurosci Lett 103:234-239.

Mazur A, Green S, Saha A, Carleton A. 1958. Mechanism of release of ferritin iron by xanthine oxidase. J Clin Invest 37:1809-1817.

McGeer PL, Itagaki S, Tago H, McGeer EG. 1987. Reactive microglia in patients with senile dementia of the Alzheimer type are positive for the histocompatibility glycoprotein HLA-DR. Neurosci Lett 79:195-200.

Mildner A, Schmitdt H, Nitsche M, Merkler D, Hanisch UK, Mack M, Heikenwalder M, Bruck W, Priller J, Prinz M. 2007. Microglia in the adult brain arise from Ly-6ChiCCR2+ monocytes only under defined host conditions. Nat Neurosci 10(12):1544-53.

Milligan C, Cunningham T, Levitt P. 1991. Differential immunochemical markers reveal the normal distribution of brain macrophages and microglia in the developing rat brain. J Comp Neurol 314(1):125-35.

Mittelbronn M, Dietz K, Schluesener HJ, Meyermann R. 2001. Local distribution of microglia in the normal adult human central nervous system differs by up to one order of magnitude. Acta Neuropathol 101:249-255.

Moran LB, Graeber MB. 2004. The facial nerve axotomy model. Brain Res Brain Res Rev 44(2-3):154-178.

Nair A, Bonneau RH. 2006. Stress-induced elevation of glucocorticoids increases microglia proliferation through NMDA receptor activation. J Neuroimmunol 171(1-2):72-85.

Nimmerjahn A, Kirchhoff F, Helmchen F. 2005. Resting microglial cells are highly dynamic surveillants of brain parenchyma in vivo. Science 308(5726):1314-1318.

Ogawa H, Nishida A, Mito T, Takashima S. 1994. Development of ferritin-positive cells in cerebrum of human brain. Pediatr Neurol 10:44-48.

Oide T, Kinoshita T, Arima K. 2006. Regression stage senile plaques in the natural course of Alzheimer's disease. Neuropathol Appl Neurobiol 32:539-556.

Overmyer M, Helisalmi S, Soininen S, Soininen H, Laakso M, Riekkinen P, Alafuzoff I. 1999. Reactive microglia in aging and dementia: an immunohistochemical study of postmortem human brain tissue. Acta Neuropathol 97:383-392.

Peinado MA, Quesada A, Pedrosa JA, Torres MI, Martinez M, Esteban FJ, Del Moral ML, Hernandez R, Rodrigo J, Peinado JM. 1998. Quantitative and ultrastructural changes in glia and pericytes in the parietal cortex of the aging rat. Microsc Res Tech 43:34-42.

Ponka P, Lok CN. 1999. The transferrin receptor: role in health and disease. Int J Biochem Cell Biol 31:1111-1137.

Qian ZM, Wang Q. 1998. Expression of iron transport proteins and excessive iron accumulation in the brain in neurodegenerative disorders. Brain Res Brain Res Rev 27(3):257-267.

Roberts ES, Masliah E, Fox HS. 2004. CD163 identifies a unique population of ramified microglia in HIV encephalitis (HIVE). J Neuropath Exp Neurol 63(12):1255-1264.

Roskams AJ, Connor JR. 1994. Iron, transferrin and ferritin in the rat brain during development and aging. J Neurochem 63:709-716.

Rozovsky I, Finch C, Morgan T. 1998. Age-related activation of microglia and astrocytes: in vitro studies show persistent phenotypes of aging, increased proliferation, and resistance to down-regulation. Neurobiol Aging 19:97-103.

Schmidt OI, Heyde CE, Ertel W, Stahel PF. 2005. Closed head injury -- an inflammatory disease? Brain Res Rev 48(2):388-399.

Sedgwick JD, al. e. 1991. Isolation and direct characterization of resident microglial cells from the normal and inflamed central nervous system. PNAS 88:7438-7442.

Seehafer SS, Pearce DA. 2006. You say lipofuscin, we say ceroid: Defining autofluorescent storage material. Neurobiol Aging 27:576-588.

Selkoe DJ. 2004. Alzheimer's disease: mechanistic understanding predicts novel therapies. Ann Intern Med 140:627-638.

Semmler A, Okulla T, Sastre M, Dumitrescu-Ozimek L, Heneka MT. 2005. Systemic inflammation induces apoptosis with variable vulnerability of different brain regions. J Chem Neuroanat 30:144-157.

Sheffield LG, Berman NEJ. 1998. Microglial expression of MHC class II increases in normal aging of nonhuman primates. Neurobiol Aging 19(1):47-55.

Sierra A, Gottfried-Blackmore AC, McEwen BS, Bulloch K. 2007. Microglia derived from aging mice exhibit an altered inflammatory profile. Glia 55:412-424.

Simard AR, Soulet D, Gowing G, Julien J-P, Rivest S. 2006. Bone marrow-derived microglia play a critical role in restricting senile plaque formation in Alzheimer's disease. Neuron 49:489-502.

Simmons DA, Casale M, Alcon B, Pham N, Narayan N, Lynch G. 2007. Ferritin accumulation in dystrophic microglia is an early event in the development of Huntington's disease. Glia 55:1074-1084.

Sitte N, Merker K, Grune T, von Zglinicki T. 2001. Lipofuscin accumulation in proliferating fibroblasts in vitro: an indicator of oxidative stress. Exp Neurol 36(3):475-86.

Sloane JA, Hollander W, Moss MB, Rosene DL, Abraham CR. 1999. Increased microglial activation and nitration in white matter of the aging monkey. Neurobiol Aging 20:395-405.

Stolzing A, Grune T. 2003. Impairment of protein homeostasis and decline of proteasome activity in microglial cells from adult Wistar rats. J Neurosci Res 71:264-271.

Stolzing A, Sethe S, Grune T. 2005. Chronically active: activation of microglial proteolysis in aging and neurodegeneration. Redox Rep 10(4):207-213.

Stolzing A, Wengner A, Grune T. 2002. Degradation of oxidized extracellular proteins by microglia. Arch Biochem Biophys 400:171-179.

Stolzing A, Widmer R, Tobias J, Voss P, Grune T. 2006. Tocopherol-mediated modulation of age-related changes in microglial cells: Turnover of extracellular oxidized protein material. Free Rad Biol Med 40:2126-35.

Streit WJ. 2000. Microglial response to brain injury: A brief synopsis. Toxicol Pathol 28(1):28-30.

Streit WJ. 2001. Microglia and macrophages in the developing CNS. Neuro Toxicol 22:619-624.

Streit WJ. 2002. Microglia as neuroprotective, immunocompetent cells of the CNS. Glia 40(2):133-139.

Streit WJ. 2004. Microglia and Alzheimer's disease pathogenesis. J Neurosci Res 77(1):1-8.

Streit WJ. 2006. Microglial senescence: does the brain's immune system have an expiration date? Trends Neurosci 29(9):506-510.

Streit WJ, Miller KR, Lopes KO, Njie E. 2008. Microglial degeneration in the aging brain - bad news for neurons? Front Biosci 13:3423-38.

Streit WJ, Sammons NW, Kuhns AJ, Sparks DL. 2004. Dystrophic microglia in the aging human brain. Glia 45(2):208-212.

Streit WJ, Sparks DL. 1997. Activation of microglia in the brains of humans with heart disease and hypercholesterolemic rabbits. J Mol Med 75(2):130-138.

Streit WJ, Walter SA, Pennell NA. 2000. Reactive microgliosis. Prog Neurobiol 57(6):563-581.

Sugama S, Fujita M, Hashimoto M, Conti B. 2007. Stress induced morphological microglial activation in the rodent brain: involvement of interleukin-18. Neuroscience 146(3):1388-1399.

Taneja V, Mishra K, Agarwal KN. 1986. Effect of early iron deficiency in rat on the gamma-aminobutyric acid shunt in brain. J Neurochem 46(6):1670-1674.

Terman A, Brunck UT. 2004. Lipofuscin. Int J Biochem Cell Biol 36:1400-1404.

Thal DR, Capetillo-Zarate E, Del Tredici K, Braak H. 2006. The development of amyloid-[beta] protein deposits in the aged brain. Sci Aging Knowledge Environ 6:1-9.

Torti FM, Torti SV. 2002. Regulation of ferritin genes and protein. Blood 99:3505-3516.

Twig G, Jung SK, Messerli MA, Smith PJ, Shirihai OS. 2001. Real-time detection of reactive oxygen intermediates from single microglial cells. Biol Bull 201:261-2.

Vogt M, Haggblom C, Yeargin J, Christiansen-Weber T, Haas M. 1998. Independent induction of senescence by p16INK4a and p21CPI1 in spontaneously immortalized human fibroblasts. Cell Growth Diff 9(2):139-46.

von Eitzen U, Egensperger R, Kosel S, Grasbon-Frodl EM, Imai Y, Bise K, Mehraein P, Graeber MB. 1998. Microglia and the development of spongiform change in Creutzfeldt-Jakob disease. J Neuropath Exp Neurol 57:246-256.

Wang W, Ji P, Dow KE. 2003. Corticotropin-releasing hormone induces proliferation and TNF-α release in cultured rat microglia via MAP kinase signalling pathways. J Neurochem 84(1):189-195.

Wang W, Ji P, Riopelle RJ, Dow KE. 2002. Functional expression of corticotropin-releasing hormone (CRH) receptor 1 in cultured rat microglia. J Neurochem 80(2):287-294.

Wierzba-Bobrowicz T, Lewandowska E, Kosno-Kruszewska E, Lechowicz W, Pasennik E, Schmidt-Sidor B. 2004. Degeneration of microglial cells in frontal and temporal lobes of chronic schizophrenics. Folia Neuropathol 42(3):157-165.

Wierzba-Bobrowicz T, Lewandowska E, Lechowicz W, Stepien T, Pasennik E. 2005. Quantitative analysis of activated microglia, ramified and damage of processes in the frontal and temporal lobes of chronic schizophrenics. Folia Neuropathol 43(2):81-89.

Wirenfeldt M, Babcock AA, Ladeby R, Lambertsen KL, Dagnaes-Hansen F, Leslie RGQ, Owens T, Finsen B. 2005. Reactive microgliosis engages distinct responses by microglial subpopulations after minor central nervous system injury. J Neurosci Res 82:507-514.

Xu H, Chen M, Manivannan A, Lois N, Forrester JV. 2008. Age-dependent accumulation of lipofuscin in perivascular and subretinal microglia in experimental mice. Aging Cell 7(1):58-68.

Yamaguchi H, Hirai S, Morimatsu M, Shoji M, Ihara Y. 1988. A variety of cerebral amyloid deposits in the brains of the Alzheimer-type dementia demonstrated by beta protein immunostaining. Acta Neuropathol 76(6):541-549.

Yamasaki R, Zhang J, Koshiishi I, Sastradipura Suniarti DF, Wu Z, Peters C, Schwake M, Uchiyama Y, Kira J, Saftig P and others. 2007. Involvement of lysosomal storage-induced p38 MAP kinase activation in the overproduction of nitric oxide by microglia in cathepsin D-deficient mice. Mol Cell Neurosci 35(3):573-84.

Yanishevsky R, Mendelsohn ML, Mayall BH, Cristofalo VJ. 1974. Proliferative capacity and DNA content of aging human diploid cells in culture: A cytophotometric and autoradiographic analysis. J Cell Physiol 84:165-170.

Ye SM, Johnson RW. 1999. Increased interleukin-6 expression by microglia from brain of aged mice. J Neuroimmunol 93:139-148.

BIOGRAPHICAL SKETCH

Kryslaine Oliveira Lopes was born in Manaus, Amazonas, Brazil. In her senior year in high school in Manaus, Kryslaine participated in an exchange student program that brought her to the United States. Kryslaine ended up finishing both her secondary and undergraduate education in the U.S.A. earning a bachelor's degree with honors in biological sciences from Illinois State University in 2001. Kryslaine then joined the neuroscience department at the University of Chicago as a full-time research technician. In 2004, Kryslaine began her doctorate studies in neuroscience at the University of Florida College of Medicine under the mentorship of Dr. Wolfgang (Jake) Streit. Upon completion of her Ph.D. program, Kryslaine will join the department of neurosciences at the University of California-San Diego as a postdoctoral scholar.